UNIVERSITY OF OKLAHOMA

GRADUATE COLLEGE

USE OF THE HLD EQUATION TO DETERMINE SURFACTANT ADSORPTION AT SOLID SURFACES

A THESIS

SUBMITTED TO THE GRADUATE FACULTY

in partial fulfillment of the requirements for the

Degree of

MASTER OF SCIENCE

By

KEVIN CARR
Norman, Oklahoma
2016

Downloaded from SHAREOK. Persistent Handle URL: https://hdl.handle.net/11244/44588

USE OF THE HLD EQUATION TO DETERMINE SURFACTANT ADSORPTION AT SOLID SURFACES

A THESIS APPROVED FOR THE
SCHOOL OF CHEMICAL, BIOLOGICAL AND MATERIALS ENGINEERING

BY

_____
Dr. Brian Grady, Chair

_____
Dr. Jeffrey Harwell

_____
Dr. Benjamin Shiau

© Copyright by KEVIN CARR 2016
All Rights Reserved.

Acknowledgements

I would like to thank my parents for their unwavering support.

I would like to thank Richard Steger, Brian Majeska, David Reynolds, Joe Lorenc, Jason Bausano, and Dennis Muncy for being great to work with.

I would like to thank Dr. Grady, Dr. Harwell, and Dr. Shiau for being on my committee and for all the help they provided with my research.

I would like to thank JJ Hamon, Dr. Danielle Baker, and Donna Stacy for teaching me how to use the instruments and methods necessary for this research.

I would like to thank Gabriel Ratcliff for his help with the experiments and for Dr. Martina Dreyer for getting this project started.

And finally I would like to thank JJ, Zahra, Maria, and Alex for being great to work with for these two years.

Table of Contents

Acknowledgements iv

List of Tables vii

List of Figures viii

Chapter 1: Introduction 1

Objective 2

Chapter II. Literature Review 3

Surfactant Overview 3

Surfactant Adsorption 5

Surfactant Solubilization 7

Modeling Surfactant Systems 8

The Hydrophilic-Lipophilic Difference 10

Determining Characteristic Curvature 11

Determining Equivalent Alkane Carbon Number 12

Enhanced Oil Recovery 13

Hydrophilic-Lipophilic Difference Modification 15

Chapter III. Experimental 17

Materials 17

Zeta Potential 18

Equvalent Alkane Carbon Number Salinity Scans 18

Characteristic Curvature Salinity Scans 20

Critical Micelle Concentration 21

Adsorption Studies 22

Chapter IV. Result and Conclusions 24
Zeta Potentials of Minerals 24
Equivalent Alkane Carbon Numbers of Heavy Petroleum Oils 25
Characteristic Curvatures of Surfactants 32
Critical Micelle Concentrations of Surfactants 36
Adsorption Isotherms 40
Model Fitting 52
Conclusions and Discussion 66
References 69
Appendix A: Sample Equivalent Alkane Carbon Number Determination 72
Materials Needed 72
Procedure 72
Appendix B: Sample Characteristic Curvature Determination 77
Materials Needed 77
Procedure 77
Example 79
Appendix C: Sample Critical Micelle Concentration Determination 85
Materials Needed 85
Procedure 85
Critical Micelle Concentration 85
Area Per Surfactant Head Group 87
Example 87

List of Tables

Table 1: Zeta potentials of mineral fines 25

Table 2: Equivalent Alkane Number Summary 31

Table 3: Toluene and Alkane mixtures 32

Table 4: Summary of the characteristic curvatures for Surfactant 1 and additives 35

Table 5: CMC and Area per head group for Surfactant 1 and additives 39

Table 6: Maximum Adsoprtion (g/m2) for Granite RS 51

Table 7: Maximum Adsoprtion (g/m2) for Granite WS 51

Table 8: Maximum Adsoprtion (g/m2) for Granite 51

Table 9: Maximum Adsoprtion (g/m2) for Ft. Payne Limestone 52

Table 10: Maximum Adsoprtion (g/m2) for Warsaw 52

Table 11: Maximum Adsoprtion (g/m2) for Limestone A 52

Table 12: Salinity Graph Data 74

Table 13: Stock solutions 80

Table 14: Mole Fraction of Surfactant 3 80

Table 15: Vial Preparation 81

Table 16: Optimal Salinities for mole fractions of Surfactant 3 82

Table 17: Mole fraction and corresponding natural logarithm of salinities 83

Table 18: Surfactant concentration and corresponding surface tensions 87

List of Figures

Figure 1: General surfactant structure of a nonionic, anionic, cationic, and amphoteric surfactants 3

Figure 2: Graphic of surfactant existing as monomers in solution, adsorbing at the air-water interface, and micelle formation 5

Figure 3: Adsorption schematic of surfactant adsorbing at the solid-liquid interface..... 7

Figure 4: (a) schematic of a normal micelle and (b) schematic of reverse micelle 8

Figure 5: Image through the Zeta Meter 3.0 microscope looking at the electric cell..... 24

Figure 6: Sample Scan for 0.1M AMA, toluene for salinities 2.8, 2.9, 3.0, 3.1, 3.2 g NaCl/100mL H2O 26

Figure 7: Optimal Salinity vs. Weight Fraction AMA, toluene, and the Refinery 13 heavy petroleum oil 27

Figure 8: Sample Scan for 0.1M AMA, toluene, and 3 wt% Refinery 13 heavy petroleum oil for salinities 3.0, 3.4, 3.5, 3.6, 4.0, and 5.0 g NaCl/100mL H2O 27

Figure 9: Optimal Salinity vs. Weight Fraction AMA, toluene, and Oil #15169 28

Figure 10: Sample Scan for 0.1M AMA, toluene, and 1 wt% Oil #15169 for salinities 2.5, 3.0, 3.3, 3.4, 3.5, 3.6, 3.7, 4.0, and 4.5 g NaCl/100mL H2O 28

Figure 11: Optimal Salinity vs. Weight Fraction AMA, toluene, and Refinery 4 heavy petroleum oil..... 29

Figure 12: Sample Scan for 0.1M AMA, toluene, and 1 wt% Refinery 4 heavy petroleum oil for salinities 2.5, 3.0, 3.3, 3.4, 3.5, 3.6, 3.7, 3.8, and 4.0 g NaCl/100mL H2O 29

Figure 13: Optimal Salinity vs. Weight Fraction AMA, toluene, and Refinery 12 heavy petroleum oil 30
Figure 14: Sample Scan for 0.1M AMA, toluene, and 1 wt% Refinery 12 heavy petroleum oil for salinities 2.5, 3.0, 3.3, 3.4, 3.5, 3.6, 3.7, 3.8, and 3.9 g NaCl/100mL H2O 30
Figure 15: Sample salinity scan for 0.0474M AMA, 0.003M Surfactant 1 with 5 wt% Additive 5, and toluene for salinities 3.0, 3.6, 3.8, 4.0, 4.2, and 4.4 g NaCl/100 mL H2O 33
Figure 16: Characteristic curvature determination graph for Surfactant 1 with 5wt% Additive 5 33
Figure 17: Sample salinity scan for 0.0474M AMA, 0.003M Surfactant 1 with 10 wt% Additive 6, and toluene for salinities 3.0, 3.3, 3.5, 3.7, 3.9, and 4.1 g NaCl/100 mL H2O 34
Figure 18: Characteristic curvature determination graph for Surfactant 1 with 10 wt% Additive 6 34
Figure 19: Sample salinity scan for 0.054M BCl and toluene for salinities 4.0, 4.6, 4.7, 4.8, 4.9, 5.0, 5.1, 5.2, 5.3, 5.4, and 6.0 g NaCl/100 mL H2O 35
Figure 20: Sample salinity scan for 0.01M BCl and hexane for salinities 10.5, 11.3, 11.4, 11.5, 11.6, 11.7, 11.8, 11.9, 12.0, 12.1, and 13.0 g NaCl/100 mL H2O ... 36
Figure 21: Sample salinity scan for 0.01M BCl and decane for salinities 21.5, 22.7, 22.8, 22.9, 23.0, 23.1, 23.2, 23.3, 23.4, and 23.5 g NaCl/100 mL H2O 36
Figure 22: Surface Tension vs. Concentration for Surfactant 2 37
Figure 23: Surface Tension vs. Concentration for Surfactant 1 37

Figure 24: Surface Tension vs. Concentration for Surfactant 1 + 1wt% Additive 5..... 37

Figure 25: Surface Tension vs. Concentration for Surfactant 1 + 3wt% Additive 5..... 38

Figure 26: Surface Tension vs. Concentration for Surfactant 1 + 5wt% Additive 5..... 38

Figure 27: Surface Tension vs. Concentration for Surfactant 1 + 3wt% Additive 6..... 38

Figure 28: Surface Tension vs. Concentration for Surfactant 1 + 5wt% Additive 6..... 39

Figure 29: Surface Tension vs. Concentration for Surfactant 1 + 10wt% Additive 6.... 39

Figure 30: Adsorption isotherm for Surfactant 1 and 1wt% Additive 5 in EACN 7.1 on Granite RS, Warsaw, Ft. Payne Limestone, Limestone A, Granite, and Granite WS mineral fines 41

Figure 31: Adsorption isotherm for Surfactant 1 and 1wt% Additive 5 in EACN 9.0 on Granite RS, Warsaw, Ft. Payne Limestone, Limestone A, Granite, and Granite WS mineral fines 41

Figure 32: Adsorption isotherm for Surfactant 1 and 1wt% Additive 5 in EACN 9.7 on Granite RS, Warsaw, Ft. Payne Limestone, Limestone A, Granite, and Granite WS mineral fines 42

Figure 33: Adsorption isotherm for Surfactant 1 and 3wt% Additive 5 in EACN 7.1 on Granite RS, Warsaw, Ft. Payne Limestone, Limestone A, Granite, and Granite WS mineral fines 42

Figure 34: Adsorption isotherm for Surfactant 1 and 3wt% Additive 5 in EACN 9.0 on Granite RS, Warsaw, Ft. Payne Limestone, Limestone A, Granite, and Granite WS mineral fines 43

Figure 35: Adsorption isotherm for Surfactant 1 and 3wt% Additive 5 in EACN 9.7 on Granite RS, Warsaw, Ft. Payne Limestone, Limestone A, Granite, and Granite WS mineral fines 43
Figure 36: Adsorption isotherm for Surfactant 1 and 5wt% Additive 5 in EACN 7.1 on Granite RS, Warsaw, Ft. Payne Limestone, Limestone A, Granite, and Granite WS mineral fines 44
Figure 37: Adsorption isotherm for Surfactant 1 and 5wt% Additive 5 in EACN 9.0 on Granite RS, Warsaw, Ft. Payne Limestone, Limestone A, Granite, and Granite WS mineral fines 44
Figure 38: Adsorption isotherm for Surfactant 1 and 5wt% Additive 5 in EACN 9.7 on Granite RS, Warsaw, Ft. Payne Limestone, Limestone A, Granite, and Granite WS mineral fines 45
Figure 39: Adsorption isotherm for Surfactant 1 and 3wt% Additive 6 in EACN 7.1 on Granite RS, Warsaw, Ft. Payne Limestone, Limestone A, Granite, and Granite WS mineral fines 45
Figure 40: Adsorption isotherm for Surfactant 1 and 3wt% Additive 6 in EACN 9.0 on Granite RS, Warsaw, Ft. Payne Limestone, Limestone A, Granite, and Granite WS mineral fines 46
Figure 41: Adsorption isotherm for Surfactant 1 and 3wt% Additive 6 in EACN 9.7 on Granite RS, Warsaw, Ft. Payne Limestone, Limestone A, Granite, and Granite WS mineral fines 46

Figure 42: Adsorption isotherm for Surfactant 1 and 5wt% Additive 6 in EACN 7.1 on Granite RS, Warsaw, Ft. Payne Limestone, Limestone A, Granite, and Granite WS mineral fines 47
Figure 43: Adsorption isotherm for Surfactant 1 and 5wt% Additive 6 in EACN 9.0 on Granite RS, Warsaw, Ft. Payne Limestone, Limestone A, Granite, and Granite WS mineral fines 47
Figure 44: Adsorption isotherm for Surfactant 1 and 5wt% Additive 6 in EACN 9.7 on Granite RS, Warsaw, Ft. Payne Limestone, Limestone A, Granite, and Granite WS mineral fines 48
Figure 45: Adsorption isotherm for Surfactant 1 and 10wt% Additive 6 in EACN 7.1 on Granite RS, Warsaw, Ft. Payne Limestone, Limestone A, Granite, and Granite WS mineral fines 48
Figure 46: Adsorption isotherm for Surfactant 1 and 10wt% Additive 6 in EACN 9.0 on Granite RS, Warsaw, Ft. Payne Limestone, Limestone A, Granite, and Granite WS mineral fines 49
Figure 47: Adsorption isotherm for Surfactant 1 and 10wt% Additive 6 in EACN 9.7 on Granite RS, Warsaw, Ft. Payne Limestone, Limestone A, Granite, and Granite WS mineral fines 49
Figure 48: Adsorption isotherm for Surfactant 1 in EACN 7.1 on Granite RS, Warsaw, Ft. Payne Limestone, Limestone A, Granite, and Granite WS mineral fine 50
Figure 49: Adsorption isotherm for Surfactant 1 in EACN 9.0 on Granite RS, Warsaw, Ft. Payne Limestone, Limestone A, Granite, and Granite WS mineral fines..... 50

Figure 50: Adsorption isotherm for Surfactant 1 in EACN 9.7 on Granite RS, Warsaw, Ft. Payne Limestone, Limestone A, Granite, and Granite WS mineral fines..... 51
Figure 51: HLD adsorption values calculated using b'TOTAL, allowing K to vary, allowing J to vary, and excluding Granite WS 54
Figure 52: HLD adsorption values calculated using b'INDIV, allowing K to vary, allowing J to vary, and excluding Granite WS 54
Figure 53: HLD adsorption values calculated using b'TOTAL, allowing K to vary, allowing J to vary, and excluding Granite WS for only Surfactant 1..... 55
Figure 54: HLD adsorption values calculated using b'TOTAL, allowing K to vary, allowing J to vary, and excluding Granite WS for only Surfactant 1 and the Additive 5 56
Figure 55: HLD adsorption values calculated using b'TOTAL, allowing K to vary, allowing J to vary, and excluding Granite WS for only Surfactant 1 and the Additive 6 56
Figure 56: HLD adsorption values calculated using b'TOTAL, allowing K to vary, allowing J to vary, and excluding Granite WS for only Surfactant 1 and 1 wt% Additive 5 57
Figure 57: HLD adsorption values calculated using b'TOTAL, allowing K to vary, allowing J to vary, and excluding Granite WS for only Surfactant 1 and 3 wt% Additive 5 58
Figure 58: HLD adsorption values calculated using b'TOTAL, allowing K to vary, allowing J to vary, and excluding Granite WS for only Surfactant 1 and 5 wt% Additive 5 58

Figure 59: HLD adsorption values calculated using b'TOTAL, allowing K to vary, allowing J to vary, and excluding Granite WS for only Surfactant 1 and 3 wt% Additive 6 59
Figure 60: HLD adsorption values calculated using b'TOTAL, allowing K to vary, allowing J to vary, and excluding Granite WS for only Surfactant 1 and 5 wt% Additive 6 59
Figure 61: HLD adsorption values calculated using b'TOTAL, allowing K to vary, allowing J to vary, and excluding Granite WS for only Surfactant 1 and 10 wt% Additive 6 60
Figure 62: HLD adsorption values calculated using b'TOTAL, allowing K to vary, and allowing J to vary for EACN 7.1 61
Figure 63: HLD adsorption values calculated using b'TOTAL, allowing K to vary, and allowing J to vary for EACN 9.0 61
Figure 64: HLD adsorption values calculated using b'TOTAL, allowing K to vary, and allowing J to vary for EACN 9.7 62
Figure 65: HLD adsorption values calculated using b'INDIV, allowing K to vary, and allowing J to vary for Granite RS 63
Figure 66: HLD adsorption values calculated using b'INDIV, allowing K to vary, and allowing J to vary for Granite WS 63
Figure 67: HLD adsorption values calculated using b'INDIV, allowing K to vary, and allowing J to vary for Granite 64
Figure 68: HLD adsorption values calculated using b'INDIV, allowing K to vary, and allowing J to vary for Ft. Payne Limestone 64

Figure 69: HLD adsorption values calculated using b'INDIV, allowing K to vary, and allowing J to vary for Warsaw 65
Figure 70: HLD adsorption values calculated using b'INDIV, allowing K to vary, and allowing J to vary for Limestone A 65
Figure 71: Example Meniscus Markings 73
Figure 72: Salinity Scan Graph Example 76
Figure 73: Aqueous phase meniscus lines 81
Figure 74: Completed Scan for 14mM AMA and 1.0mM Surfactant 3 82
Figure 75: Optimal Salinity vs. Mole Fraction for Surfactant 3 84
Figure 76: Surface Tension vs. Concentration for Surfactant 570S 88
Figure 77: CMC approximation 89
Figure 78: CMC Determination 90

Chapter 1: Introduction

Oil recovery from reservoirs typically occurs in three stages. The first stage, known as primary recovery, is driven by natural causes such as gas expansion in the oil reservoir, natural water displacing the oil, or drainage due to gravity and will typically account for only a small percentage of the total oil reservoir. The second stage, known as secondary recovery, occurs after the natural drives have ceased and requires an artificial drive to continue the oil recovery process. And lastly the third stage, known as tertiary recovery or enhanced oil recovery, alters the mobility of the oil in order to increase the amount that can be extracted. Enhanced oil recovery can be categorized into three main methods: gas injection, thermal injection, and chemical injection. This study focuses on the chemical injection method of enhance oil recovery, specifically surfactant injection, and attempts to describe adsorption of a surfactant onto the mineral surfaces of a reservoir in order to predict wettability alteration. Wettability alteration of the permeable rock is an important aspect in enhanced oil recovery as a more water-wet surface will allow oil to flow more easily than an oil-wet surface. Factors such as oil composition, natural charge of the mineral surface, and the curvature of the surfactant at an interface are examined with respect to the adsorption of the surfactant onto the mineral surface in the oil phase. Temperature effects would also be an important component of this model but are not included in the scope of this study. This study was performed on one surfactant with two additives (applied at different weight percentages to change their effect on how the surfactant adsorbed), six different minerals (three granites and three limestones), and three different oil phases that were artificially created based on the range of compositions of heavy petroleum oils that were provided.

Adsorptions of the surfactant onto the minerals is studied in the presences of the oil phase to examine the various effects that each component of the system has on the adsorption phenomena and by extension the wettability alteration of the oil reservoir. This study is fairly limited in its scope and would be improved by expanding the ranges of the crucial parameters of the model as well as the addition of a temperature variable.

Objective

The objective of this work is to develop and refine a mathematical model based on the fundamentals of the hydrophilic-lipophilic deviation equation in order to describe and predict surfactant adsorption onto reservoir rocks in the presences of heavy petroleum oils.

Chapter II. Literature Review

Surfactant Overview

Surface active agents or surfactants are amphiphilic molecules which have two distinct components, namely a hydrophilic head group and a hydrophobic tail group.[1] Surfactants are known by a variety of other functional names such as wetting agents, emulsifiers, dispersants, detergents, etc. based on their intended uses. While a wide assortment of surfactants exist, they can be classified into four main subgroups based on the behavior of their head groups: anionic, cationic, nonionic, and amphoteric (sometimes referred to as ampholytic).

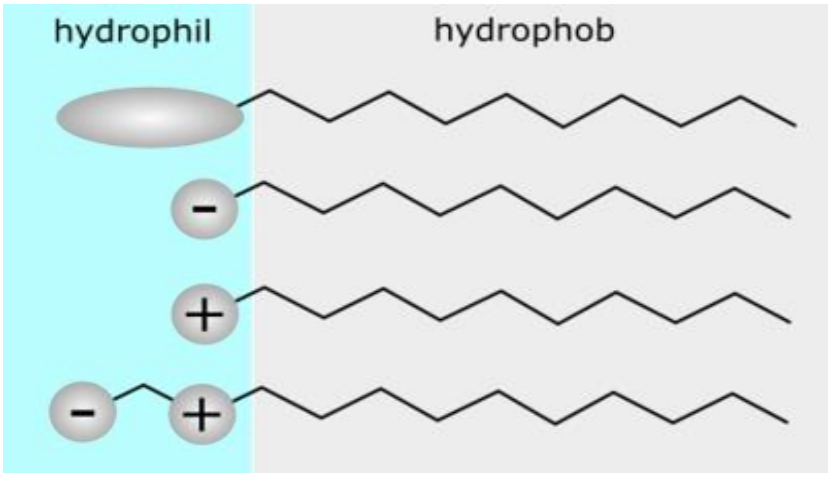

Figure 1: General surfactant structure of a nonionic, anionic, cationic, and amphoteric surfactants

Anionic surfactants have a negatively charged head group and are used for a variety of applications such as detergents, enhanced oil recovery, wetting agents, cosmetics, and many others. Since most naturally occurring surfaces are negatively charged, anionic surfactants do not adsorb well on these surfaces which makes them effective cleaning agents. Anionic surfactants may also adsorb onto positively charged surfaces and make them hydrophobic. Cationic surfactants have a positively charged head group and,

therefore, adsorb strongly on many surfaces. They exhibit poor compatibility with anionic surfactants and are in general more expensive than their anionic counterparts. Cationic surfactants are used as fabric softeners, corrosion inhibitors, asphalt emulsifiers, and in many other ways. Nonionic surfactants typically have good compatibility when mixed with other surfactants and are generally tolerant to significant electrolyte concentrations. Since nonionic surfactants do not dissociate, they are soluble in both organic and aqueous phases and are used in agriculture, detergents, as wetting agents, as well as in other applications. Ampholytic surfactants, as their name suggests, have a variable head group which can change between cationic, anionic, and nonionic depending on pH. Ampholytic surfactants can be used in conjunction with other surfactants well and are typically used in detergents, as foam boosters, and as wetting agents.

The hydrophobic tail group can consist of a straight chain of alkyl groups both unsaturated and saturated, branched chains of alkyl groups, propylene oxide groups, aromatic groups, or even polymer-like lignin derivatives. The composition of the tail group will affect how the surfactant interacts with the surrounding media. For example a longer chain will decrease the surfactants solubility in water while increasing solubility in the organic phase. A longer chain will also increase the Krafft temperature of ionic surfactants, which is the temperature below which surfactants precipitate instead of forming micelles. A longer chain will decrease the cloud point of nonionic surfactants, which is the temperature above which surfactants will no longer be fully soluble in an aqueous phase. Branching of the tail group (at a constant total number of carbons) tends to have the opposite effect as having a longer chain length i.e. the Krafft

temperature of ionic surfactants will be decreased and the cloud point of nonionic surfactants will be decreased.

Surfactant Adsorption

Surfactants are utilized to achieve low interfacial tension and high solubilization.[2] Low interfacial tension is achieved because the surfactant molecules in aqueous solution tend to adsorb at the interface such as at the air-water interface with the hydrophilic head group remaining in the aqueous solution and the hydrophobic tail groups sticking out of the aqueous solution. These hydrophobic tail groups create an oil-like "film" at the air-water interface thereby lowering the surface tension of the solution. Adsorption at the air-water interface occurs due to a release of entropy into the system as there exists a cage-like structure of water molecules around the hydrophobic surfactant tail groups when the surfactant molecules are in solution. This cage-like structure is thereby released when the surfactant monomers adsorb at the air-water interface thereby returning these water molecules to the bulk solution.[3]

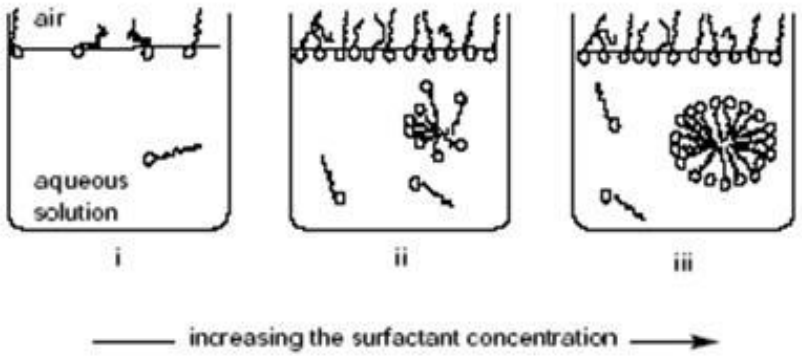

Figure 2: Graphic of surfactant existing as monomers in solution, adsorbing at the air-water interface, and micelle formation

Adsorption of surfactants on a solid interface results from more energetically favorable interactions between the surfactants and the chemical species in the interfacial region than between the surfactants in the bulk solution.[4] Adsorption of surfactants onto a surface interface from a bulk solution occurs primarily by way of electrostatic attraction, covalent bonding, hydrogen bonding, hydrophobic bonding, or lateral interaction between the adsorbed species.[4] [5] [6] Surfactant orientation at the solid interface will determine how the surface will be altered i.e. the surface may become positively or negatively charged or more oil-wet or water-wet.[7] [8] [9] [10] [11] Surfactant orientation at the solid interface is determined primarily by the chemical nature of the surfactant molecule itself, surface properties of the rock and temperature. Solvent identity and solvent conditions (especially if water is the solvent) also play a role.[11]

Surfactant adsorption typically occurs in four regions on a mineral surface from water. In region I the surfactant molecules adsorb mainly via electrostatic attractions between the surfactant head group and charged sites on the mineral surface.[5] [11] [12] [13] Adsorption in this region obeys Henry's Law and only unassociated first layer molecules are present.[12] [13] Region II is marked by an increase in surfactant adsorption due to lateral interaction between the hydrophobic chains of the adsorbed surfactants.[5] [11] The adsorbed surfactants begin to form aggregates on the surface and hemimicelles are present.[5] [14] [12] [13] In region III adsorption begins to slow in relation to concentration.[5] [11] Finally in region IV surfactant adsorption reaches a plateau at concentrations above the CMC.[5] [11] The surface is largely covered with hemicmicelles with sizeable second layer adsorption.[12] [13] The plateau of surfactant

adsorption does not necessarily mean that all active sites are filled as it is with gas adsorption.[12] [13] Above the critical micelle concentration, monomer concentration remains constant regardless of total surfactant concentration, and micelles do not adsorb significantly.[12] Steric hindrance between the surfactant monomers on the surface may also prohibit additional adsorption. Qualitatively this picture is found for adsorption from oils as well.

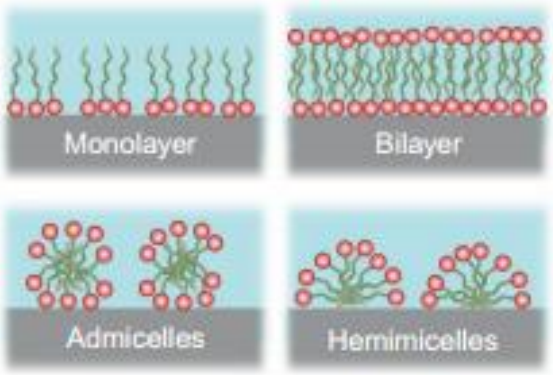

Figure 3: Adsorption schematic of surfactant adsorbing at the solid-liquid interface

Surfactant Solubilization

Surfactant monomers, when above a certain concentration, will no longer continue to adsorb at the interface but will self-assemble into structures known as micelles (or reverse micelle in oil). The concentration at which this phenomena occurs is known as the critical micelle concentration (CMC) and is unique to each surfactant. These micelles allow for increased solubilization of two previously immiscible liquids such as oil and water, which is referred to as an emulsion. A normal micelle consists of an oil droplet surrounded by surfactant monomers with the hydrophobic tail groups oriented inward toward the oil drop and with the hydrophilic head groups oriented outward into the continuous aqueous phase. A reverse micelle consists of a water droplet surrounded

by surfactant monomers with the hydrophilic head groups oriented inward toward the water drop and with the hydrophobic tail groups oriented outward into the continuous organic phase. Not only can surfactants form these spherical micelles, but also they can form more complex shapes such as rod-like micelles, hexagonal micelles, cubic phase micelles or lamellar micelles.

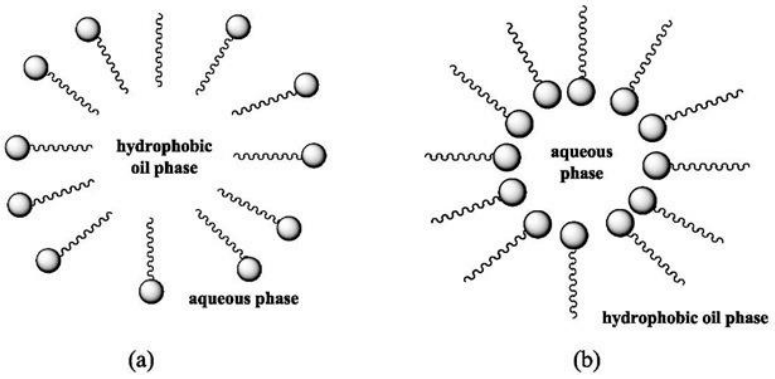

Figure 4: (a) schematic of a normal micelle and (b) schematic of reverse micelle

Modeling Surfactant Systems

Determining the formulation for solubilizing an oil in water with surfactant depends on the oil needed to be solubilized as well as restrictions for the temperature, electrolyte type and concentration, and the allowed surfactant concentration based on the application.[15] Even though describing the phase behavior of a given system of surfactant, oil, and water is of great importance, there exists limited means to accurately do so.[15] Such descriptors like the critical micelle concentration (CMC), hydrophilic-lipophilic balance (HLB), Krafft temperature, cloud point, and critical packing factor exist to help in the selection of surfactants for a given system.[15] The CMC of a surfactant can be used to predict the point at which micelles begin to form instead of surfactant monomers simply existing in solution. The Krafft temperature and cloud

point address the solubility of the surfactant, either ionic or nonionic respectively, in the aqueous media. The critical packing factor describes what type of micelles will form. The commonly used HLB value is used to predict solubilization; in general, the best (i.e. the most oil solubilized for the least amount of surfactant) solubilization occurs when the HLB of the surfactant equals the HLB of the oil to be solubilized. However, the HLB value has been found lacking for some classes of surfactant and more importantly fails to account for system variables such as surfactant concentration, temperature, salinity, and the presence of alcohols or other co-surfactants.[2] Phenomenological models exist that attempt to incorporate the natural curvature at the oil-water interface produced by the surfactant and the Helfrich free energy balance, but once again fail to address the system variables that also affect surfactant behavior.[15] Empirical correlations such as the Windsor R-ratio and the net average curvature (NAC) model are complex equations which require the determination of many parameters and as such are not practical to use.[2] [16] [17] The NAC model in particular measures the distance of the surfactant, oil, and water system from a point of net zero curvature at the interface where the same volume of oil and water is solubilized.[18] The NAC model accomplishes this by examining the free energy cost of such a change in curvature.[15] Salager et al. proposed the hydrophilic-lipophilic difference (HLD) equation to approximate the value of the NAC model by expressing the free energy change as a change in the chemical potential of the surfactant.[15] Similar to the Windsor R-ratio as well, the HLD value measures the departure of the system from the optimum point (i.e. net zero curvature) by means of easily quantifiable parameters of the system.[2]

The Hydrophilic-Lipophilic Difference

The hydrophilic-lipophilic difference or HLD equation is a semi-empirical equation used to calculate the chemical potential difference for the transfer of a surfactant from the oil phase into the aqueous phase as a function of formulation variables such as electrolyte concentration, surfactant type, oil, and temperature.[19] [20] [21] [17] In other word the HLD equation predicts at what point a system of oil, water, and surfactant will have the lowest interfacial tension and the greatest solubilization capacity. This point of optimal surfactancy for a given oil and water microemulsion occurs when the HLD value is 0.[21] When HLD is negative, the system forms oil in water microemulsions or Windsor type I; and when HLD is positive, the system forms water in oil microemulsions or Windsor type II.[22] The HLD equation for ionic surfactants is given below

$$HLD = \ln S - K\ (EACN) - f(A) + \sigma - a_T(\Delta T)$$

where S is the salinity in grams of NaCl per 100mL of water, K is an empirically determined constant, EACN is the equivalent alkane carbon number, f(A) is a function of the cosolvent present which is typically an alcohol, σ is the characteristic curvature which reflects the hydrophilic or lipophilic nature of the surfactant, α(T) is the temperature coefficient, and ΔT is the change in temperature from 25˚C.[2] Similarly there exists an HLD variant for non-ionic surfactants where the HLD value no longer varies logarithmically with salinity,

$$HLD = \mathrm{b} * S - K\ (EACN) - f(A) + \sigma - c_T(\Delta T)$$

where b is an empirically determined coefficient.[23] HLD can even be correlated with a net average curvature component that can predict the morphology of microemulsions.[18] [16]

The HLD can be manipulated a number of ways to determine particular parameters such as characteristic curvature for an unknown surfactant or equivalent alkane carbon number for an unknown oil if linear mixing is assumed.[15] [21]

Determining Characteristic Curvature

The characteristic curvature (Cc) of a surfactant as defined by Acosta et al. describes how the surfactant molecule will behave in a system with negative Cc values indicating a hydrophilic surfactant with a proclivity to forming normal micelles and with positive Cc values indicating a hydrophobic surfactant tending to form reverse micelles.[15] Salager's method for determining the σ parameter of an ionic surfactant involved measuring the interfacial tension of microemulsions containing 1g of NaCl per 100mL of water, thereby negating the natural logarithm of salinity term by having it equal zero, at different reference oils with known alkane carbon number values.[15] These values are then extrapolated to the alkane carbon number that would produce the lowest interfacial tension i.e. the HLD value is 0.[15] Acosta proposed another method for determining the characteristic curvature of the surfactant because of the difficulty in measuring interfacial tension, the error associated with the extrapolation process, and in some cases the insoluble phases produced by the surfactants when conducting this scan.[15] Acosta's method involves the use of a well-studied reference surfactant with well-defined HLD parameters and increasing concentrations of the test surfactant.[15] Increasing the concentration of the test surfactant will also change the salinity at which

Windsor type III microemulsions are formed thereby allowing the HLD parameters of the test surfactant to be calculated. This method assumes linear mixing of the two surfactant system, that all of the surfactant is present at the interface, and that the K coefficients that affect the alkane carbon number parameter of the system are equal for both surfactants.[15] Both methods are performed in an alcohol free system.[15]

Determining Equivalent Alkane Carbon Number

The equivalent alkane carbon number (EACN) is an essential parameter in the hydrophilic-lipophilic difference (HLD) model and describes the hydrophobicity of an oil. Because heavy petroleum oil consists of many different carbon species, it is helpful to determine the EACN of a heavy petroleum oil in order to adjust the emulsifier additive. Heavy petroleum oils consist of hydrocarbons with aromatic and acyclic rings with multiple varying side chains and heteroatomic species like oxygen, nitrogen, and/or sulfur which may also be included in ring structures, links between molecules, or as functional groups. Since EACN describes how hydrophobic a specific mixture of hydrocarbon species is, higher EACNs indicate a more hydrophobic system of hydrocarbons. Alkanes like hexane, octane, and decane have EACNs corresponding to the number of aliphatic carbons in the chain i.e. 6, 8, and 10. Species like benzene and toluene, which exist in aromatic rings, have EACNs of 0 and 1 respectively despite have 6 and 7 carbons each. EACN can be negative for species that contain Cl atoms. EACN is determined via a titration method which utilizes a surfactant with known HLD parameters and a reference oil with a known EACN.[24] Increasing amounts of the heavy crude oil with an unknown EACN value are mixed with the reference oil and the change in optimal salinity in forming a Windsor type III microemulsion is determined.

By manipulation of the HLD equation, similar to the method of determining characteristic curvature, a linear relationship can be seen between salinity and EACN.[24] Increasing the electrolyte concentration will cause the ionic surfactant molecules to become more hydrophobic thereby causing the surfactant to distribute more towards the oil-water interface eventually reaching an optimum point of lowest interfacial tension, where equal parts of oil and water are solubilized in the middle phase of a Windsor type III microemulsion.[24]

Enhanced Oil Recovery

Enhanced oil recovery (EOR) is an important process for the production of crude oil. Despite being a limited resource, the demand for crude oil worldwide has increased requiring crude oil to be produced by means other than the conventional techniques. Recently enhanced oil recovery methods have attracted attention and increased research due to the diminishing effectiveness of the conventional methods for the production of oil.[25] Crude oil from a reservoir is acquired generally by depletion first and then using water flooding techniques. Most reservoir fields are currently under water flooding conditions leaving some residual oil trapped in the crevices of the rock.[26] Many mature fields, despite have between 50 and 75% of their crude oil left in the reservoir, have decreasing production even under water flooding.[11] [8] Chemical recovery processes for EOR attempt to alter the wettability of the reservoir rocks, reduce the interfacial tension in the reservoir, and control the mobility so that the residual oil may flow more easily out of previously inaccessible areas by injecting alkali, surfactants, and/or polymers.[26] [27] [25] The low interfacial tension conditions and altered wettability of the reservoir rocks are achieved by surfactant or

polymer flooding.[26] The lowered interfacial tension allows the oil droplets to flow more easily through pores they previously would not have been able to flow through due to capillary trapping.[26] The surfactants allow the oil to be solubilized more easily in the water as well increasing crude oil production from the wells.[26] The reservoir rocks are also affected by adsorption of the surfactant or polymer onto them making them more water wet which also allows oil recovery to be increased.[26]

Many factors may affect the efficiency of the surfactant flooding process but most critically are the surfactant chemistry and its concentration, electrolyte concentration, composition of the crude oil, and reservoir conditions such as temperature and pressure.[11] [26] Oil viscosity and formation permeability also have an effect on the efficiency but are less important.[26] Surfactant flooding, while considered by some to be the most promising EOR technique, can be rendered uneconomical due to surfactant loss by adsorption onto the porous media of the reservoir and precipitation.[11] [28] [27] [25] [12] Surfactant molecules can adsorb significantly even at low concentrations.[11] This adsorbed surfactant layer on the porous media adds an additional resistance to the flow as well as contributing to surfactant loss.[27] One way to inhibit such adsorption of the surfactant onto the porous media is to introduce chemical species, known as sacrificial agents, which compete with the surfactants for the adsorption sites on the reservoir rocks.

Anionic surfactants have high adsorption in carbonite formations and cationic surfactants are not only expensive but also exhibit high adsorption on calcite formations.[26] [9] Cationic surfactants are able to alter the wettability of these calcite

formations by forming ion pairs with the acidic components of the crude oil which have adsorbed onto the calcite formation surface.

Hydrophilic-Lipophilic Difference Modification

When the HLD equation is at the optimal point of 0, it suggests that in effect there is maximum surfactant coverage at the oil/water interface where interfacial tension is minimized. For enhanced oil recovery, maximum surface coverage of the surfactant on the minerals is desired in order change the wettability of the rock to allow oil to flow more easily. Therefore, it is proposed that the HLD equation be modified in order to predict surface coverage. This will be achieved by replacing the salinity term with the zeta potential of the rock, a characteristic unique to each mineral. Like the salinity term, zeta potential accounts for the charge present in the system. Zeta potential is a measure of the difference in potential between the bulk fluid, in this case DI water, and the fluid layer surrounding the fine particle. The modified HLD adsorption equation is given below

$$HLD_{adsorption} = b' * ZP - K' * (EACN) - f(A) + J * \sigma - a'_T(\Delta T)$$

with a maximum now at 1 i.e. an HLD adsorption value of 1 indicates the highest surface coverage has been achieved. A coefficient J is introduced so that ($b' * ZP$), ($K' * (EACN)$), and ($J * \sigma$) are all effectively the same order of magnitude. Since there is no alcohol present in the system and the experiments will be performed at 25°C, the modified HLD adsorption equation reduces to

$$HLD_{adsorption} = b' * ZP - K' * (EACN) + J * \sigma$$

The modified HLD adsorption equation indicates that surface coverage of the surfactant at the interface of the hydrophilic rock and the hydrophobic liquid is affected by surface

charge of the mineral, oil characteristics, and the hydrophobic or hydrophilic nature of the surfactant. Therefore, it is necessary to develop a data set of adsorption values for many combinations of minerals, alkanes, and surfactants and fit the corresponding parameters to the modified HLD adsorption equation.

Chapter III. Experimental

In order to develop the necessary data set that is to be fitted to the modified HLD adsorption equation and used to determine the equation coefficients the various parameters must be measured; specifically zeta potentials for each individual mineral type, equivalent alkane carbon numbers for the heavy petroleum oils originating from many different refineries, characteristic curvatures for the surfactant along with the various fatty acid additives that can be used along with it, and adsorption isotherms for the many combinations of heavy petroleum oils, surfactant, and minerals. These data points will be fitted to the modified HLD adsorption equation. In addition to these parameters, the critical micelle concentrations of the surfactant and the fatty acid additives are determined to explore the effects that these additives have on the behavior of the surfactant as well as to calculate the effective area per head-group for each surfactant system.

Materials

Surfactants are supplied by Ingevity and are designated as Surfactant 1 and Surfactant 2, the same company supplied Additives 5 and 6. Toluene, octane, decane, hexadecane, heptadecane, and icosane were used to simulate the heavy petroleum oils for use in determining the adsorption isotherms. Sodium dihexyl sulfosuccinate and benzethonium chloride from Sigma Aldrich were used as the reference surfactants for determining the characteristic curvatures of Surfactant 1 and the various concentrations of Additive 5 and Additive 6 fatty acid additives, and the sodium dihexyl sulfosuccinate was also used in determining the EACNs of the heavy crude oils. Six minerals were provided by Ingevity on which to conduct the adsorption studies. Sodium chloride from

Sigma Aldrich was used for the salinity scans for determination of the characteristic curvatures and EACNs

Zeta Potential

Electrophoretic mobility of the mineral fines was measured using a Zeta Meter 3.0 from Zeta-Meter Inc. by suspending a sample of the mineral fines in DI water and observing particle movement via microscope as a voltage is applied to either end of the zeta meter cell. Three different voltages are applied to the cell containing the mineral fine, 40V, 50V, and 75V. Five electrophoretic mobility measurements are taken at each voltage for a total of fifteen measurements. Then using the Smoluchowski equation, the zeta potentials of the mineral fines are calculated along with standard deviations

$$ZP = 113000\ \mu_t/D_t \text{ x } EM$$

where EM is the electrophoretic mobility, μ_t is the viscosity of the suspending liquid in poises, D_t is the dielectric constant of the suspending liquid, and ZP is the zeta potential in millivolts.

Equvalent Alkane Carbon Number Salinity Scans

EACN of an unknown heavy petroleum oil is determined by using a reference oil and a well characterized surfactant. The reference oil used in the EACN determinations is toluene, which has an EACN of 1, and the surfactant used is sodium dihexyl sulfosuccinate (AMA), which is an anionic surfactant with well described HLD parameters. If it is assumed that there is no alcohol present in the system, that all measurements are done at 25°C, and that the optimum HLD occurs at 0, then the HLD equation reduces to

$$\ln S^* = K\,(EACN) - Cc$$

Since the parameters K and Cc are well defined for AMA, the EACN of an unknown heavy petroleum oil can be determined as there exists a linear relationship between the natural logarithm of optimal salinity and EACN. An indirect titration method is utilized for EACN determination where the heavy petroleum oil with unknown EACN is mixed with toluene at varying weight percentages from 1 wt% to 9 wt%.

A salinity scan is performed on the different weight percentages of heavy petroleum oil in toluene: different amounts of sodium chloride are added to the microemulsions in order to locate the optimal salinity of the heavy petroleum oil (HPO) mixture and observe by how much the optimal salinity shifts from a microemulsion using pure toluene. The optimal salinity is the point at which a Windsor Type III microemulsion exists with equal parts oil and water solubilized in the middle phase indicating the lowest interfacial tension i.e. HLD is 0. Assuming linear mixing of the hydrocarbons, the HLD equation for the mixture reduces to

$$HLD_{mix} = x_{Toluene}[\ln(S^*_{mix}) - K * EACN_{Toluene} + Cc] + x_{HPO}[\ln(S^*_{mix}) - K * EACN_{HPO} + Cc]$$

$$0 = \ln(S^*_{mix}) + Cc - K(x_{Toluene}EACN_{Toluene} + x_{HPO}EACN_{HPO})$$

$$HLD_{Toluene} = \ln(S^*) - K * EACN_{Toluene} + Cc$$

$$0 = \ln(S^*_{mix}) - \ln(S^*) - K\big((1 - x_2)EACN_{Toluene} + x_{HPO}EACN_{HPO}\big) + K * EACN_{Toluene}$$

Once the optimal salinities are measured, the natural logarithm of the optimal salinity of the AMA and toluene system divided by the optimal salinity of the mixture is then graphed against the mass fraction of the heavy petroleum oil dissolved in toluene. This is done for each weight percent of heavy petroleum oil in toluene, and the slope of the

resulting line subtracted from the reference oil EACN is the EACN of the unknown heavy petroleum oil.

$$\frac{\ln\left(\frac{S^*}{S^*_{mix}}\right)}{K} = x_2(EACN_{Toluene} - EACN_{HPO})$$

Where S* is the optimal salinity for a microemulsion of AMA, toluene, and water and S^*_{mix} is the optimal salinity for the mixture of toluene and unknown heavy petroleum oil, AMA, and water. The salinity scans were performed in 16mL round bottomed glass test tubes with 5mL of aqueous phase and 5mL of oil phase. See Appendix A for a full procedure and example.

Characteristic Curvature Salinity Scans

Cc is determined by performing a scan of the optimal salinities of differing mole fractions of surfactants; a reference surfactant, in this case AMA (sodium dihexyl sulfosuccinate), with a known Cc and the target surfactant with an unknown Cc denoted as TS. The optimal salinity of the system will change depending on the relative mole fractions of each surfactant in the microemulsion. In order to determine the Cc of the target surfactant, it will be assumed no alcohol and 25°C so the HLD equation reduces to;

$$HLD = \ln(S) - K * EACN + Cc$$

Assuming linear mixing occurs between the two surfactants;

$$HLD_{mix} = x_{AMA}HLD_{AMA} + x_{TS}HLD_{TS}$$

$$HLD_{mix} = x_{AMA}[\ln(S_{mix}) - K_{AMA} * EACN + Cc_{AMA}] + x_{TS}[\ln(S) - K_{TS} * EACN + Cc_{TS}]$$

Assume the K constants are equal and the optimum point occurs at $HLD_{mix} = 0$;

$$0 = (x_{AMA} + x_{TS})\ln(S_{mix}) - K * EACN(x_{AMA} + x_{TS}) + x_{AMA}Cc_{AMA} + x_{TS}Cc_{TS}$$

$$x_{AMA} + x_{TS} = 1$$

$$0 = \ln(S_{mix}) - K * EACN + x_{AMA}Cc_{AMA} + x_{TS}Cc_{TS}$$

Subtracting the optimum HLD for AMA (i.e. $0 = \ln(S_{AMA}) - K * EACN + Cc_{AMA}$) gives;

$$\ln \frac{S_{mix}}{S_{AMA}} = x_{XD70} * (Cc_{AMA} - Cc_{TS})$$ for ionic surfactants

The natural logarithm of the optimal salinity of the mixture divided by the optimal salinity of the reference surfactant will then be graphed against the mole fraction of the target surfactant. The linear slope of the data points is equal to the Cc of the target surfactant subtracted from the Cc of the reference surfactant.

Characteristic curvatures were determined for Surfactant 1, Surfactant 1 and three differing weight percentages of the fatty acid Additive 5, Surfactant 1 and three differing weight percentages of the fatty acid Additive 6, and Surfactant 2. The salinity scans were performed in 16mL round bottomed glass test tubes with 5mL of aqueous phase and 5mL of oil phase. See Appendix B for a full procedure and example.

Critical Micelle Concentration

Also, while not a parameter in the modified HLD adsorption equation, the CMCs and surfactant head group areas are measured to learn more about the effects of the fatty acid additives and for potential use in the modified equation. The area per surfactant head group is determined by taking the inverse of the surface excess energy multiplied by the inverse of Avogadro's number (N_A). The surface excess energy is determined by the Gibbs adsorption formulas where the differential term is found by taking the slope of the linear portion of graphs of surface tension with respect to the log scale of surfactant concentration just below the CMC.[29]

$$Area = \frac{1}{\Gamma_{2,1} N_A}$$

$$\Gamma_{2,1} = \frac{1}{RT}\frac{d\pi}{d(lnC)} = -\frac{1}{2.303 * 2 * RT}\frac{d\gamma}{d(logC)} \; ionic$$

The CMC occurs where the linear decrease in surface tension with respect to the log scale of surfactant concentration changes to a constant surface tension with respect to the log scale of concentration. For reference, the surface tension of deionized water is 72.4 dynes/cm. See Appendix C for a full procedure and example.

Adsorption Studies

Adsorption of the Surfactant 1 surfactant and the various additives onto the six different mineral surfaces in representative EACNs was measured using the Agilent 1100 HPLC. Samples were prepared by filling vials with the mineral and adding various concentrations of surfactant dissolved in a mixture of toluene and some alkane ranging from 0.2 wt% to 1.0 wt%. After vigorous shaking and allowing enough time for adsorption to reach equilibrium, the vials were centrifuged and an aliquot of the supernatant was removed in order to be analyzed by the HPLC in order to determine surfactant concentration change in the bulk solution. Isocratic flow of 82 vol% methanol and 18 vol% water with an ultraviolet detector set at 235nm wavelength was the method used to elute and detect the surfactant. While this method was successful for detecting surfactant in EACNs of 7.1, 9.0, and 9.7, it showed limited success for the higher EACNs. In an effort to delay the elution of the surfactant for the higher EACNs and achieve better separation, the methanol volume was reduced to 79 vol% and then 65 vol%, but these methods have shown little improvement. Once an adsorption isotherm is made for a particular pairing of mineral, surfactant, and EACN, the plateau is identified and a maximum adsorption is determined. Maximum adsorptions are found

for every different combination of the seven surfactants, three EACNs, and six rock minerals.

Chapter IV. Result and Conclusions

Zeta Potentials of Minerals

The movement of the mineral fines was tracked using the Zeta Meter 3.0 which calculated the electrophoretic mobility. These electrophoretic mobilities were then used to calculate the zeta potentials based on the dielectric constant of deionized water in which the mineral fines were suspended and the voltage applied to the electric cell. Part of the apparatus can be seen below in Figure 5 which was used to track the mineral fines as they moved across the electric cell.

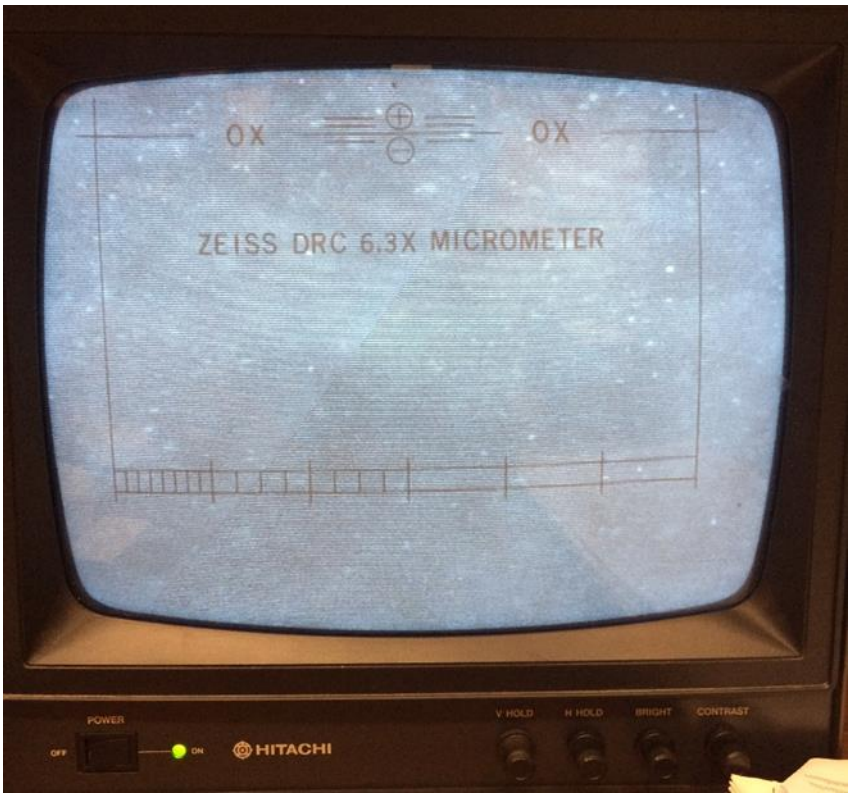

Figure 5: Image through the Zeta Meter 3.0 microscope looking at the electric cell

The zeta potentials of the mineral fines that are used in the model fitting for the modified HLD adsorption equation are summarized below in Table 1. As will be discussed in a later section the washed screened granite (Granite WS) shows a low zeta

potential as compared to the other granites closer to that of the limestones. It seems that the washed screening process cleans the mineral of the more negative zeta potential components such as clays which in turn causes the zeta potential of the mineral to become less negative.[30] The zeta potential measurements were performed at natural pH in deionized water.

Table 1: Zeta potentials of mineral fines

Mineral	Zeta potential in DI water (mw)
Granite RS	-41
Granite WS	-23
Granite	-41
Ft. Payne Limestone	-20
Warsaw	-16
Limestone A	-20

Equivalent Alkane Carbon Numbers of Heavy Petroleum Oils

EACNs were determined for a number of heavy petroleum oils. A sample scan of sodium dihexyl sulfosuccinate (AMA), toluene, sodium chloride, and deionized water is provided below in Figure 6. As reported in the literature, the optimal salinity of AMA in a toluene-water system can be seen at 3.2 g NaCl/100 mL H_2O. This value will be used in the determination of the EACNs of the heavy petroleum oils based on the amount by which the optimal salinity shifts when the heavy petroleum oils are dissolved in the toluene.

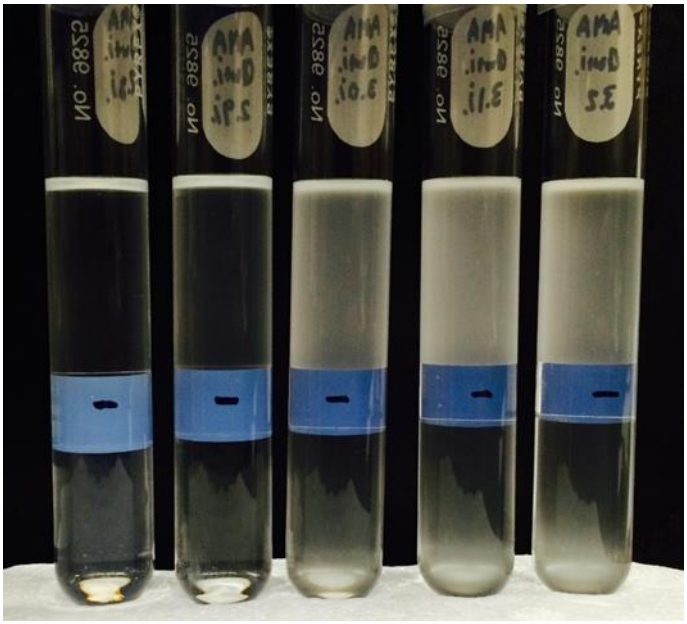

Figure 6: Sample Scan for 0.1M AMA, toluene for salinities 2.8, 2.9, 3.0, 3.1, 3.2 g NaCl/100mL H2O

The determination of four heavy petroleum oils are shown below in Figures 7, 9, 11, and 13 with accompanying sample scans to demonstrate the range of EACNs demonstrated by the heavy petroleum oils.

Figure 7 shows that the linear slope of the salinity scan of a heavy petroleum oil from Refinery 13 was determined to be -16.5. Since toluene has an EACN of 1, it was determined that the EACN of the heavy petroleum oil from Refinery 13 is 17.5 = (1+16.5). A sample salinity scan for the heavy petroleum oil from Refinery 13 is shown in Figure 8. This value is relatively high, indicating that this material is hydrophobic.

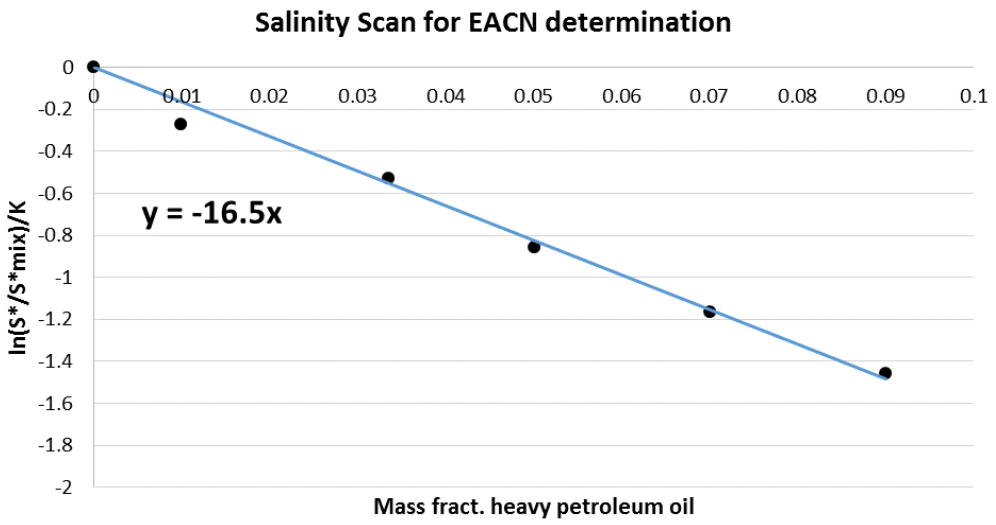

Figure 7: Optimal Salinity vs. Weight Fraction AMA, toluene, and the Refinery 13 heavy petroleum oil

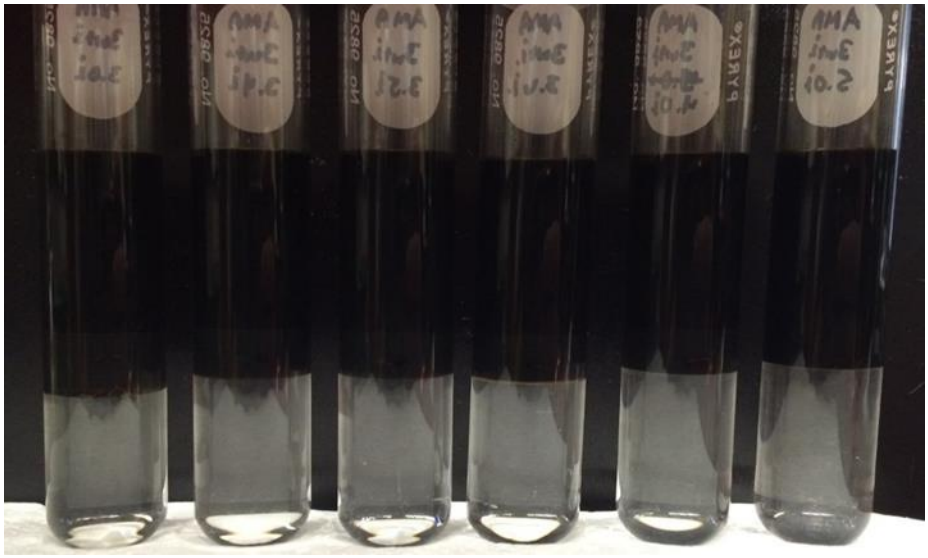

Figure 8: Sample Scan for 0.1M AMA, toluene, and 3 wt% Refinery 13 heavy petroleum oil for salinities 3.0, 3.4, 3.5, 3.6, 4.0, and 5.0 g NaCl/100mL H2O

Figure 9 shows that the linear slope of the salinity scan of Oil #15169 was determined to be -20.5. Since toluene has an EACN of 1, it was determined that the EACN of the Oil #15169 is 21.5 = (1+20.5). A sample salinity scan for Oil #15169 is shown in

Figure 10. This value is extremely high, indicating that this material is extremely hydrophobic.

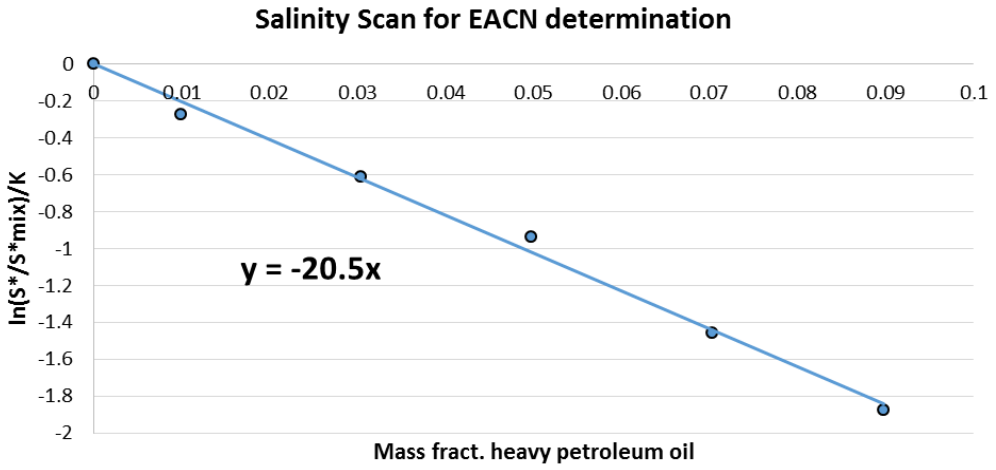

Figure 9: Optimal Salinity vs. Weight Fraction AMA, toluene, and Oil #15169

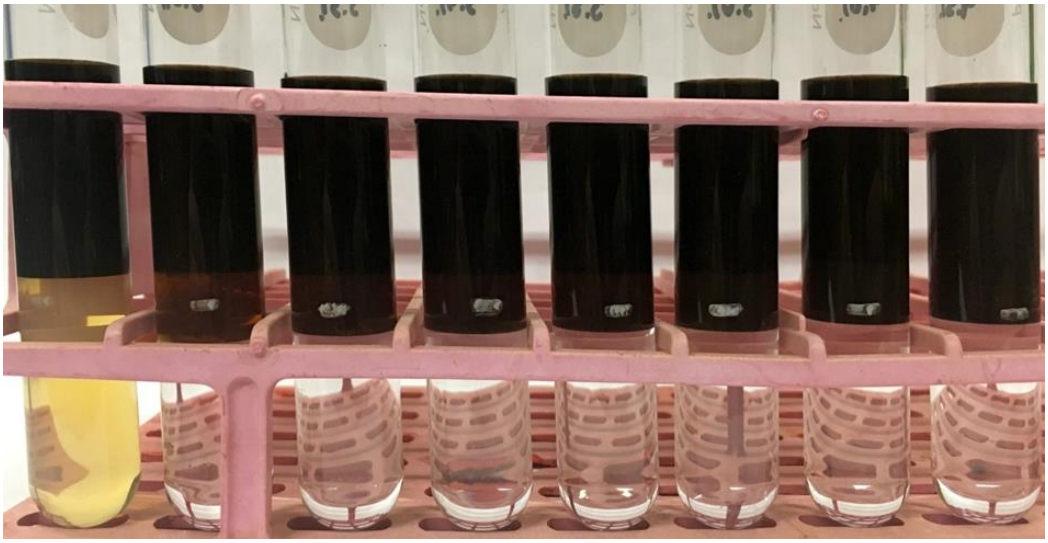

Figure 10: Sample Scan for 0.1M AMA, toluene, and 1 wt% Oil #15169 for salinities 2.5, 3.0, 3.3, 3.4, 3.5, 3.6, 3.7, 4.0, and 4.5 g NaCl/100mL H2O

Figure 11 shows that the linear slope of the salinity scan of a heavy petroleum oil from Refinery 4 was determined to be -12.5. Since toluene has an EACN of 1, it was determined that the EACN of the heavy petroleum oil from Refinery 4 is 13.5 =

(1+12.5). A sample salinity scan for the heavy petroleum oil from Refinery 4 is shown in Figure 12. This value is relatively high, indicating that this material is comparable in hydrophobicity to tetradecane.

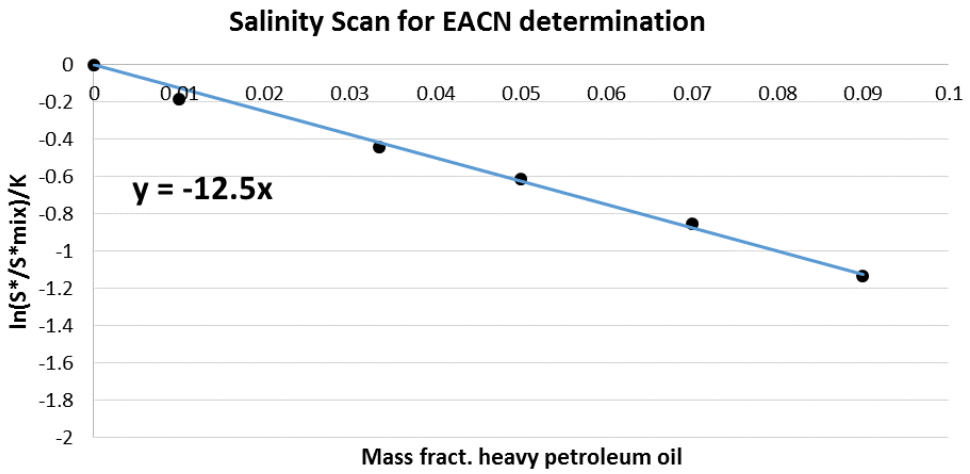

Figure 11: Optimal Salinity vs. Weight Fraction AMA, toluene, and Refinery 4 heavy petroleum oil



Figure 12: Sample Scan for 0.1M AMA, toluene, and 1 wt% Refinery 4 heavy petroleum oil for salinities 2.5, 3.0, 3.3, 3.4, 3.5, 3.6, 3.7, 3.8, and 4.0 g NaCl/100mL H2O

Figure 13 shows that the linear slope of the salinity scan of a heavy petroleum oil from Refinery 12 was determined to be -8.7. Since toluene has an EACN of 1, it was determined that the EACN of the heavy petroleum oil from Refinery 12 is 9.7 = (1+8.7). A sample salinity scan for the heavy petroleum oil from Refinery 12 is shown in Figure 14. This value is comparable in hydrophobicity of decane.

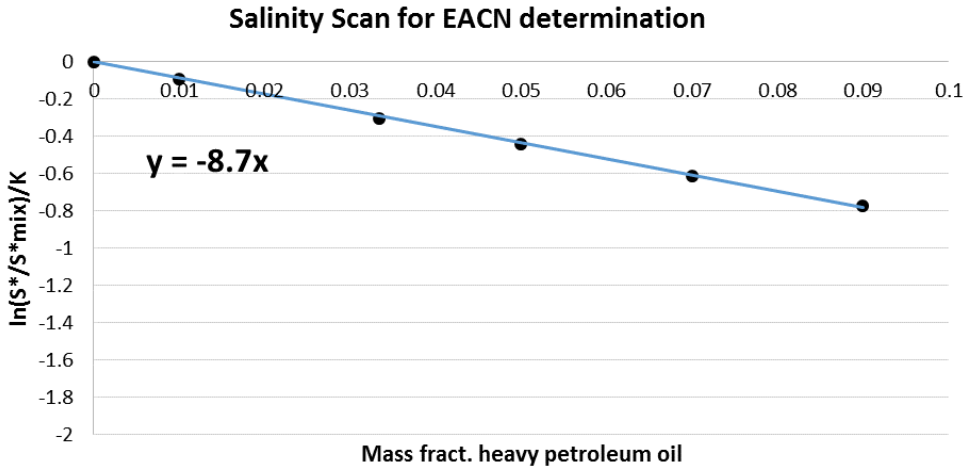

Figure 13: Optimal Salinity vs. Weight Fraction AMA, toluene, and Refinery 12 heavy petroleum oil

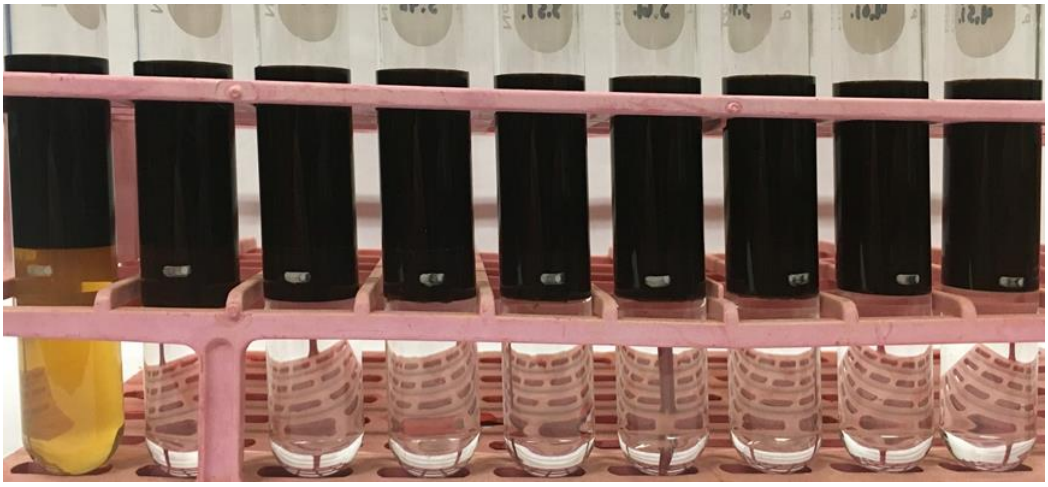

Figure 14: Sample Scan for 0.1M AMA, toluene, and 1 wt% Refinery 12 heavy petroleum oil for salinities 2.5, 3.0, 3.3, 3.4, 3.5, 3.6, 3.7, 3.8, and 3.9 g NaCl/100mL H2O

Below in Table 2 is the complete list of the EACNs for all of the heavy petroleum oils provided. The range of EACNs for these crude oils is very large, between 7.1 and 21.5. Since these crude oils come from many different wells from across the country, a range of EACNs was to be expected, but such a wide range indicates very different compositions in these wells which must be accounted for.

Table 2: Equivalent Alkane Number Summary

Heavy Petroleum Oil	EACN
Refinery 1	17.4
Refinery 2	11.8
Refinery 3	13.5
Refinery 4	13.5
Refinery 5	19.0
Refinery 6	18.0
Refinery 7	20.7
Refinery 8	9.7
Refinery 9	11.8
Refinery 10	10.8
Refinery 11	7.1
Refinery 12	9.7
Refinery 13	17.5
Oil #15169	21.5
Oil #15369	20.7

The alkanes were used to mimic the heavy petroleum oils since the crude oils themselves could not be put through the HPLC when adsorption is being measured because they would foul the column. A mixture of straight chain alkanes and toluene were used in the preparation for these artificial EACNs. The toluene serves to allow the EACN number to be tailored to a specific value and to solubilize the surfactant. The EACNs chosen to represent the range of EACNs measured from the crude oils are 7.1, 9.0, 9.7, 13.1, 16.1, and 18.7. These EACNs are prepared by mixing toluene and

alkanes together at specific weight percentages to make the desired EACN and these mixtures are specified in Table 3.

Table 3: Toluene and Alkane mixtures

EACN	Alkane	Vol. of toluene (mL)	Vol. of alkanes (mL)
7.1	octane	1	8.36
9	decane	1	9.5
9.7	undecane	1	7.84
13.1	hexadecane	1	4.7
16.1	heptadecane	1	18.89
18.7	icosane	1	15.33

Characteristic Curvatures of Surfactants

The addition of the fatty acid additives, Additive 5 and Additive 6, changes the characteristic curvature of the surfactant system to being less negative. The characteristic curvatures of Surfactant 1, Surfactant 1 with 1, 3, and 5 wt% Additive 5, and Surfactant 1 with 3, 5, and 10 wt% Additive 6 were determined via the Acosta method of salinity scans.

A sample salinity scan for Surfactant 1 and 5 wt% Additive 5 is displayed below in Figure 15 and the characteristic curvature determination is shown in Figure 16 which shows the linear slope is 0.75. Since AMA has a characteristic curvature of -0.93, the characteristic curvature of Surfactant 1 with 5 wt% Additive 5 is -1.68 = -(0.75+0.93).

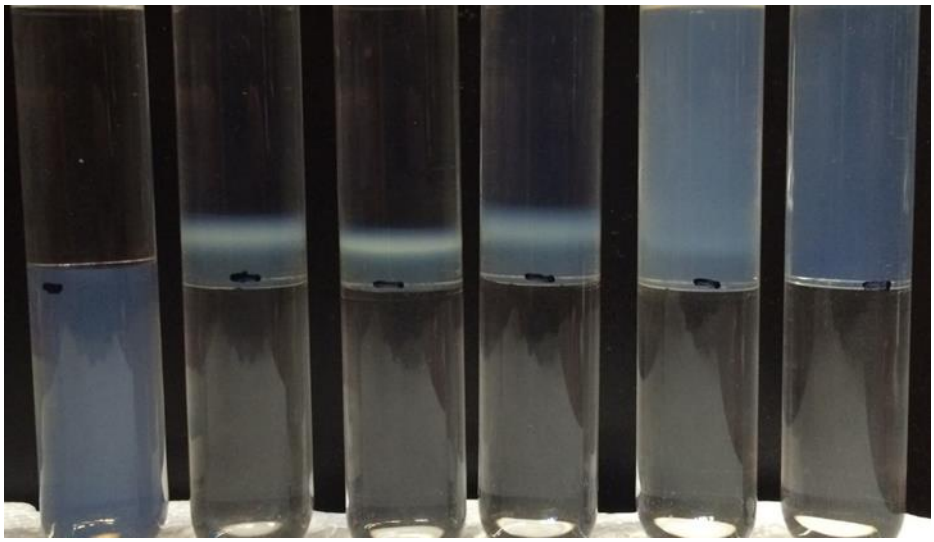

Figure 15: Sample salinity scan for 0.0474M AMA, 0.003M Surfactant 1 with 5 wt% Additive 5, and toluene for salinities 3.0, 3.6, 3.8, 4.0, 4.2, and 4.4 g NaCl/100 mL H2O

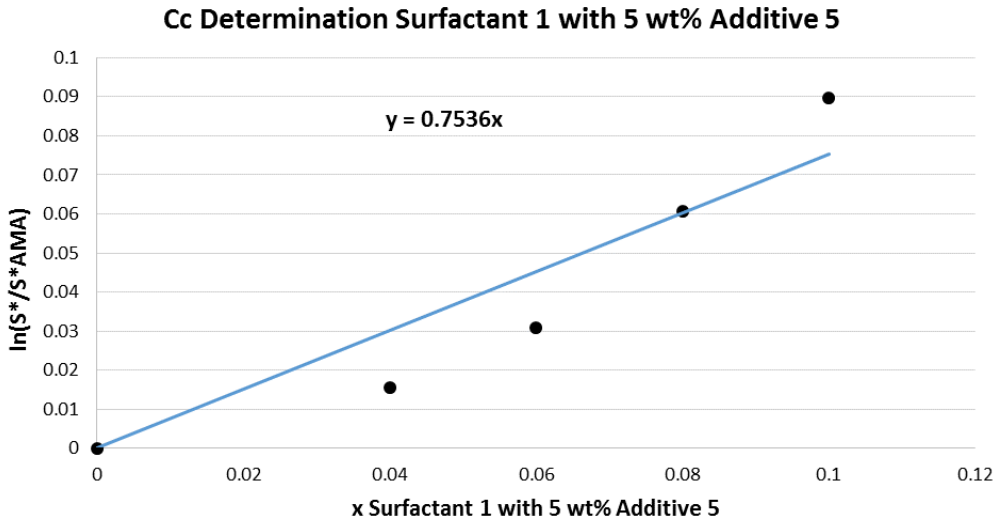

Figure 16: Characteristic curvature determination graph for Surfactant 1 with 5wt% Additive 5

A sample salinity scan for Surfactant 1 and 10 wt% Additive 6 is displayed below in Figure 17 and the characteristic curvature determination is shown in Figure 18 which

shows the linear slope is 1.10. Since AMA has a characteristic curvature of -0.93, the characteristic curvature of Surfactant 1 with 10 wt% Additive 6 is -2.03 = -(1.10+0.93).

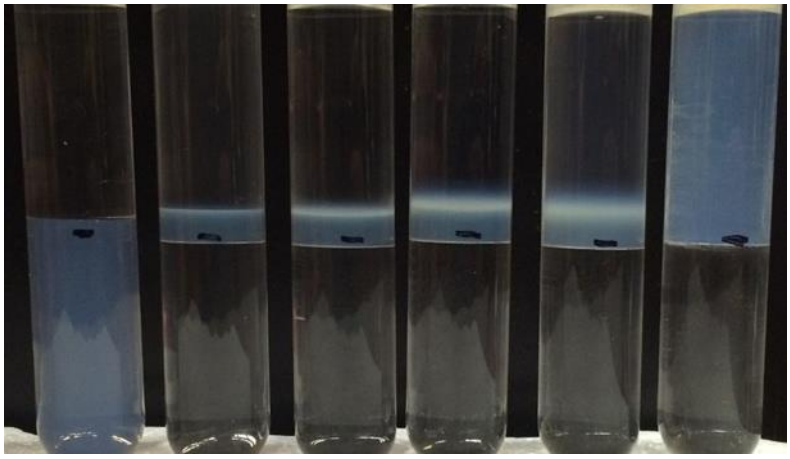

Figure 17: Sample salinity scan for 0.0474M AMA, 0.003M Surfactant 1 with 10 wt% Additive 6, and toluene for salinities 3.0, 3.3, 3.5, 3.7, 3.9, and 4.1 g NaCl/100 mL H2O

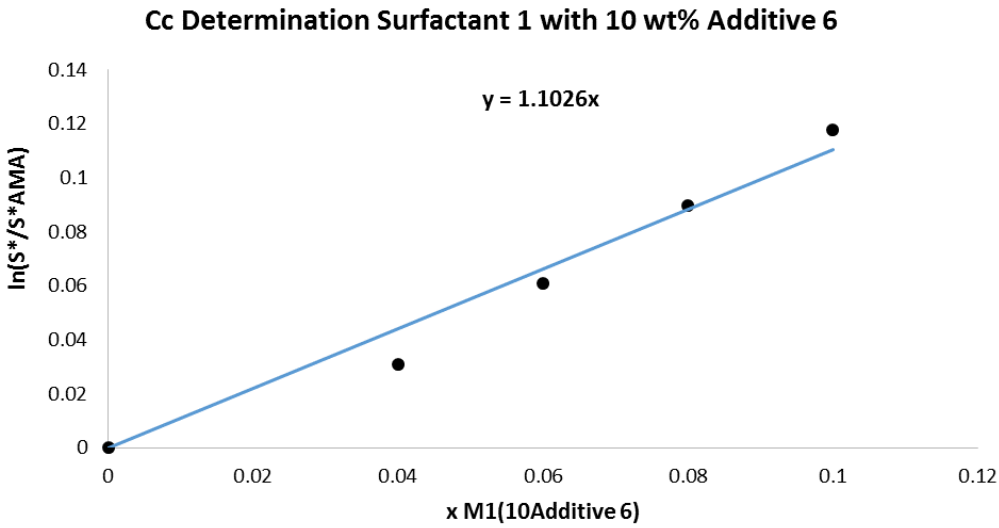

Figure 18: Characteristic curvature determination graph for Surfactant 1 with 10 wt% Additive 6

Below is a summary table of the characteristic curvatures of Surfactant 1 with the differing weight percentages of the fatty acid additives.

Table 4: Summary of the characteristic curvatures for Surfactant 1 and additives

Surfactant	Cc
Surfactant 1	-3.07
Surfactant 1 with 1 wt% Additive 5	-2.79
Surfactant 1 with 3 wt% Additive 5	-2.24
Surfactant 1 with 5 wt% Additive 5	-1.68
Surfactant 1 with 3 wt% Additive 6	-2.76
Surfactant 1 with 5 wt% Additive 6	-2.55
Surfactant 1 with 10 wt% Additive 6	-2.03
Surfactant 2	-2.61
AMA	-0.93

Since AMA is an anionic surfactant and Surfactant 1 is a cationic surfactant, there could be a large systematic error associated with these characteristic curvature values due to nonlinear mixing. Attempts were made to use benzethonium chloride as a reference surfactant, however, it was discovered that the salinity range at which benzethonium chloride forms a Windsor type III microemulsion in a toluene-water system is too large to provide an accurate optimal salinity as seen in Figure 19. Attempts were also made for benzethonium chloride in a hexane-water system and a decane-water system, however, a gel formed in the hexane-water system and a precipitate formed in the decane-water system as seen in Figures 20 and 21.

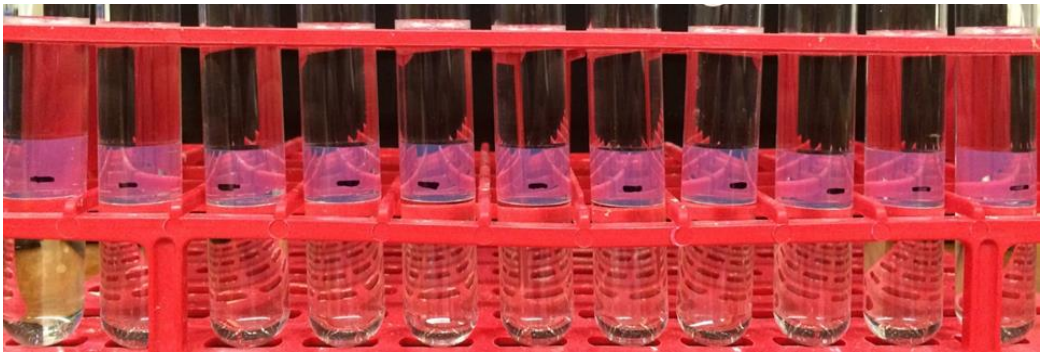

Figure 19: Sample salinity scan for 0.054M BCl and toluene for salinities 4.0, 4.6, 4.7, 4.8, 4.9, 5.0, 5.1, 5.2, 5.3, 5.4, and 6.0 g NaCl/100 mL H2O

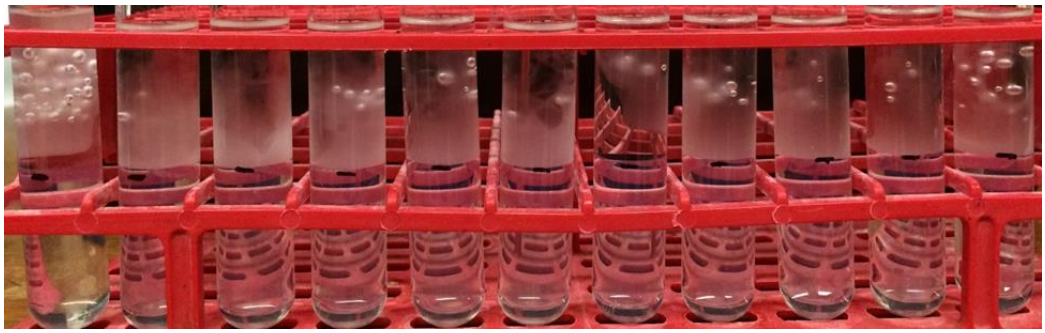

Figure 20: Sample salinity scan for 0.01M BCl and hexane for salinities 10.5, 11.3, 11.4, 11.5, 11.6, 11.7, 11.8, 11.9, 12.0, 12.1, and 13.0 g NaCl/100 mL H2O

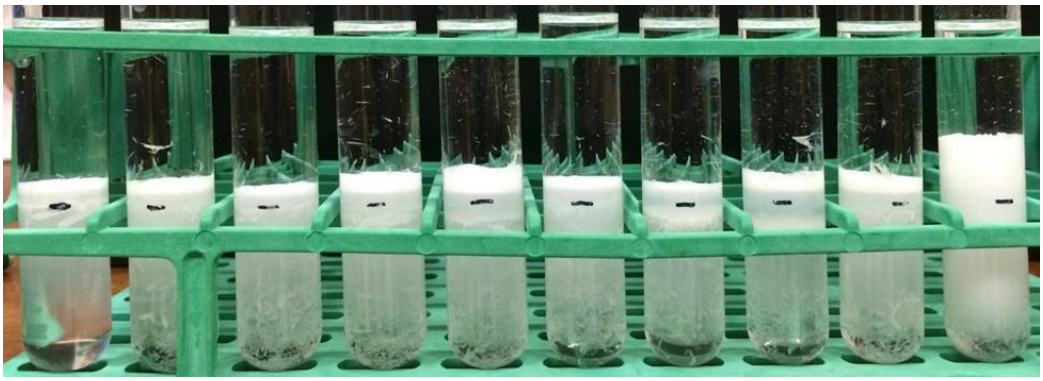

Figure 21: Sample salinity scan for 0.01M BCl and decane for salinities 21.5, 22.7, 22.8, 22.9, 23.0, 23.1, 23.2, 23.3, 23.4, and 23.5 g NaCl/100 mL H2O

Critical Micelle Concentrations of Surfactants

Below are the individual surface tension vs. concentration determination for each surfactant and various concentrations of additives. For reference, the surface tension of deionized water is 72.4 dynes/cm.

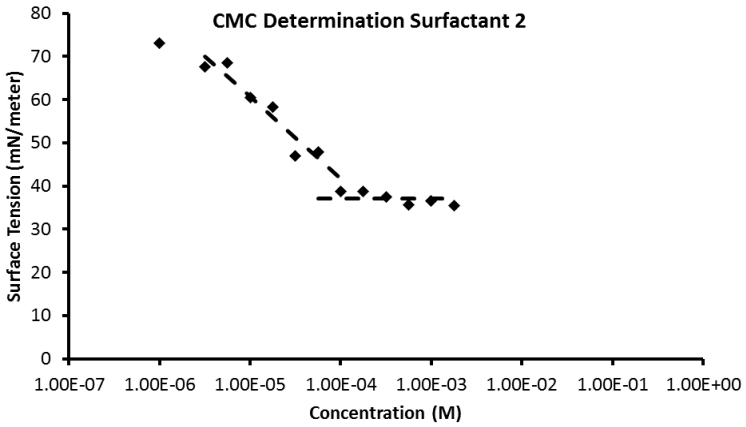

Figure 22: Surface Tension vs. Concentration for Surfactant 2

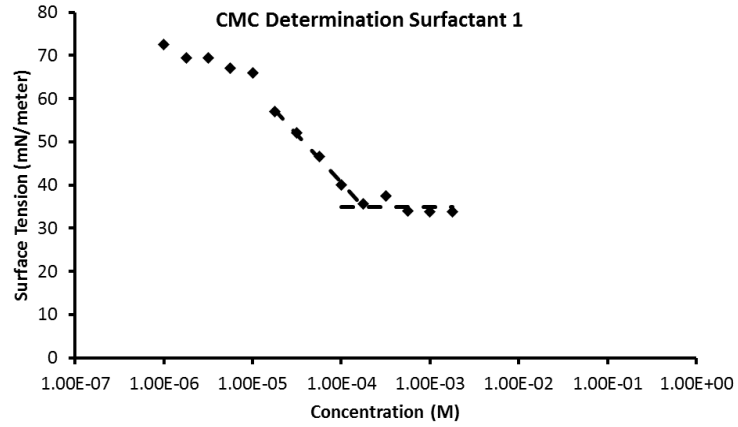

Figure 23: Surface Tension vs. Concentration for Surfactant 1

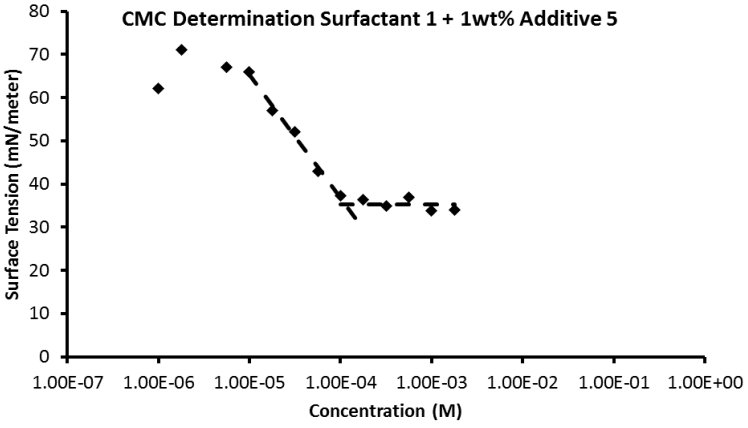

Figure 24: Surface Tension vs. Concentration for Surfactant 1 + 1wt% Additive 5

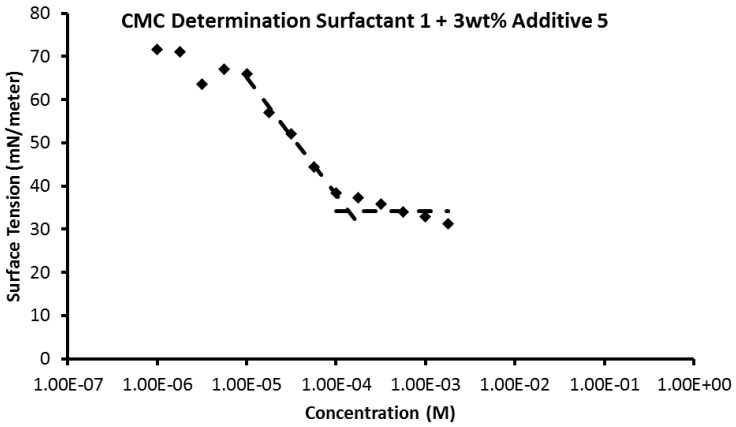

Figure 25: Surface Tension vs. Concentration for Surfactant 1 + 3wt% Additive 5

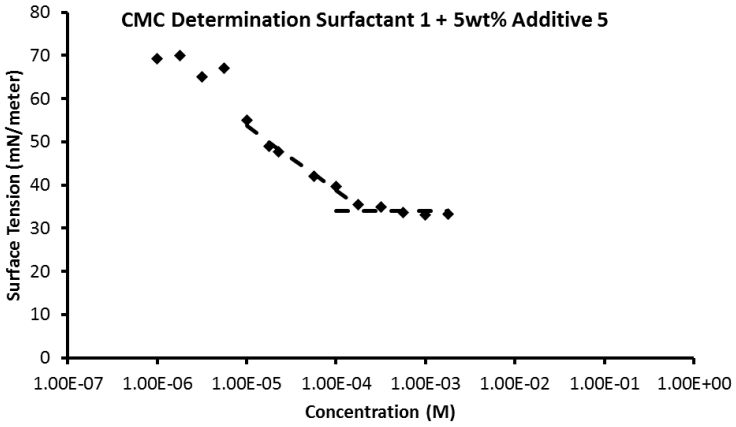

Figure 26: Surface Tension vs. Concentration for Surfactant 1 + 5wt% Additive 5

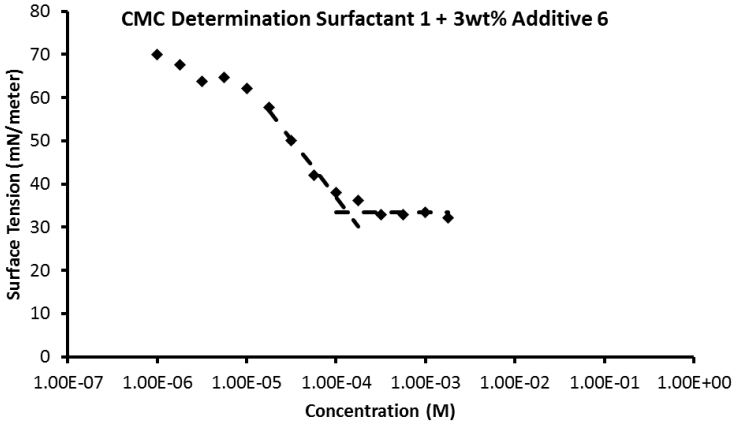

Figure 27: Surface Tension vs. Concentration for Surfactant 1 + 3wt% Additive 6

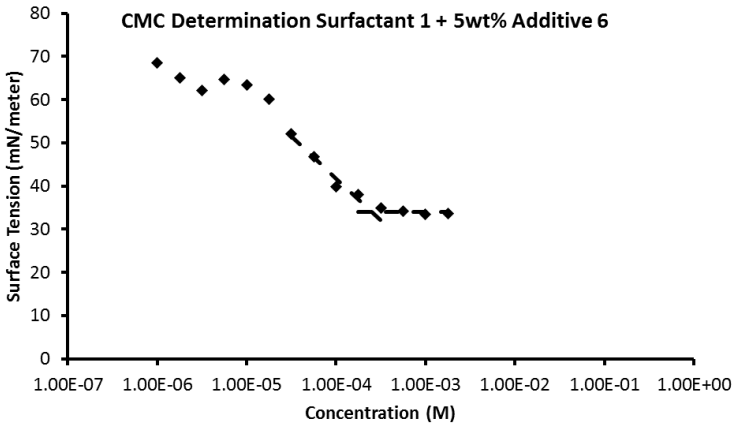

Figure 28: Surface Tension vs. Concentration for Surfactant 1 + 5wt% Additive 6

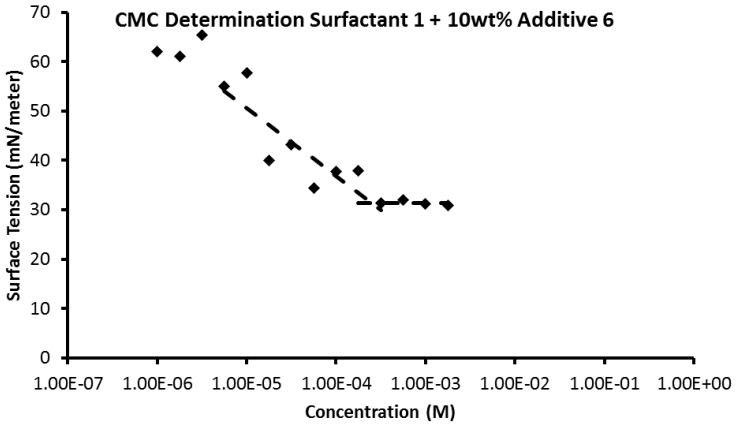

Figure 29: Surface Tension vs. Concentration for Surfactant 1 + 10wt% Additive 6

Below is a summary table of the critical micelle concentrations and area per head groups of Surfactant 1 and the differing weight percentages of fatty acid additives.

Table 5: CMC and Area per head group for Surfactant 1 and additives

Surfactant	CMC (M)	SA/headgroup (Å^2/molecule)	Surface Tension at CMC (mN/m)
Surfactant 2	1.76E-4	100.4	37.1
Surfactant 1	1.77E-4	84.4	34.9

Surfactant 1 + 1wt% Additive 5	1.13E-4	66.2	35.2
Surfactant 1 + 3wt% Additive 5	1.39E-4	70.0	34.2
Surfactant 1 + 5wt% Additive 5	2.10E-4	127.4	34.0
Surfactant 1 + 3wt% Additive 6	1.34E-4	70.6	33.5
Surfactant 1 + 5wt% Additive 6	2.47E-4	97.0	34.1
Surfactant 1 + 10wt% Additive 6	2.50E-4	137.4	31.3

Adsorption Isotherms

The adsorption isotherms are displayed below in Figures 30 to 50. These adsorption isotherms provide the maximum surfactant adsorbed once they have reached the plateau region of the isotherm. These maximum adsorptions are used to fit the model parameters. If no plateau was reached by 1 wt% of surfactant added, those particular maximum adsorptions were omitted from the model fitting.

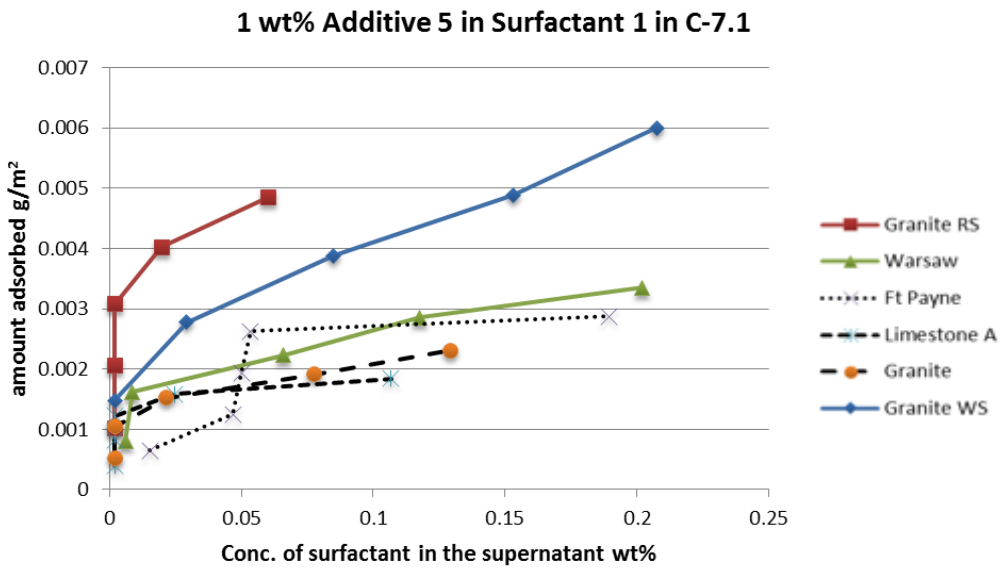

Figure 30: Adsorption isotherm for Surfactant 1 and 1wt% Additive 5 in EACN 7.1 on Granite RS, Warsaw, Ft. Payne Limestone, Limestone A, Granite, and Granite WS mineral fines

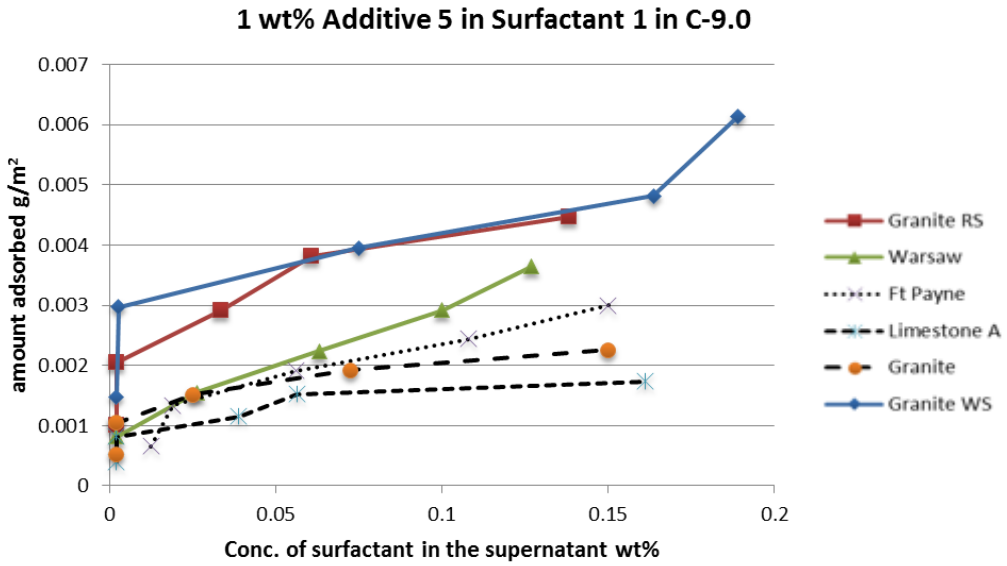

Figure 31: Adsorption isotherm for Surfactant 1 and 1wt% Additive 5 in EACN 9.0 on Granite RS, Warsaw, Ft. Payne Limestone, Limestone A, Granite, and Granite WS mineral fines

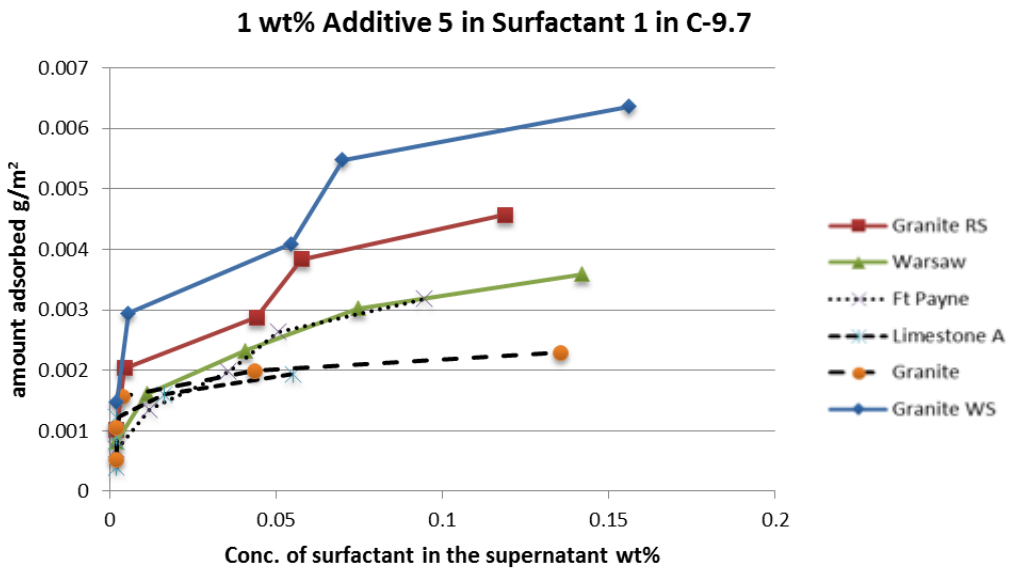

Figure 32: Adsorption isotherm for Surfactant 1 and 1wt% Additive 5 in EACN 9.7 on Granite RS, Warsaw, Ft. Payne Limestone, Limestone A, Granite, and Granite WS mineral fines

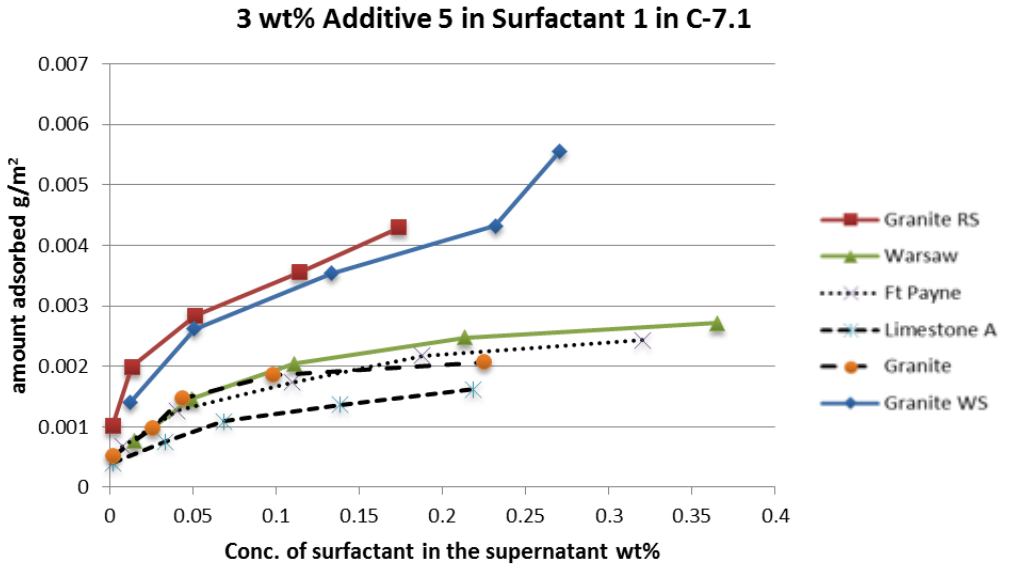

Figure 33: Adsorption isotherm for Surfactant 1 and 3wt% Additive 5 in EACN 7.1 on Granite RS, Warsaw, Ft. Payne Limestone, Limestone A, Granite, and Granite WS mineral fines

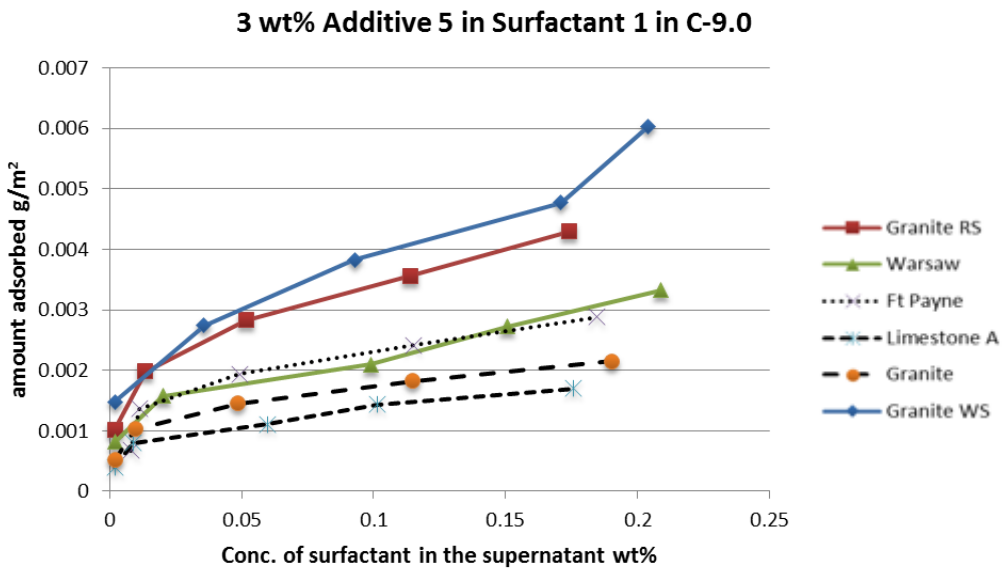

Figure 34: Adsorption isotherm for Surfactant 1 and 3wt% Additive 5 in EACN 9.0 on Granite RS, Warsaw, Ft. Payne Limestone, Limestone A, Granite, and Granite WS mineral fines

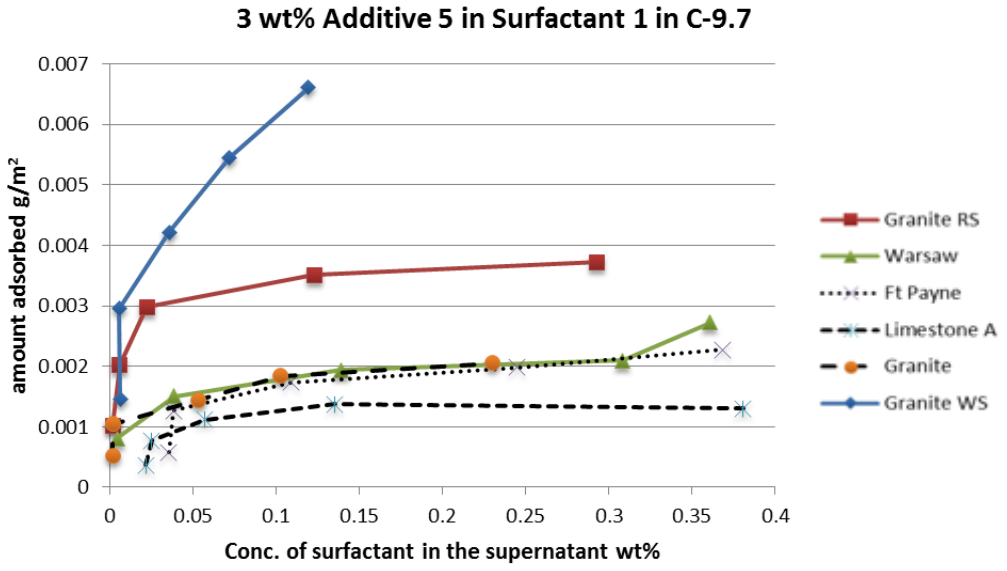

Figure 35: Adsorption isotherm for Surfactant 1 and 3wt% Additive 5 in EACN 9.7 on Granite RS, Warsaw, Ft. Payne Limestone, Limestone A, Granite, and Granite WS mineral fines

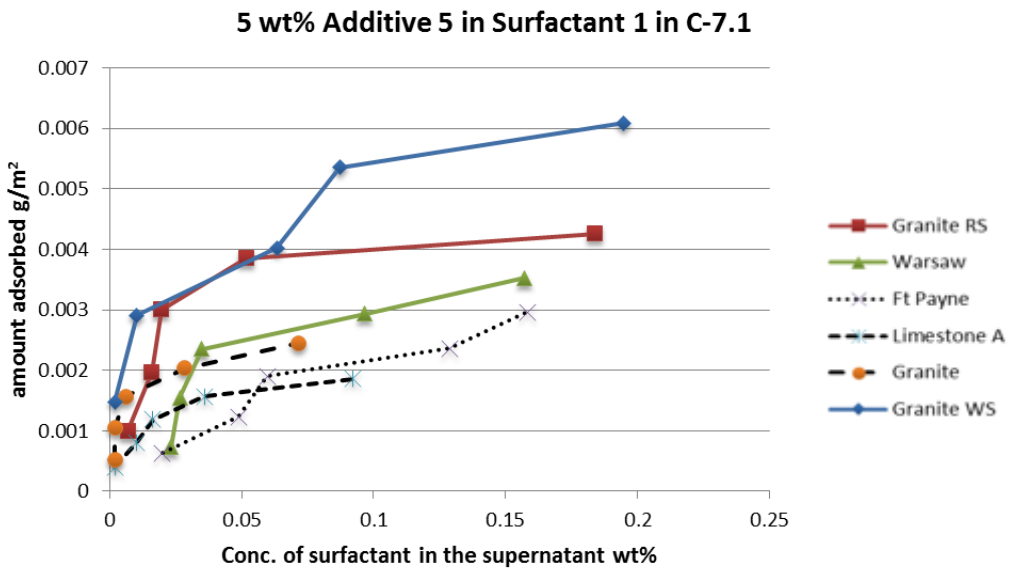

Figure 36: Adsorption isotherm for Surfactant 1 and 5wt% Additive 5 in EACN 7.1 on Granite RS, Warsaw, Ft. Payne Limestone, Limestone A, Granite, and Granite WS mineral fines

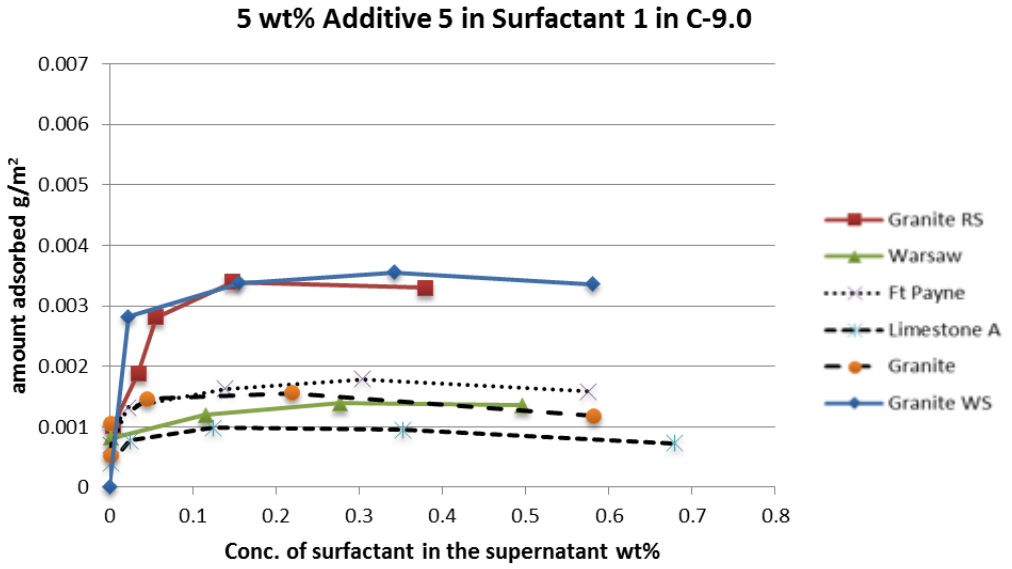

Figure 37: Adsorption isotherm for Surfactant 1 and 5wt% Additive 5 in EACN 9.0 on Granite RS, Warsaw, Ft. Payne Limestone, Limestone A, Granite, and Granite WS mineral fines

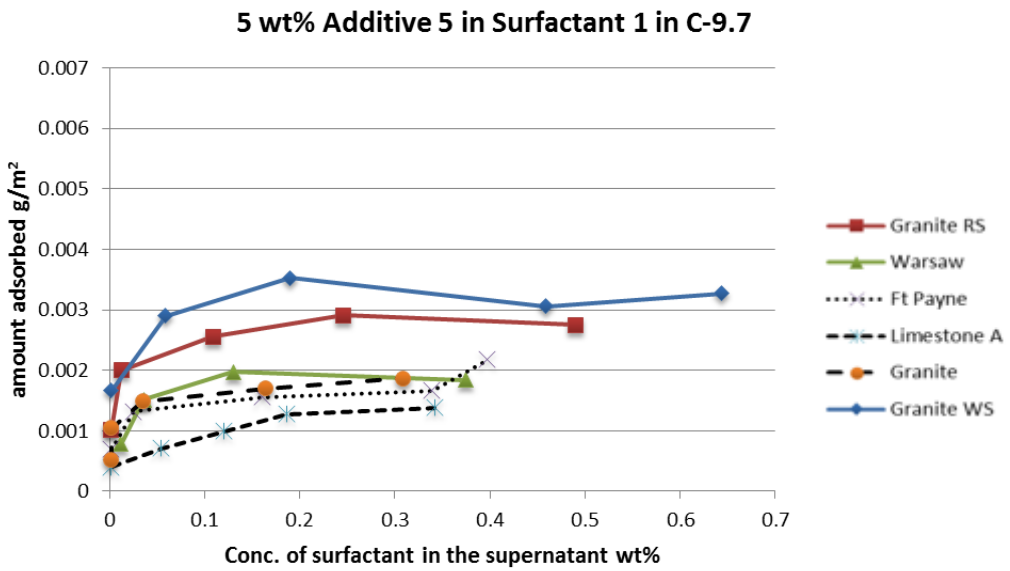

Figure 38: Adsorption isotherm for Surfactant 1 and 5wt% Additive 5 in EACN 9.7 on Granite RS, Warsaw, Ft. Payne Limestone, Limestone A, Granite, and Granite WS mineral fines

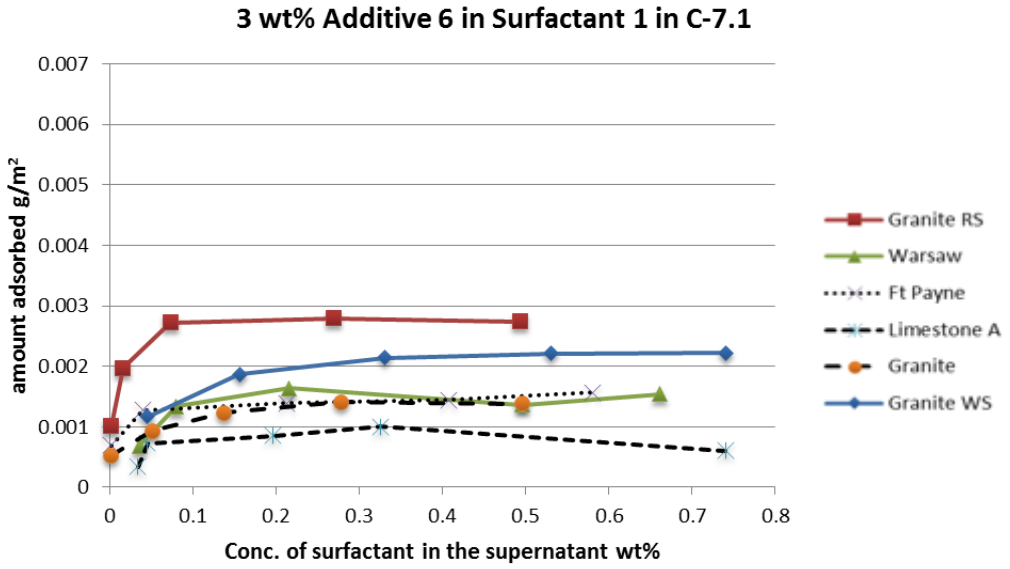

Figure 39: Adsorption isotherm for Surfactant 1 and 3wt% Additive 6 in EACN 7.1 on Granite RS, Warsaw, Ft. Payne Limestone, Limestone A, Granite, and Granite WS mineral fines

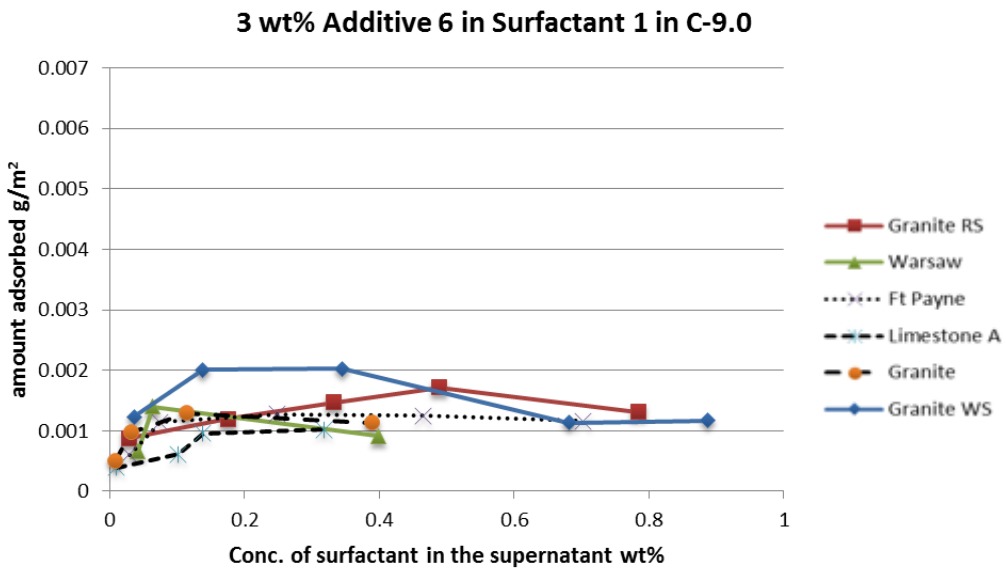

Figure 40: Adsorption isotherm for Surfactant 1 and 3wt% Additive 6 in EACN 9.0 on Granite RS, Warsaw, Ft. Payne Limestone, Limestone A, Granite, and Granite WS mineral fines

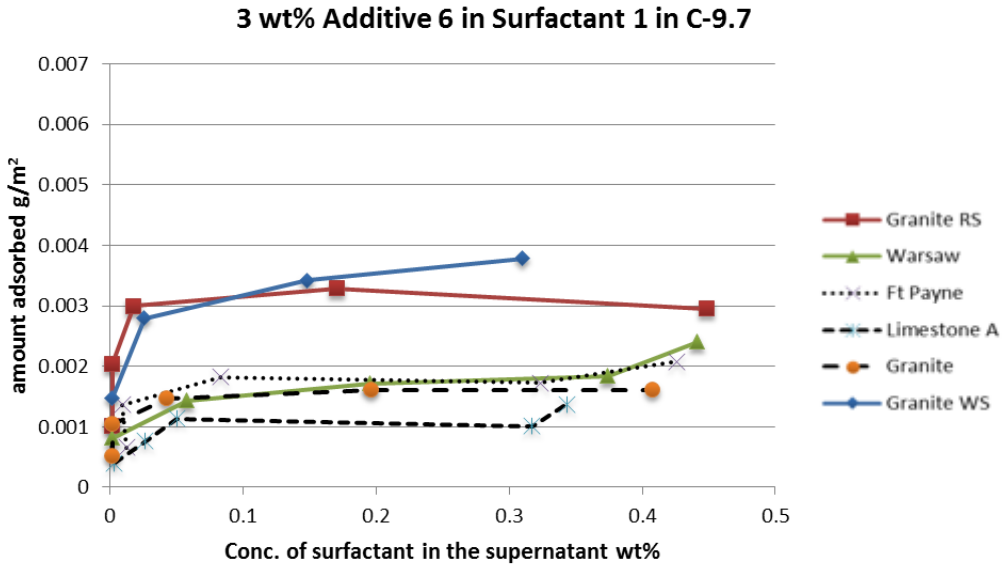

Figure 41: Adsorption isotherm for Surfactant 1 and 3wt% Additive 6 in EACN 9.7 on Granite RS, Warsaw, Ft. Payne Limestone, Limestone A, Granite, and Granite WS mineral fines

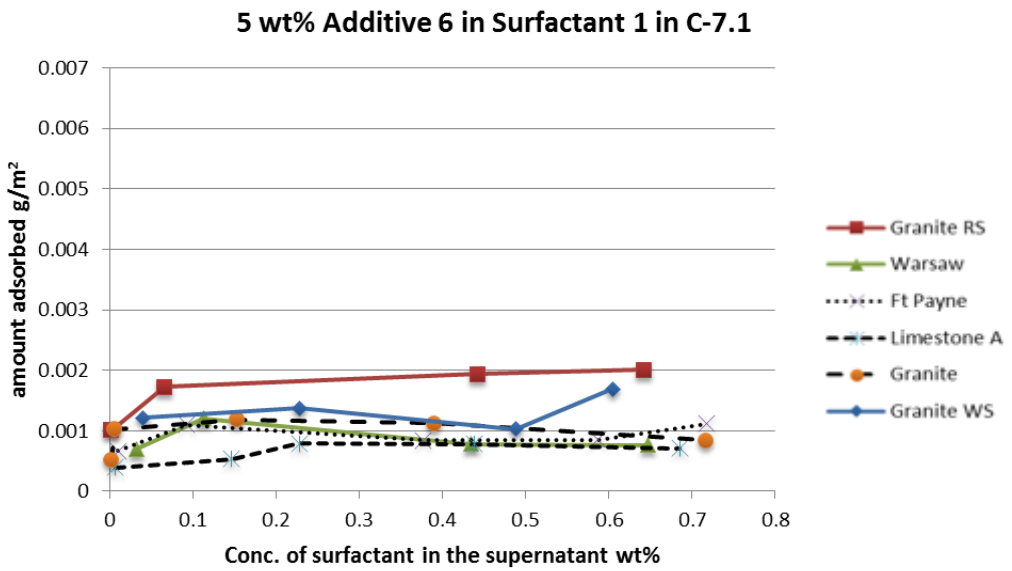

Figure 42: Adsorption isotherm for Surfactant 1 and 5wt% Additive 6 in EACN 7.1 on Granite RS, Warsaw, Ft. Payne Limestone, Limestone A, Granite, and Granite WS mineral fines

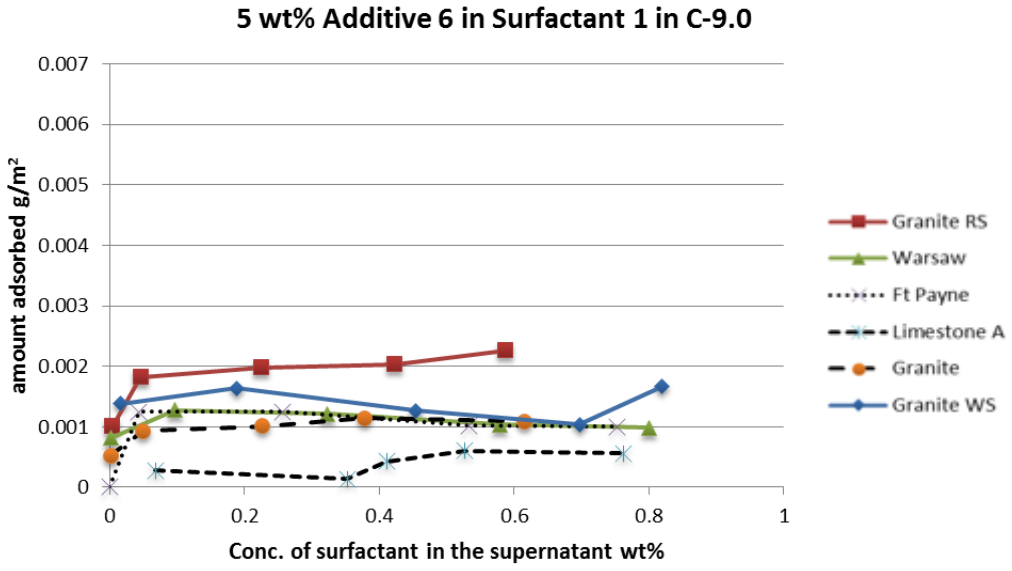

Figure 43: Adsorption isotherm for Surfactant 1 and 5wt% Additive 6 in EACN 9.0 on Granite RS, Warsaw, Ft. Payne Limestone, Limestone A, Granite, and Granite WS mineral fines

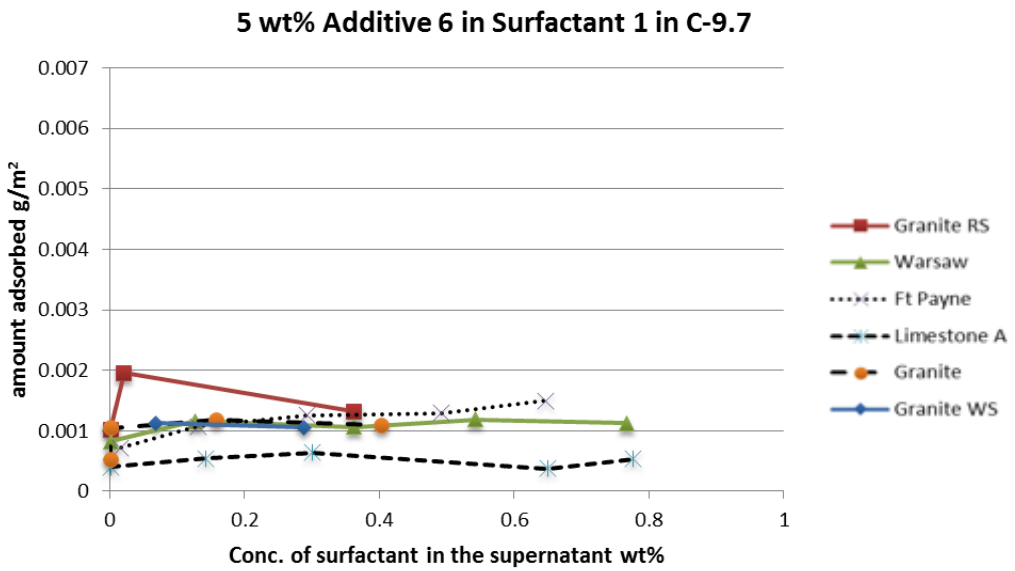

Figure 44: Adsorption isotherm for Surfactant 1 and 5wt% Additive 6 in EACN 9.7 on Granite RS, Warsaw, Ft. Payne Limestone, Limestone A, Granite, and Granite WS mineral fines

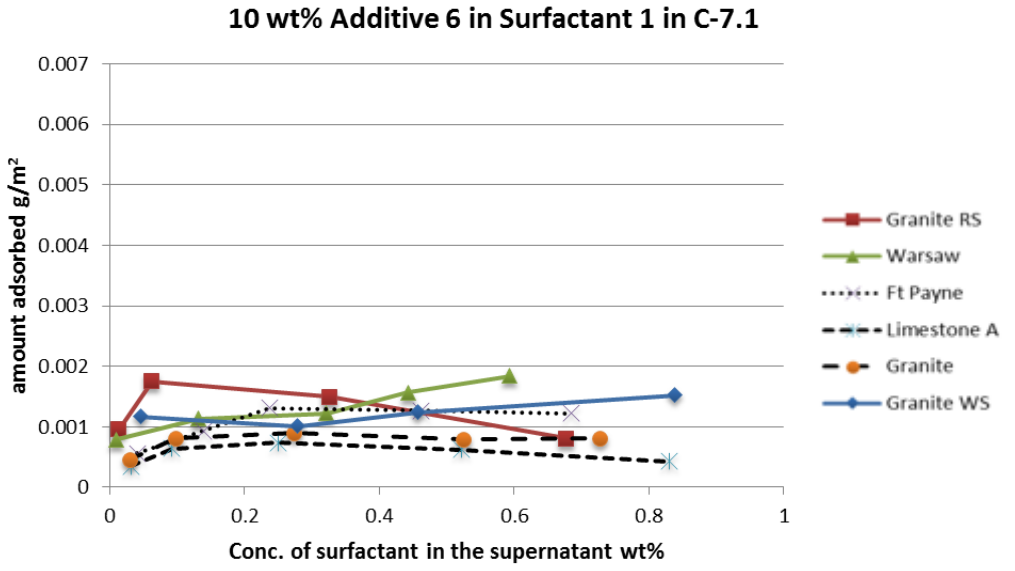

Figure 45: Adsorption isotherm for Surfactant 1 and 10wt% Additive 6 in EACN 7.1 on Granite RS, Warsaw, Ft. Payne Limestone, Limestone A, Granite, and Granite WS mineral fines

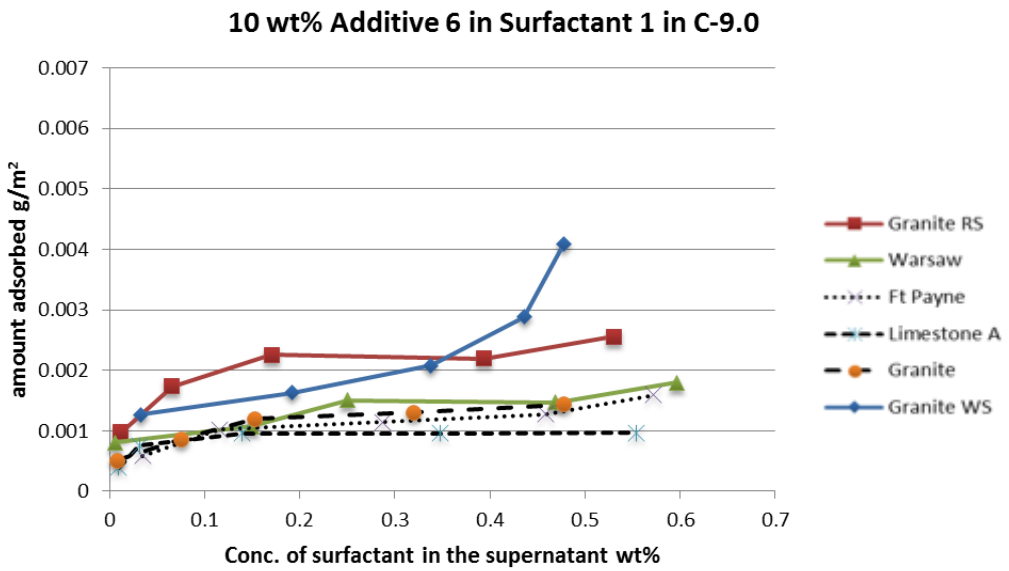

Figure 46: Adsorption isotherm for Surfactant 1 and 10wt% Additive 6 in EACN 9.0 on Granite RS, Warsaw, Ft. Payne Limestone, Limestone A, Granite, and Granite WS mineral fines

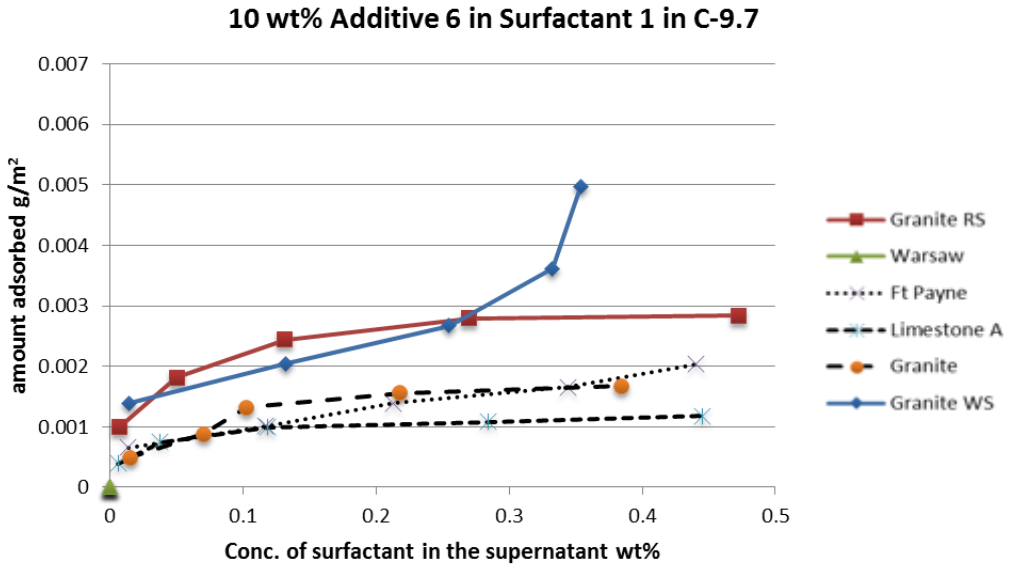

Figure 47: Adsorption isotherm for Surfactant 1 and 10wt% Additive 6 in EACN 9.7 on Granite RS, Warsaw, Ft. Payne Limestone, Limestone A, Granite, and Granite WS mineral fines

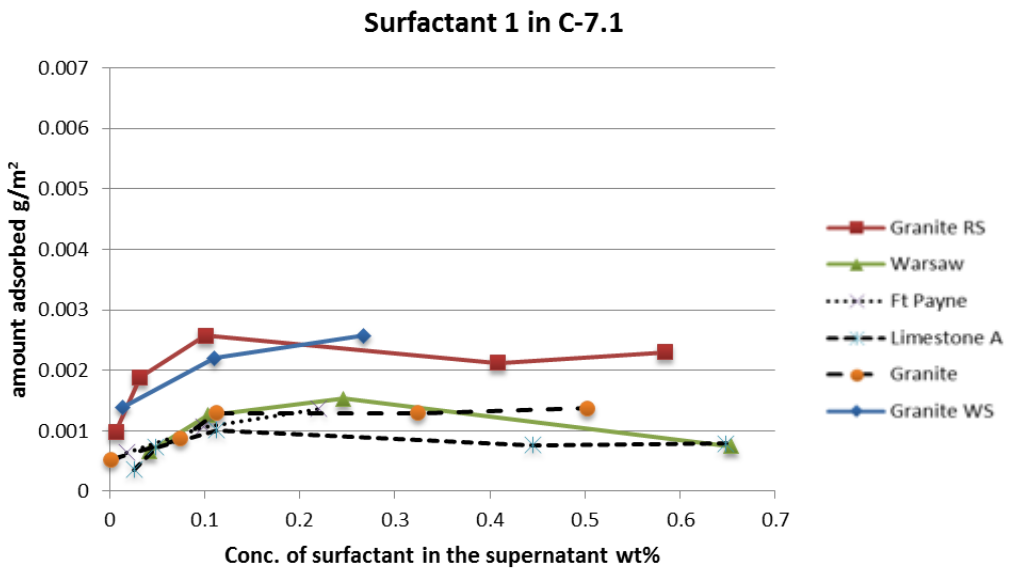

Figure 48: Adsorption isotherm for Surfactant 1 in EACN 7.1 on Granite RS, Warsaw, Ft. Payne Limestone, Limestone A, Granite, and Granite WS mineral fine

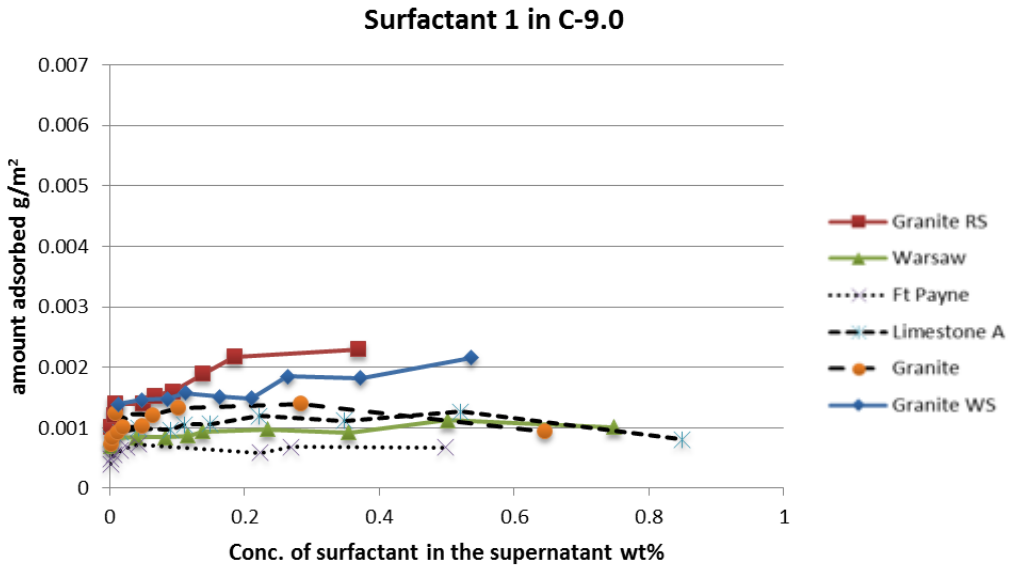

Figure 49: Adsorption isotherm for Surfactant 1 in EACN 9.0 on Granite RS, Warsaw, Ft. Payne Limestone, Limestone A, Granite, and Granite WS mineral fines

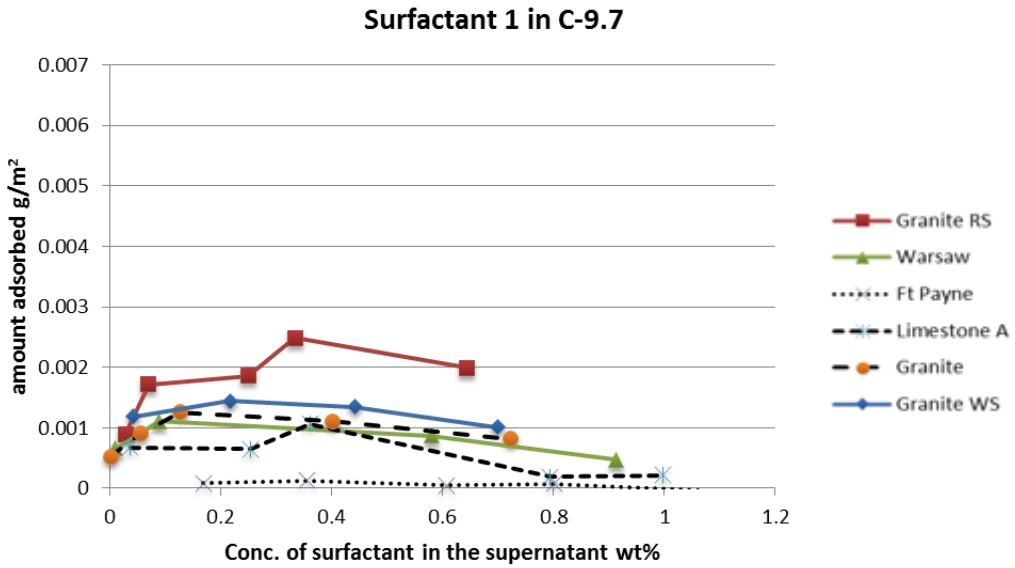

Figure 50: Adsorption isotherm for Surfactant 1 in EACN 9.7 on Granite RS, Warsaw, Ft. Payne Limestone, Limestone A, Granite, and Granite WS mineral fines

Below are the summary tables of the maximum adsorptions determined from the above adsorption isotherms divided by mineral fine.

Table 6: Maximum Adsoprtion (g/m2) for Granite RS

EACN	M1	1wt% Additive 5	3wt% Additive 5	5wt% Additive 5	3wt% Additive 6	5wt% Additive 6	10wt% Additive 6
7.1	0.00257	0.00485	N/A	0.00426	0.00274	0.00201	0.0015
9	0.0023	0.00447	N/A	0.00329	0.00147	0.00203	0.00225
9.7	0.00199	0.00456	0.00372	0.00291	0.00329	N/A	0.00284

Table 7: Maximum Adsoprtion (g/m2) for Granite WS

EACN	M1	1wt% Additive 5	3wt% Additive 5	5wt% Additive 5	3wt% Additive 6	5wt% Additive 6	10wt% Additive 6
7.1	0.00257	N/A	0.00432	0.00608	0.00222	0.00137	0.00152
9	0.00182	0.00482	0.00477	0.00336	0.00203	0.00167	N/A
9.7	0.00144	0.00636	N/A	0.00327	0.00378	N/A	N/A

Table 8: Maximum Adsoprtion (g/m2) for Granite

EACN	M1	1wt% Additive 5	3wt% Additive 5	5wt% Additive 5	3wt% Additive 6	5wt% Additive 6	10wt% Additive 6
7.1	0.00137	0.0023	0.00207	0.00245	0.00139	0.00113	0.00089
9	0.0014	0.00225	0.00215	0.00156	0.00129	0.00115	0.00144

9.7	0.00126	0.00229	0.00205	0.00187	0.00161	0.00118	0.00167

Table 9: Maximum Adsoprtion (g/m2) for Ft. Payne Limestone

EACN	M1	1wt% Additive 5	3wt% Additive 5	5wt% Additive 5	3wt% Additive 6	5wt% Additive 6	10wt% Additive 6
7.1	0.00137	0.00287	0.00244	0.00236	0.00145	0.00112	0.00131
9	0.00101	N/A	0.00289	0.00159	0.00125	0.00125	0.00128
9.7	0.00087	0.00318	0.00227	0.00167	0.00182	0.0013	0.00139

Table 10: Maximum Adsoprtion (g/m2) for Warsaw

EACN	M1	1wt% Additive 5	3wt% Additive 5	5wt% Additive 5	3wt% Additive 6	5wt% Additive 6	10wt% Additive 6
7.1	0.00153	0.00335	0.00271	0.00293	0.00154	0.00121	0.00122
9	0.00127	N/A	0.00332	0.00136	0.0014	0.00128	0.0015
9.7	0.00106	0.00359	0.0021	0.00198	0.00184	0.00118	N/A

Table 11: Maximum Adsoprtion (g/m2) for Limestone A

EACN	M1	1wt% Additive 5	3wt% Additive 5	5wt% Additive 5	3wt% Additive 6	5wt% Additive 6	10wt% Additive 6
7.1	0.00077	0.00184	0.00162	0.00186	0.00061	0.00079	0.00074
9	0.00068	0.00173	0.0017	0.00098	0.00102	0.00061	0.00097
9.7	N/A	0.00194	0.0013	0.00138	0.00173	0.00064	0.00118

The addition of both additives increases the amount of Surfactant 1 adsorbed onto the mineral fines. In general the samples where Additive 5 was added along with the Surfactant 1 exhibit the highest adsorption. Also, the granites tend to show the greatest tendency for adsorption to occur. The highest adsorption occurs on Granite WS in an EACN of 9.7 with Surfactant 1 and 1 wt% of the Additive 5.

Model Fitting

Every combination of mineral fine (ZP), surfactant (Cc), and heavy petroleum oil (EACN) produces a distinct adsorption HLD. Six minerals, seven surfactants, and three oil phases have been used to measure 126 adsorption isotherms. Maximum adsorptions taken from these adsorption isotherms are used to determine the error associated with the calculated HLD adsorption values. The maximum adsorptions taken from the adsorption isotherms will be referred to as measured maximum adsorptions, while the

maximum adsorptions calculated using the modified HLD adsorption equation will be referred to as the calculated maximum adsorptions. Since the modified HLD adsorption equation has its optimum at 1 i.e. the maximum adsorption occurs there, a scaler is applied to the measured maximum adsorptions so that the highest value is now 1, while the measured maximum adsorptions retain their trends relative to each other.

Preliminary values are assumed for b', K, and J so that calculated maximum adsorptions can be predicted. The mean squared error between each calculated maximum adsorptions and its corresponding measured maximum adsorption is found, and all of the errors are then added together. This total error is then minimized using non-linear least squares regression by iteratively changing the three coefficients in the modified HLD adsorption equation.

It was determined that granite washed screened is an outlier, since it experienced some of the highest adsorptions despite having a zeta potential comparable to that of the limestones which experienced significantly lower adsorptions. All the modified HLD adsorption equation optimizations performed were then re-optimized excluding granite washed screened from the data set. This omission showed improvement in the model fit across the board, but ultimately failed to provide enough of a reduction in error for the models to be considered successful.

Several different variations of the modified HLD adsorption equation have been optimized. These different variations have involved using different sets of coefficients for different parts of the data set. First, the entirety of the data set was examined simultaneously and a single equation and set of coefficients was used. Next, a different

b’ coefficient was optimized for each individual mineral while utilizing a single K and J coefficient for all of the minerals.

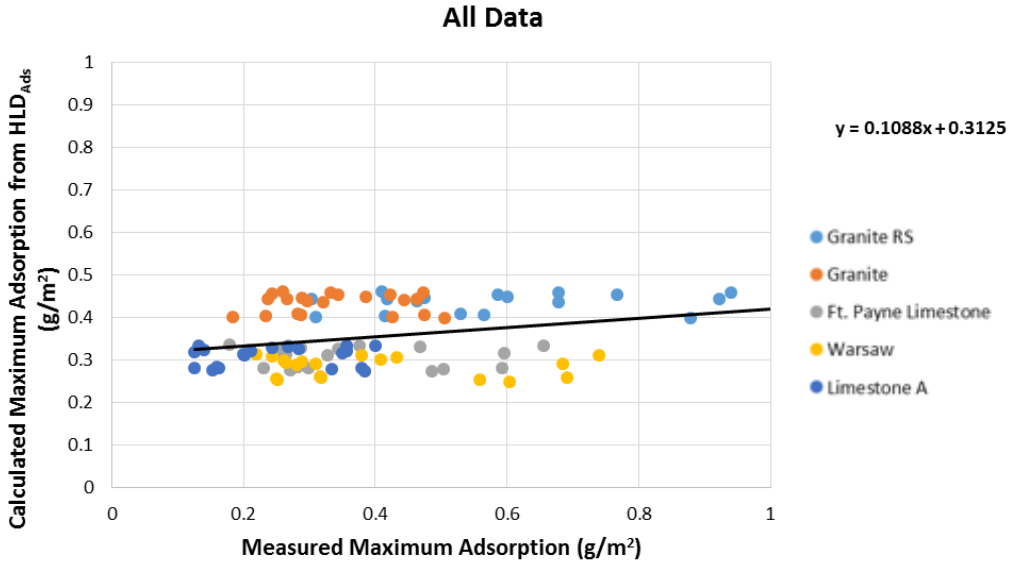

Figure 51: HLD adsorption values calculated using b’TOTAL, allowing K to vary, allowing J to vary, and excluding Granite WS

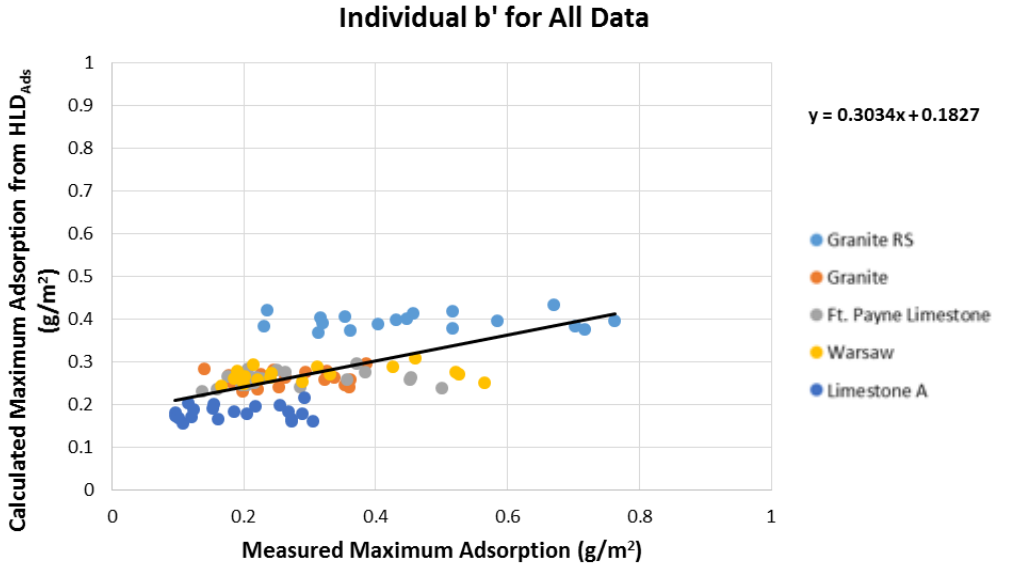

Figure 52: HLD adsorption values calculated using b’INDIV, allowing K to vary, allowing J to vary, and excluding Granite WS

Next, one of the parameters of the modified HLD adsorption equation was held constant and the rest of the equation was optimized. First, distinct coefficients (b', K, and J) were optimized for all minerals and all EACNs in three groups of surfactant data: Surfactant 1, Surfactant 1 with the Additive 5, and Surfactant 1 with the Additive 6.

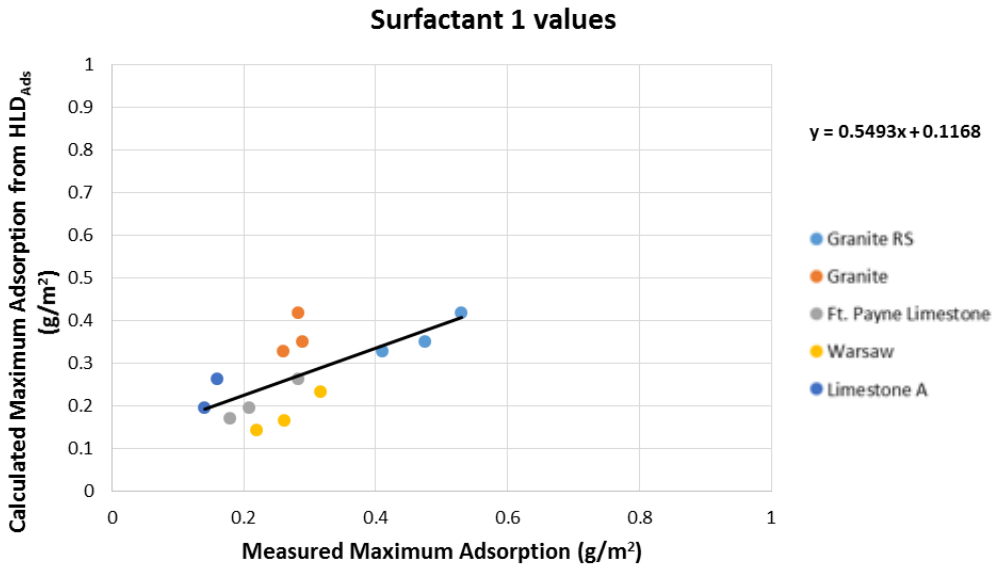

Figure 53: HLD adsorption values calculated using b'TOTAL, allowing K to vary, allowing J to vary, and excluding Granite WS for only Surfactant 1

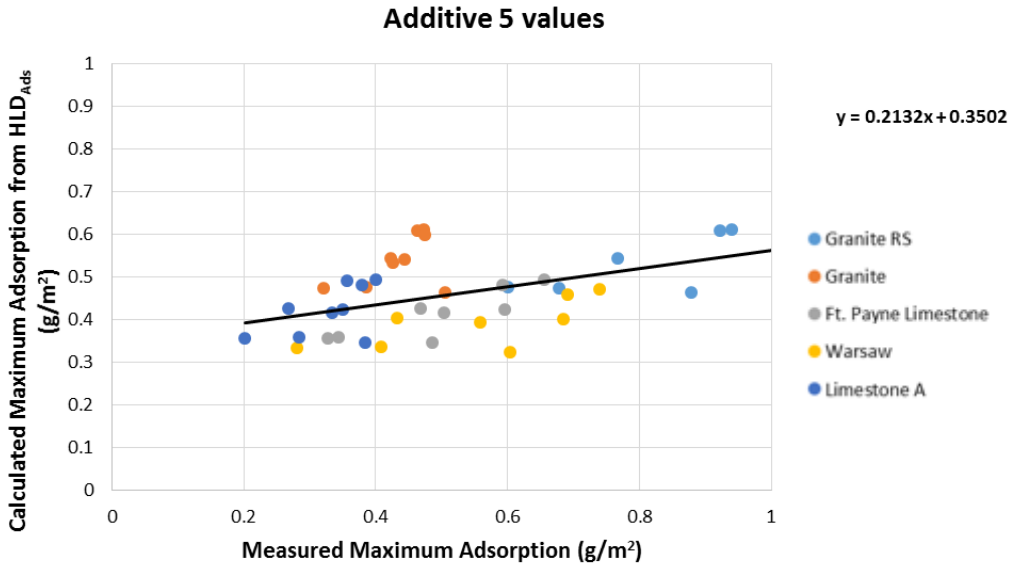

Figure 54: HLD adsorption values calculated using b'TOTAL, allowing K to vary, allowing J to vary, and excluding Granite WS for only Surfactant 1 and the Additive 5

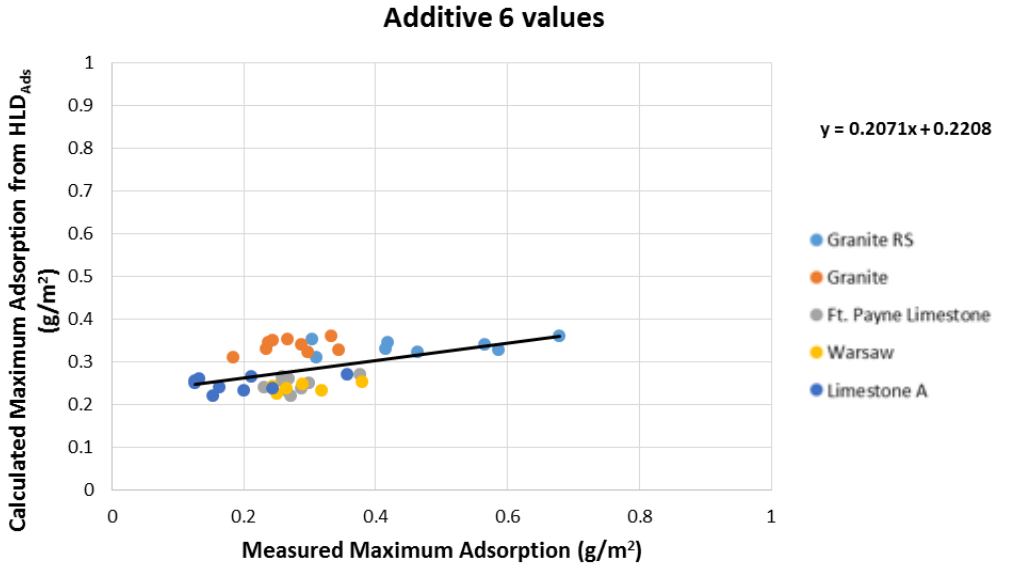

Figure 55: HLD adsorption values calculated using b'TOTAL, allowing K to vary, allowing J to vary, and excluding Granite WS for only Surfactant 1 and the Additive 6

Next, distinct coefficients (b', K, and J) were optimized for all minerals and all EACNs in seven groups of surfactant data: Surfactant 1, Surfactant 1 with 1 wt% Additive 5, Surfactant 1 with 3 wt% Additive 5, Surfactant 1 with 5 wt% Additive 5, Surfactant 1 with 3 wt% Additive 6, Surfactant 1 with 5 wt% Additive 6, and Surfactant 1 with 10 wt% Additive 6.

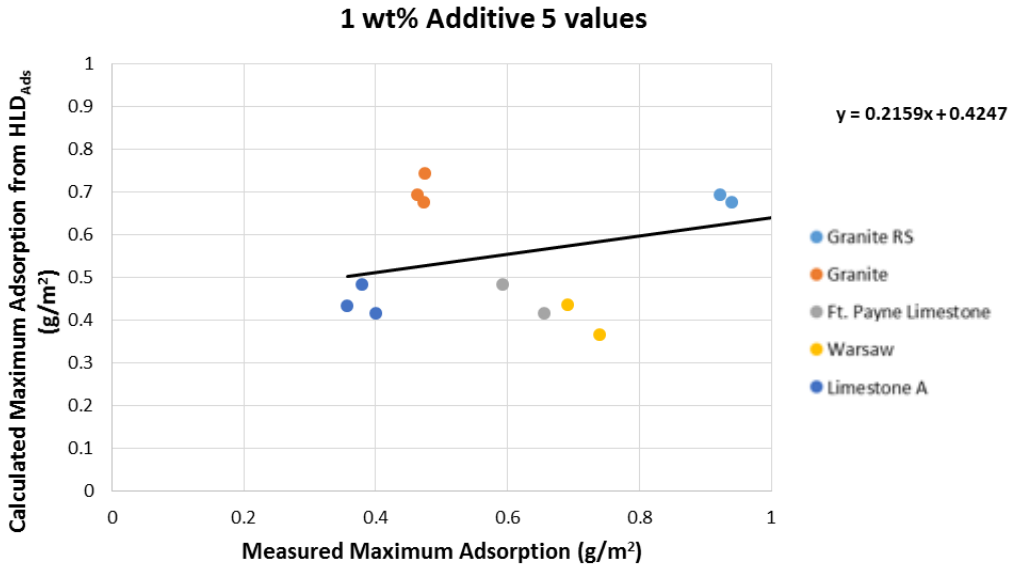

Figure 56: HLD adsorption values calculated using b'TOTAL, allowing K to vary, allowing J to vary, and excluding Granite WS for only Surfactant 1 and 1 wt% Additive 5

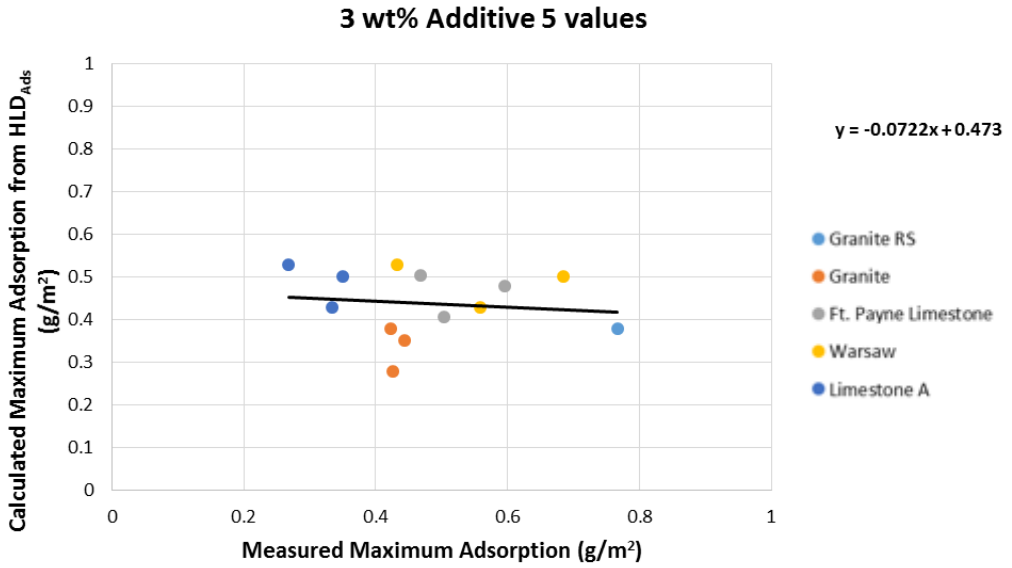

Figure 57: HLD adsorption values calculated using b'TOTAL, allowing K to vary, allowing J to vary, and excluding Granite WS for only Surfactant 1 and 3 wt% Additive 5

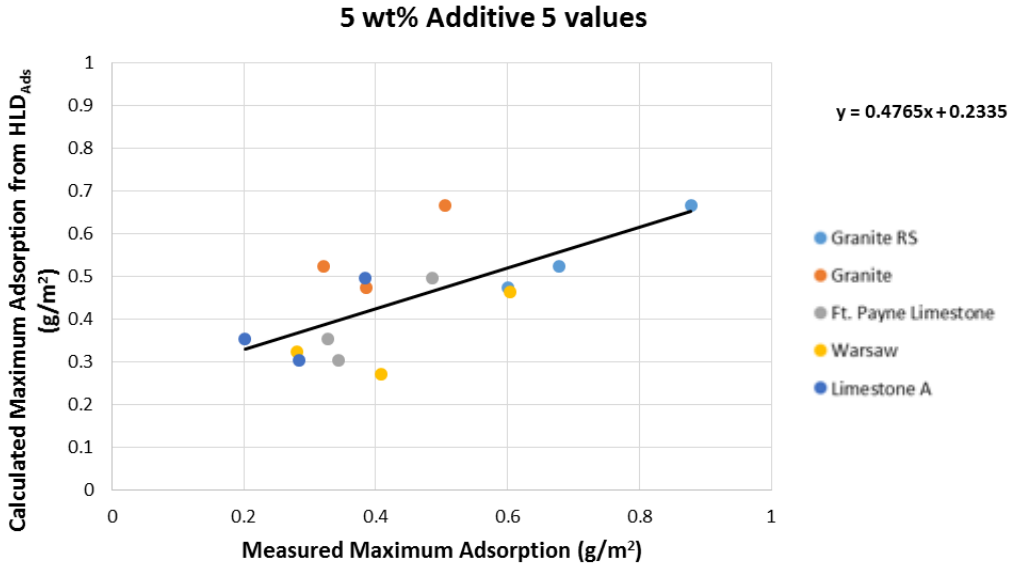

Figure 58: HLD adsorption values calculated using b'TOTAL, allowing K to vary, allowing J to vary, and excluding Granite WS for only Surfactant 1 and 5 wt% Additive 5

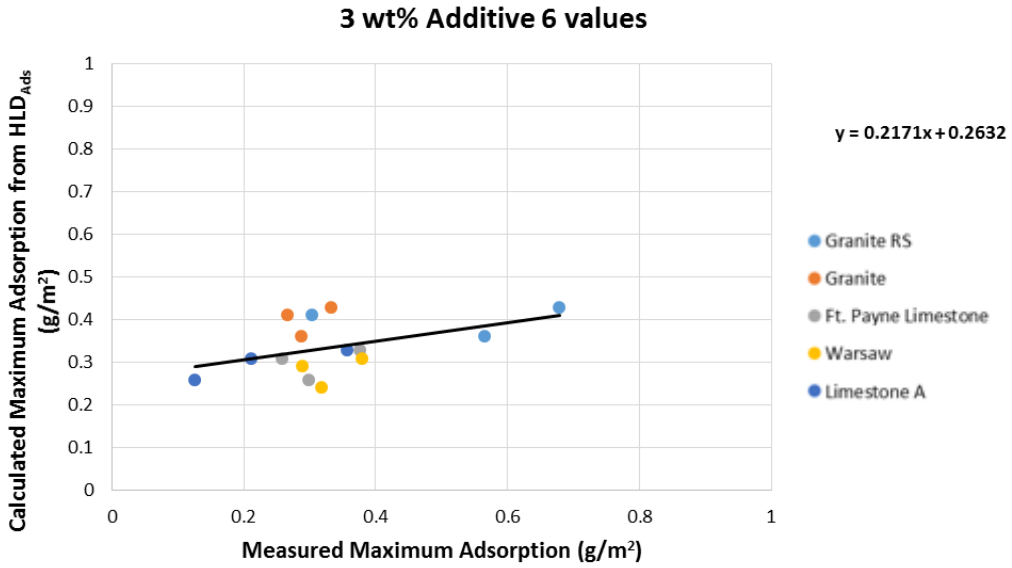

Figure 59: HLD adsorption values calculated using b'TOTAL, allowing K to vary, allowing J to vary, and excluding Granite WS for only Surfactant 1 and 3 wt% Additive 6

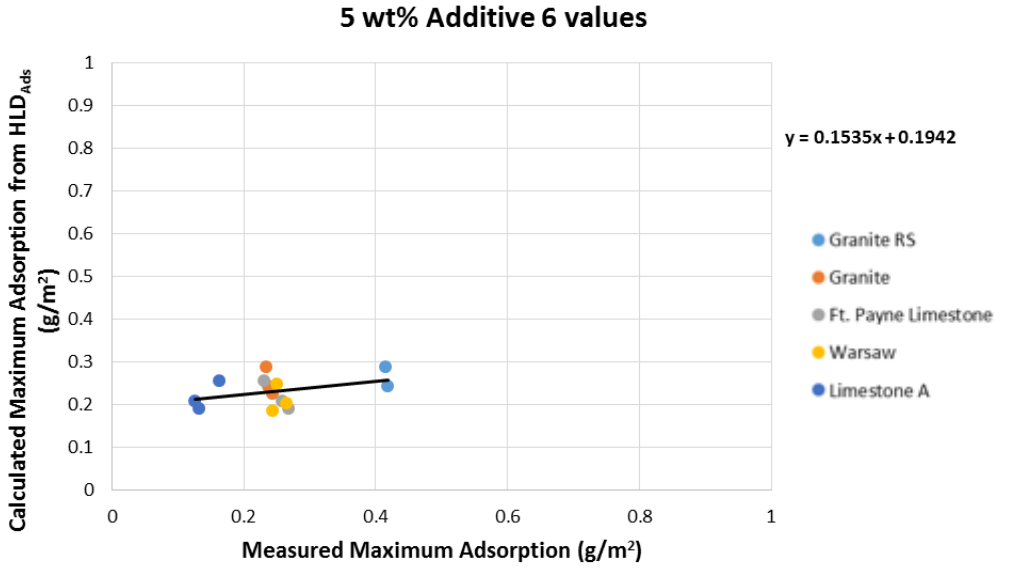

Figure 60: HLD adsorption values calculated using b'TOTAL, allowing K to vary, allowing J to vary, and excluding Granite WS for only Surfactant 1 and 5 wt% Additive 6

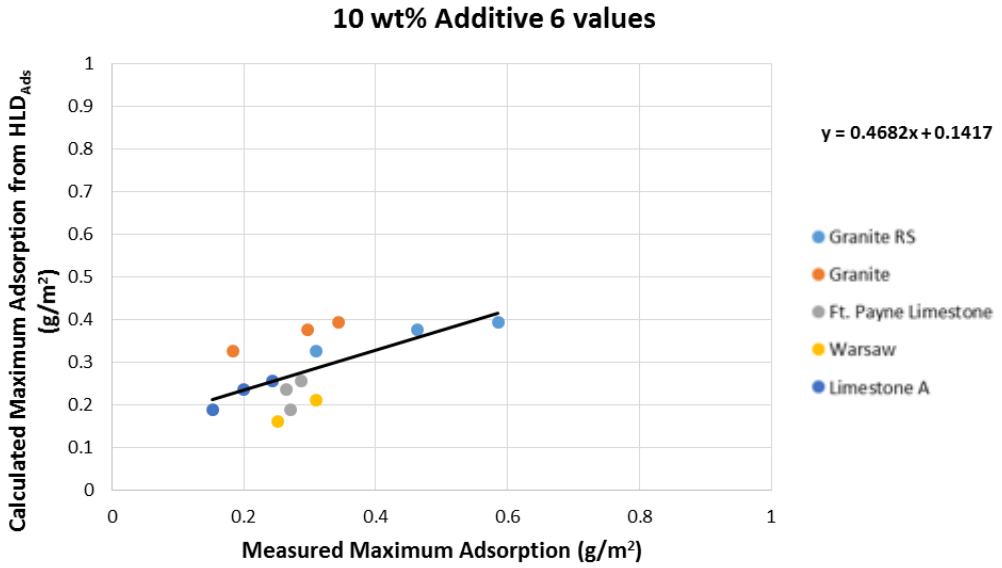

Figure 61: HLD adsorption values calculated using b'TOTAL, allowing K to vary, allowing J to vary, and excluding Granite WS for only Surfactant 1 and 10 wt% Additive 6

Then, distinct coefficients (b', K, and J) were optimized for all minerals and all surfactants in three groups of EACN data: EACN of 7.1, EACN of 9.0, and EACN of 9.7.

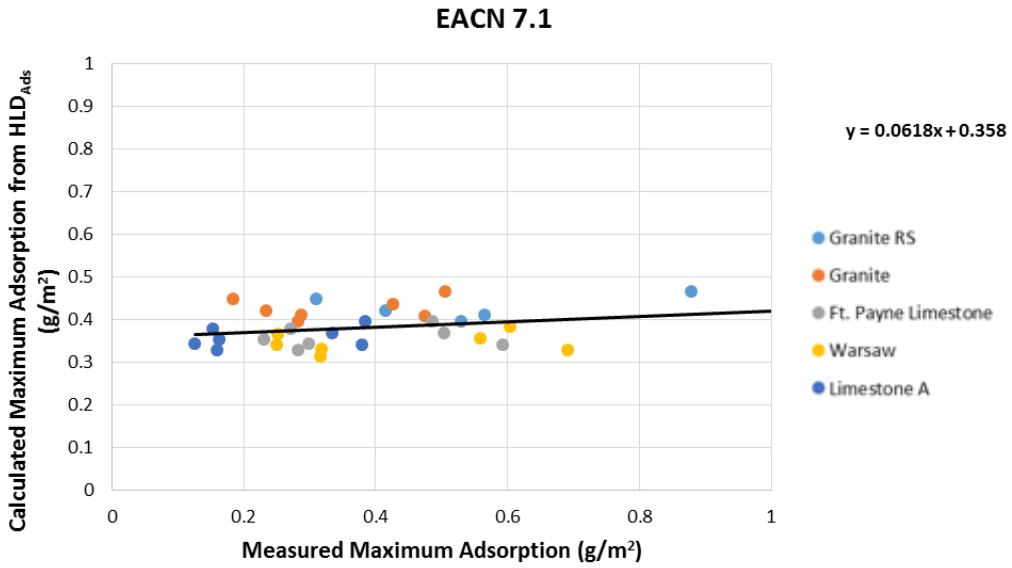

Figure 62: HLD adsorption values calculated using b'TOTAL, allowing K to vary, and allowing J to vary for EACN 7.1

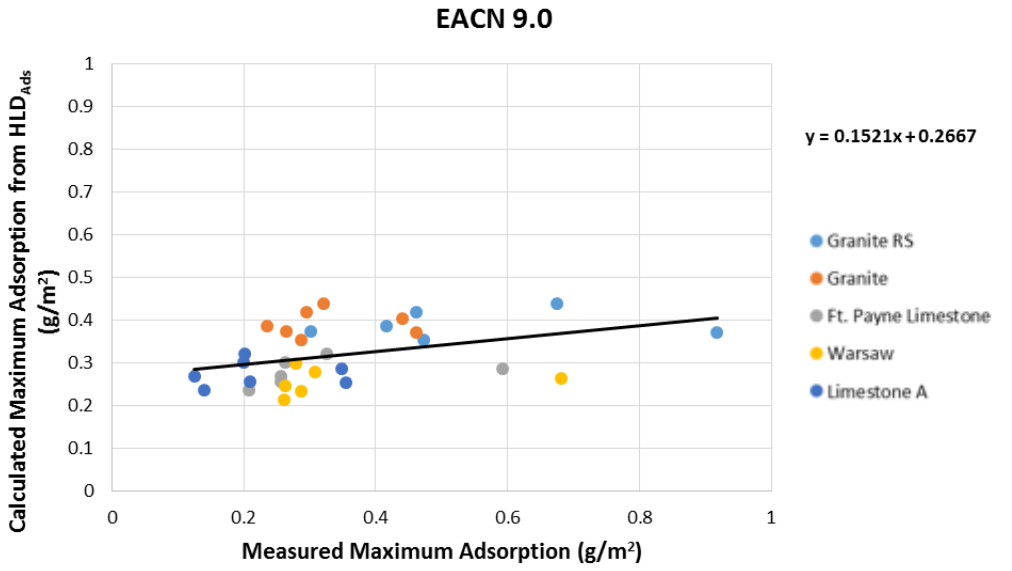

Figure 63: HLD adsorption values calculated using b'TOTAL, allowing K to vary, and allowing J to vary for EACN 9.0

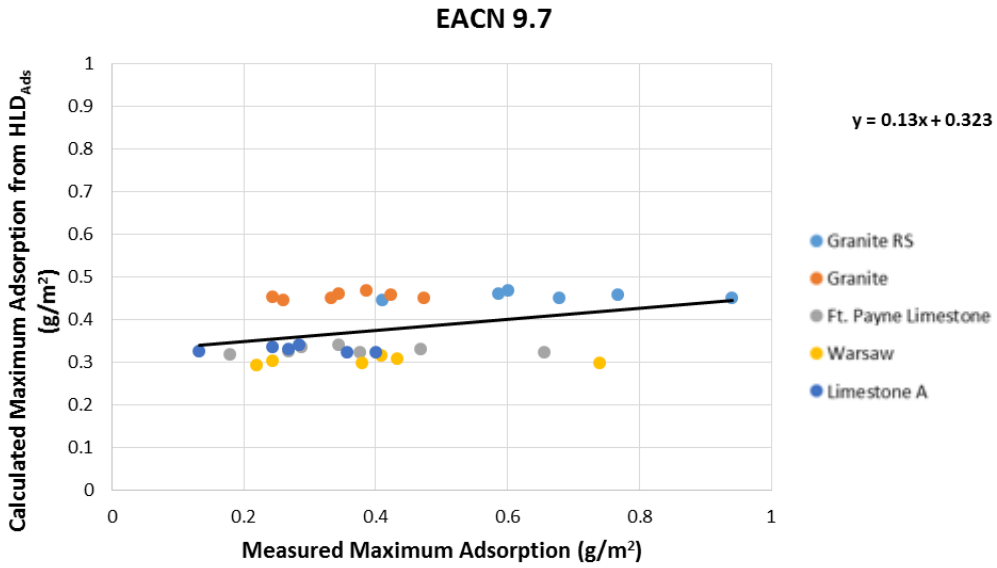

Figure 64: HLD adsorption values calculated using b'TOTAL, allowing K to vary, and allowing J to vary for EACN 9.7

Finally, distinct coefficients (b', K, and J) were optimized for all EACNs and all surfactants in six groups of mineral data: granite regular screened, granite washed screened, granite, Ft. Payne limestone, Warsaw limestone, and Limestone A.

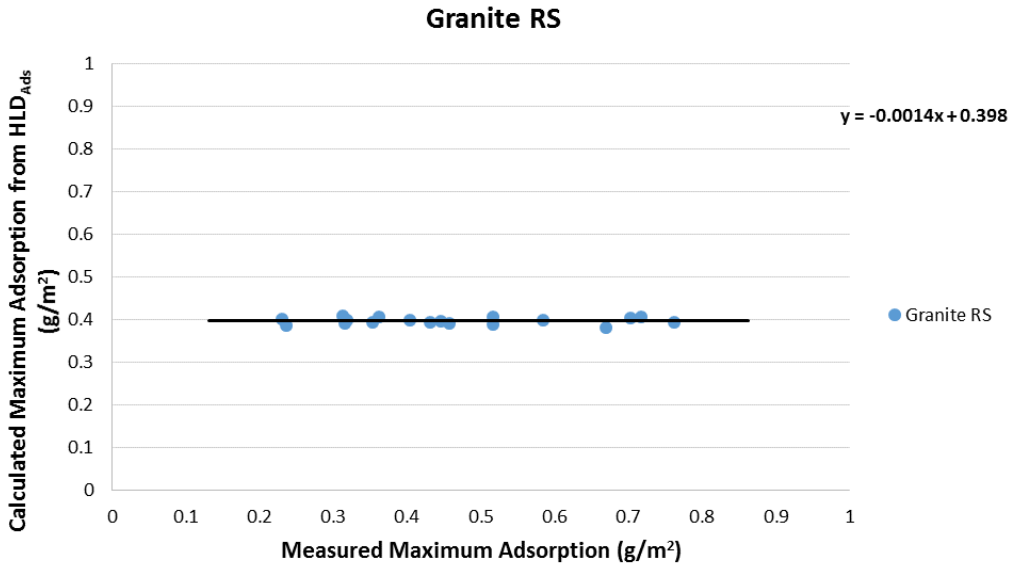

Figure 65: HLD adsorption values calculated using b'INDIV, allowing K to vary, and allowing J to vary for Granite RS

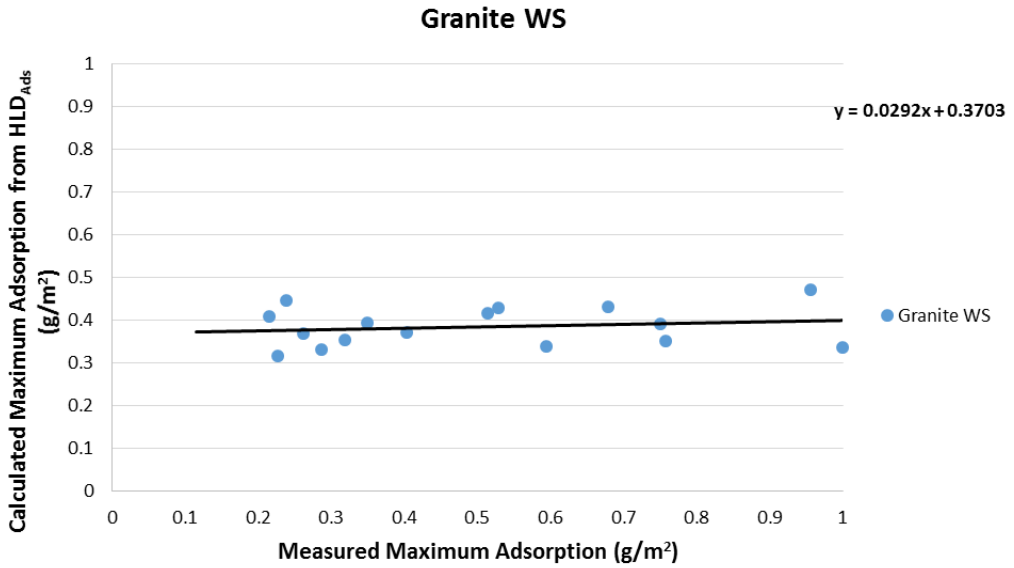

Figure 66: HLD adsorption values calculated using b'INDIV, allowing K to vary, and allowing J to vary for Granite WS

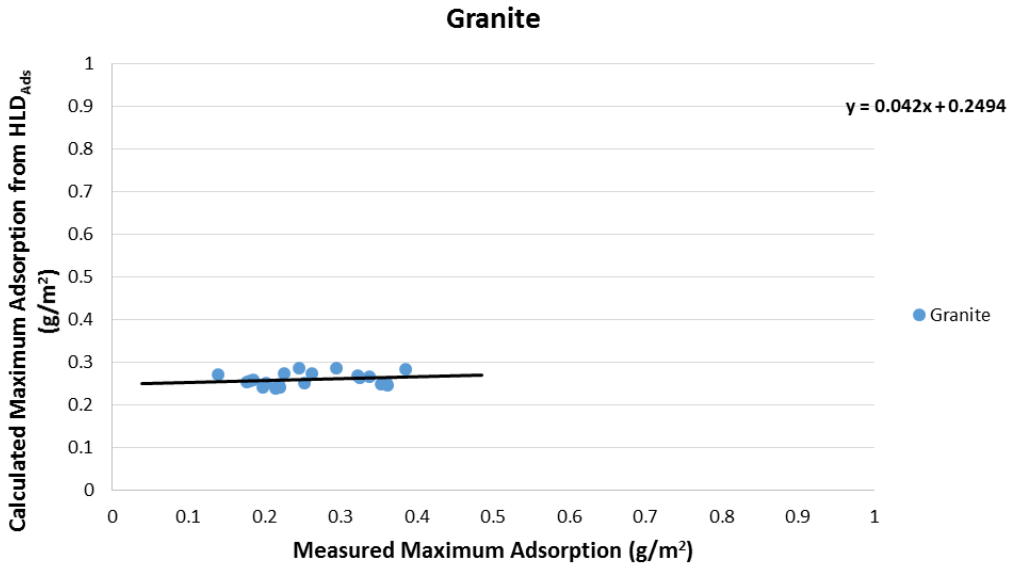

Figure 67: HLD adsorption values calculated using b'INDIV, allowing K to vary, and allowing J to vary for Granite

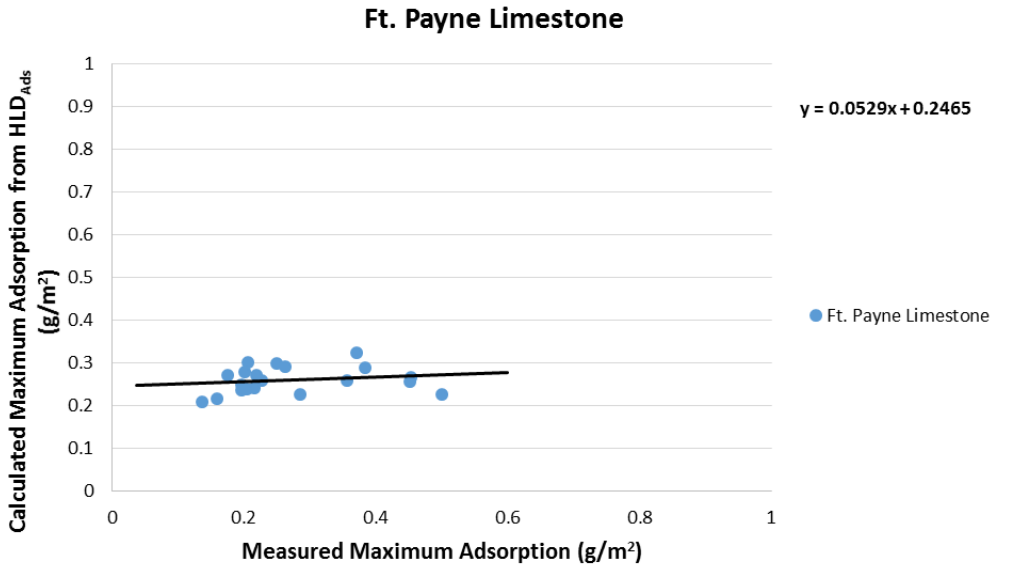

Figure 68: HLD adsorption values calculated using b'INDIV, allowing K to vary, and allowing J to vary for Ft. Payne Limestone

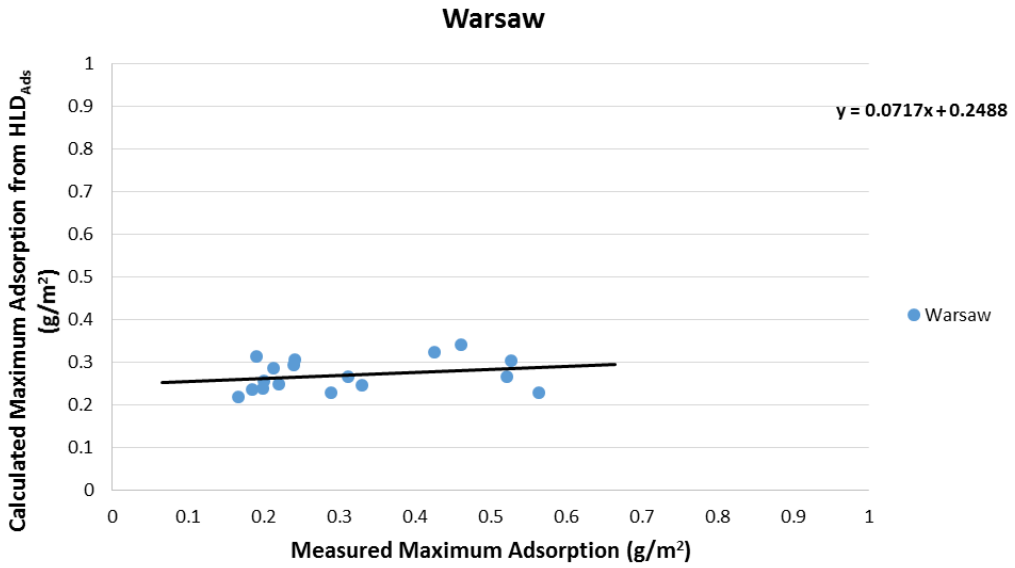

Figure 69: HLD adsorption values calculated using b'INDIV, allowing K to vary, and allowing J to vary for Warsaw

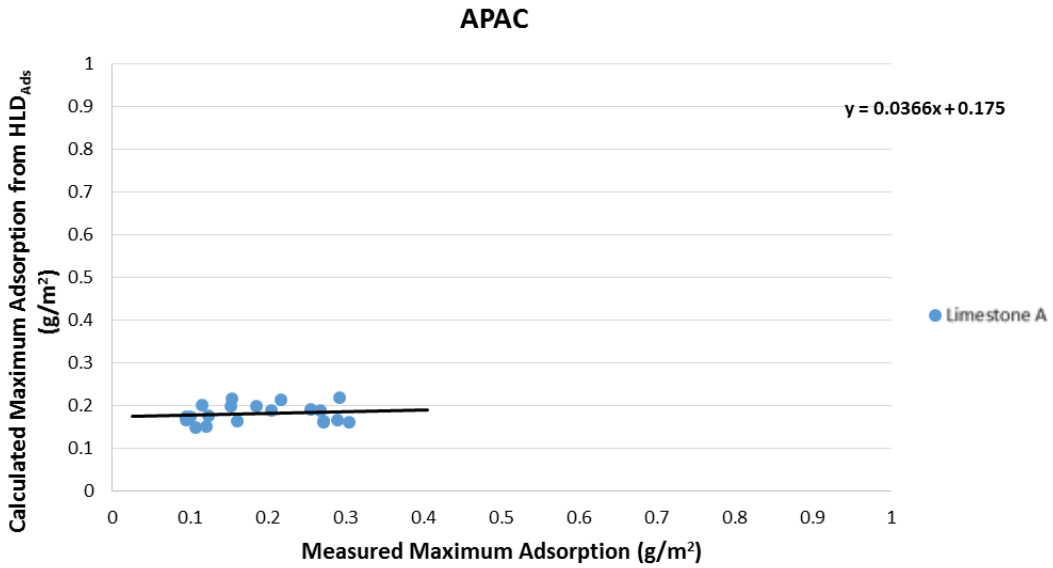

Figure 70: HLD adsorption values calculated using b'INDIV, allowing K to vary, and allowing J to vary for Limestone A

Conclusions and Discussion

An adequate correlation between the measured values of maximum adsorption and the predictive values from the modified HLD model was never achieved. A wider range of EACNs for the adsorption isotherms would have allowed for a greater understanding the effect the alkanes have on the system. The EACNs studied were essentially heptane, nonane, and decane which are relatively close together compared to the range of EACNs for the heavy petroleum oils characterized. The model, while incomplete, allows for insight to be gained on the factors that govern the adsorption of the surfactant on to the minerals in the presence of heavy petroleum oils.

Surfactant 1, being a cationic surfactant, adsorbed more strongly on the granites, which exhibited a more negative zeta potential than the limestones. This suggests that the surface chemistry of the mineral has a large effect on the performance of the adsorption. The addition of the fatty acid additives noticeably increased the adsorption of the surfactant onto the mineral. Also the Surfactant 1 when used in conjunction with the Additive 5 exhibited higher adsorption than the Surfactant 1 by itself or the Surfactant 1 used in conjunction with the Additive 6. Additive 6 is a maleated form of Additive 5 which suggests that the maleation process alters the species on the fatty acid that aids in promoting the adsorption of the surfactant exhibited by the Additive 5.

The models optimized for each individual surfactant, each individual mineral, and each individual EACN provide insight on the important forces that govern the adsorption system. These models essentially hold one term of the modified HLD equation constant and allow the other two parameters to be examined in relation to one another.

The models optimized for each individual surfactant allow the EACNs of the artificial heavy petroleum oils and the zeta potentials of the minerals to be examined together. While not a perfect correlation, there exists some correlation between the amounts of surfactant adsorbed based upon the effects of the oil EACN and the surface characteristics of the rock indicating that the relationship between these two parameters is crucial for describing the adsorption phenomena that is occurring.

The models optimized for the individual minerals allow the EACNs of the artificial heavy petroleum oils and the surfactant characteristics to be examined. These models have slopes of almost 0 indicating the relationship between the surfactant and the oil is not as important as the chemistry of the mineral which is supported by the literature.[31]

Finally the models optimized for the individual EACNs allow the relationship between the surfactant characteristics and the mineral chemistry to be examined. These exhibit a slight correlation indicating that, while not the primary driving force of the adsorption, the relationship between the surfactant characteristics and the mineral chemistry is of some importance.

It is interesting to note with the initial addition of Additives 5 and 6, the surface area of the surfactant head group decreases as compared to the surface area of Surfactant 1 by itself due to the initial attraction between the fatty acid and the cationic surfactant. With this decreased surface area per head group, adsorption of Surfactant 1 increases. As greater weight percentages of the additives are added, the surface area per head group increases and adsorption also generally decreases.

Ultimately, although the modified HLD model failed to accurately predict the adsorption of the surfactant onto a mineral surface in the presence of a heavy petroleum oil, some of the driving forces behind such adsorption were examined and compared to one another to determine how their interactions affected this adsorption.

References

1. De Gennes, P.G. and C. Taupin, Microemulsions and the flexibility of oil/water interfaces. The Journal of Physical Chemistry, 1982. 86(13): p. 2294-2304.

2. Witthayapanyanon, A., J.H. Harwell, and D.A. Sabatini, Hydrophilic–lipophilic deviation (HLD) method for characterizing conventional and extended surfactants. Journal of Colloid and Interface Science, 2008. 325(1): p. 259-266.

3. Berg, J.C., An introduction to interfaces & colloids: the bridge to nanoscience. 2010: World Scientific.

4. Somasundaran, P., S. Shrotri, and L. Huang, Thermodynamics of adsorption of surfactants at solid-liquid interface. Pure and applied chemistry, 1998. 70(3): p. 621-626.

5. Paria, S. and K.C. Khilar, A review on experimental studies of surfactant adsorption at the hydrophilic solid–water interface. Advances in Colloid and Interface Science, 2004. 110(3): p. 75-95.

6. Somasundaran, P. and L. Huang, Adsorption/aggregation of surfactants and their mixtures at solid–liquid interfaces. Advances in Colloid and Interface Science, 2000. 88(1–2): p. 179-208.

7. Atkin, R., et al., Mechanism of cationic surfactant adsorption at the solid–aqueous interface. Advances in Colloid and Interface Science, 2003. 103(3): p. 219-304.

8. Zhang, D.L., et al., Wettability alteration and spontaneous imbibition in oil-wet carbonate formations. Journal of Petroleum Science and Engineering, 2006. 52(1): p. 213-226.

9. Jarrahian, K., et al., Study of Wettability Alteration Mechanisms by Surfactants.

10. Austad, T. and J. Milter. Spontaneous imbibition of water into low permeable chalk at different wettabilities using surfactants. in International Symposium on Oilfield Chemistry. 1997. Society of Petroleum Engineers.

11. Somasundaran, P. and L. Zhang, Adsorption of surfactants on minerals for wettability control in improved oil recovery processes. Journal of Petroleum Science and Engineering, 2006. 52(1): p. 198-212.

12. Scamehorn, J., R. Schechter, and W. Wade, Adsorption of surfactants on mineral oxide surfaces from aqueous solutions: I: Isomerically pure anionic surfactants. Journal of Colloid and Interface Science, 1982. 85(2): p. 463-478.

13. Somasundaran, P. and D. Fuerstenau, Mechanisms of alkyl sulfonate adsorption at the alumina-water interface1. The Journal of Physical Chemistry, 1966. 70(1): p. 90-96.

14. Cases, J. and F. Villieras, Thermodynamic model of ionic and nonionic surfactants adsorption-abstraction on heterogeneous surfaces. Langmuir, 1992. 8(5): p. 1251-1264.

15. Acosta, E.J., J.S. Yuan, and A.S. Bhakta, The Characteristic Curvature of Ionic Surfactants. Journal of Surfactants and Detergents, 2008. 11(2): p. 145-158.

16. Kiran, S.K. and E.J. Acosta, Predicting the Morphology and Viscosity of Microemulsions Using the HLD-NAC Model. Industrial & Engineering Chemistry Research, 2010. 49(7): p. 3424-3432.

17. Acosta, E.J. and A.S. Bhakta, The HLD-NAC Model for Mixtures of Ionic and Nonionic Surfactants. Journal of Surfactants and Detergents, 2008. 12(1): p. 7-19.

18. Acosta, E., et al., Net-Average Curvature Model for Solubilization and Supersolubilization in Surfactant Microemulsions. Langmuir, 2003. 19(1): p. 186-195.

19. Salager, J.-L., et al., Enhancing solubilization in microemulsions—State of the art and current trends. Journal of Surfactants and Detergents. 8(1): p. 3-21.

20. Márquez, N., et al., Partitioning of Ethoxylated Alkylphenol Surfactants in Microemulsion−Oil−Water Systems: Influence of Physicochemical Formulation Variables. Langmuir, 2002. 18(16): p. 6021-6024.

21. Salager, J.-L. and R.E. Antón, Ionic microemulsions. 1999, Marcel Dekker: New York. p. 247-280.

22. Acosta, E.J., The HLD–NAC equation of state for microemulsions formulated with nonionic alcohol ethoxylate and alkylphenol ethoxylate surfactants. Colloids and Surfaces A: Physicochemical and Engineering Aspects, 2008. 320(1–3): p. 193-204.

23. Zarate-Muñoz, S., et al., A Simplified Methodology to Measure the Characteristic Curvature (Cc) of Alkyl Ethoxylate Nonionic Surfactants. Journal of Surfactants and Detergents, 2016: p. 1-15.

24. Wan, W., et al., Characterization of Crude Oil Equivalent Alkane Carbon Number (EACN) for Surfactant Flooding Design. Journal of Dispersion Science and Technology, 2016. 37(2): p. 280-287.

25. ShamsiJazeyi, H., R. Verduzco, and G.J. Hirasaki, Reducing adsorption of anionic surfactant for enhanced oil recovery: Part II. Applied aspects. Colloids

and Surfaces A: Physicochemical and Engineering Aspects, 2014. 453: p. 168-175.

26. Sheng, J.J., Status of surfactant EOR technology. Petroleum, 2015. 1(2): p. 97-105.

27. ShamsiJazeyi, H., R. Verduzco, and G.J. Hirasaki, Reducing adsorption of anionic surfactant for enhanced oil recovery: Part I. Competitive adsorption mechanism. Colloids and Surfaces A: Physicochemical and Engineering Aspects, 2014. 453: p. 162-167.

28. Gogoi, S.B., Adsorption–desorption of surfactant for enhanced oil recovery. Transport in porous media, 2011. 90(2): p. 589-604.

29. Zana, R., Critical micellization concentration of surfactants in aqueous solution and free energy of micellization. Langmuir, 1996. 12(5): p. 1208-1211.

30. Liu, J., et al., Bitumen–clay interactions in aqueous media studied by zeta potential distribution measurement. Journal of colloid and interface science, 2002. 252(2): p. 409-418.

31. Curtis, C.W., K. Ensley, and J. Epps, Fundamental properties of asphalt-aggregate interactions including adhesion and absorption. 1993, National Research Council Washington, DC, USA.

Appendix A: Sample Equivalent Alkane Carbon Number Determination

Materials Needed

- Heavy petroleum oil (HPO) with unknown equivalent alkane carbon number (EACN)
- Organic Solvent (assumed to be toluene here). The organic solvent must solubilize the oil with unknown EACN
- Surfactant with a known optimal salinity and characteristic curvature (e.g. AMA; sodium dihexylsulfosuccinate)
- Small vials with caps
- DI water
- Pipettes that measure in microliters

Procedure

1. Stock solutions:
    a. Prepare a surfactant stock solution to be used in the salinity scans and record the molarity. For AMA, 0.2 mol/liter is the appropriate stock solution to use. A reasonable amount is 1 liter. Record actual amount (grams) of AMA added.
    b. Prepare approximately a 20g of NaCl per 100mL water solution and record the actual amount. A reasonable amount is 1 liter, i.e. ~200 g of salt and fill to 1 L with water. Record actual amount (grams) of salt added. Be sure the salt fully dissolves.

c. Dissolve the unknown heavy petroleum oil in toluene at the desired weight percentages to make the unknown heavy petroleum oil stock solutions. It is recommended approximately 1 wt%, 3 wt%, 5 wt%, 7 wt% and 9 wt% be made. Record the actual weight percentages for all the solutions.

2. Using the previously recorded concentrations of surfactant and salt stock solutions, determine the amount of each solution and additional water needed to make the mixture contain 0.1M AMA, the desired concentration of salt, and ensure the mixture adds up to 5mL of water total and add this to a vial. As a starting point, it is recommended a total of 5 vials ranging in salt concentration from 2 to 4 g of NaCl per 100mL at 0.5 intervals for each heavy petroleum oil weight percent be made.
3. Mark the bottom of the meniscus of the water solution on the vial with a permanent marker.

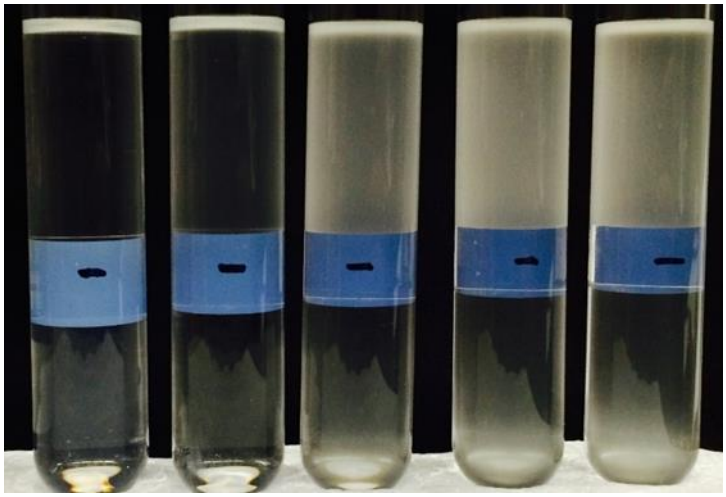

Figure 71: Example Meniscus Markings

4. Add 5mL of the toluene/heavy petroleum oil mixture to each vial and shake each vial vigorously until well mixed.
5. Allow the vials to sit for about a day to let the emulsions settle.
6. Look for where the drawn line from step 5 is in the middle of the type III emulsion. This will indicate the optimal salinity is around this salt concentration and a new scan can be performed around this salt concentration with smaller 0.1 g of NaCl per 100mL salt intervals
7. Repeat steps 2-7 until the optimal salinity can be determined.
8. Once the optimal salinity has been determined, record it along with the weight percent of heavy petroleum oil used in the experiments.
9. Repeat steps 2-8 with different weight percentages of heavy petroleum oil in toluene.

Table 12: Salinity Graph Data

wt%	wt frac	S*	S*mix	ln(S*/S*mix)/K
1	0.01	3.2	3.2	0
3	0.03	3.2	3.6	-0.692841386
5	0.05	3.2	3.8	-1.010883864
7	0.07	3.2	4	-1.312609125
9	0.09	3.2	4.3	-1.738024782

$$HLD_{mix} = x_1 HLD_1 + x_2 HLD_2$$

Assuming no alcohol, 25°C, and HLD is 0 for optimum salinity:

$$HLD = \ln(S) - K * EACN + Cc$$

$$HLD_{mix} = x_1[\ln(S^*_{mix}) - K * EACN_1 + Cc] + x_2[\ln(S^*_{mix}) - K * EACN_2 + Cc]$$

$$0 = (x_1 + x_2)\ln(S^*_{mix}) + (x_1 + x_2)Cc - K(x_1 EACN_1 + x_2 EACN_2)$$

$$1 = (x_1 + x_2)$$

$$0 = \ln(S^*_{mix}) + Cc - K(x_1 EACN_1 + x_2 EACN_2)$$

For toluene, species 1:

$$HLD_1 = \ln(S^*) - K * EACN_1 + Cc$$

Subtracting the toluene HLD equation from the HLD equation of the mixture

$$0 = \ln(S^*_{mix}) - \ln(S^*) - K\big((1 - x_2)EACN_1 + x_2 EACN_2\big) + K * EACN_1$$

$$0 = \ln(\frac{S^*_{mix}}{S^*}) + K * x_2(EACN_1 - EACN_2)$$

$$\frac{\ln\left(\frac{S^*}{S^*_{mix}}\right)}{K} = x_2(EACN_1 - EACN_2)$$

10. Graph the natural logarithm of the optimal salinity of the surfactant chosen over the determined salinity of the mixture against the weight percent of the heavy petroleum oil in the toluene.

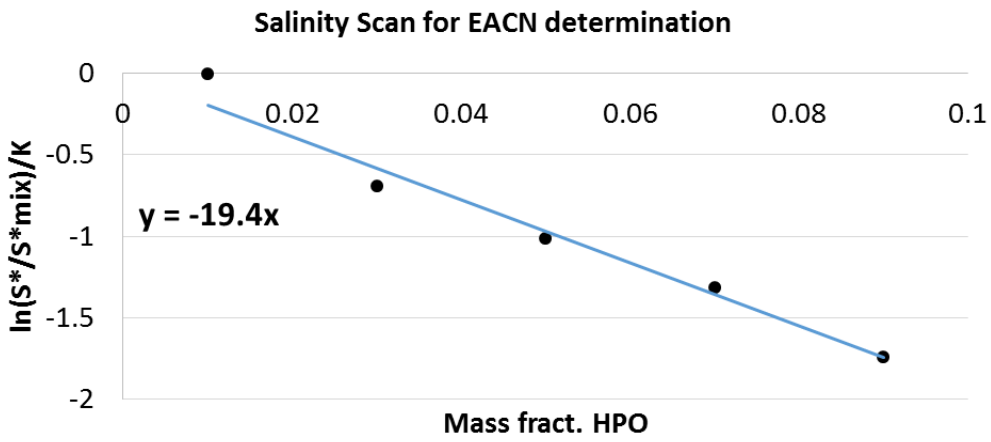

Figure 72: Salinity Scan Graph Example

11. The slope of the line from the graph in step 13 should be the EACN of the heavy petroleum oil subtracted from the EACN of the toluene. So in this case, the slope of the line is -19.4 which means that the EACN of the unknown heavy petroleum oil is 20.4.

Appendix B: Sample Characteristic Curvature Determination

Materials Needed

- Surfactant to be tested
- Reference Surfactant with a known characteristic curvature (e.g. AMA)
- Sodium Chloride
- Reference organic oil with a known EACN (e.g. toluene, decane)
- DI water
- Small vials with caps
- Microliter pipette
- Various glassware

Procedure

1. Stock solution preparation:

a. Prepare a surfactant stock solution that will be used for the salinity scans and record the molarity. Ensure that the stock solution is reasonably above the desired concentrations to be tested so as to allow enough room for the other surfactant and the salt in the aqueous phase. A liter in total volume is a reasonable amount.

b. Prepare a reference surfactant stock solution that will be used in the salinity scans and record the molarity. A liter is a reasonable amount.

c. Prepare approximately a 20g – 25g NaCl per 100mL of water solution and record the actual concentration. A liter is again a reasonable amount (i.e. 200g – 250g of NaCl in a liter of water).

2. Using the previously recorded concentrations of surfactant and salt stock solutions, determine the amount of each solution and additional DI water that is needed to make the mixture contain the desired concentrations of surfactant, reference surfactant, and NaCl and add them to the vial so that the total volume is 5mL. These will consist of the aqueous phase.
    a. As a starting point, it is recommended a total of 5 vials are used ranging in salt concentrations of 0.5 g of NaCl per 100mL intervals around the optimal salinity of the reference surfactant in the designated oil phase.
    b. It is recommended the mole fraction of the target surfactant should not exceed 0.5, since this will defeat the purpose of using a reference surfactant as it may cause the system to behave differently than when the reference surfactant is present in a larger fraction.
    c. An appropriate amount of total surfactant added is 0.1M, but this may be adjusted if the surfactant is not soluble enough to produce such concentrations (e.g. 0.01M of target surfactant and 0.09M of reference surfactant, 0.02M of target surfactant and 0.08M of reference surfactant etc.)
    d. Add the DI water first, reference surfactant next, then target surfactant, and lastly add the salt. Ensure the salt solution is added last to avoid salt shock to the system.
3. Mark the bottom of the meniscus of the aqueous phase on the vial with a permanent marker.

4. Add 5mL of the organic oil with known EACN to each vial and shake vigorously until well mixed.
5. Allow the vials to equilibrate for about a day to allow the emulsions to settle.
6. Observe where the line drawn in step 3 is located with respect to the type of emulsion that exists in the vial. If the line is in the middle of the type III emulsion then this indicates the optimal salinity has been found. A new scan can then be performed in smaller salt concentration intervals.
7. Repeat steps 2-7 until the optimal salinity can be determined.
8. Once optimal salinity has been determined, record it along with the mole fraction of target surfactant used in the experiments.
9. Repeat steps 2-8 with different mole fractions of the target surfactant.
10. Graph either the natural logarithm of the optimal salinity of the surfactant mixture over the optimal salinity of the reference surfactant for ionic surfactants or the "b" coefficient (typically ~ 0.13) multiplied by the difference of the optimal salinity of the mixture and the optimal salinity of the reference surfactant for nonionic surfactants against the mole fraction of the target surfactant.
11. The linear slope of the line between these points and the origin is the Cc of the target surfactant subtracted from the Cc of the reference surfactant.

Example

As described in the procedure for salinity scans, a spreadsheet was setup in excel to determine the appropriate amounts of each stock solution used. In this example Surfactant 3 was used. Stock solutions were first made and recorded.

Table 13: Stock solutions

AMA stock	0.197	M
Surfactant 3 stock	0.00818	M
NaCl stock	33.6	gNaCl/100mLH_2O

It was then decided which mole fractions would be used in the experiments.

Table 14: Mole Fraction of Surfactant 3

AMA (M)	Surfactant 3 (M)	x Surfactant 3 (mole frac.)
0.015	0	0
0.014	0.001	0.067
0.013	0.002	0.13
0.012	0.003	0.20
0.01	0.005	0.33

For a desired mole fraction of Surfactant 3 of 0.067, concentrations of 0.014M AMA and 0.001M Surfactant 3 are required. To determine around which salinity the scan should begin, the optimal salinity of AMA in decane can be found using the HLD equation for ionic surfactants.

$$HLD = \ln(S) - K * EACN + Cc - \alpha_T * \Delta T$$

Since the optimal salinity will occur at and HLD of 0, K is approximately 0.173, the change in temperature from 25°C is 0, the EACN of decane is 10, and the Cc of AMA is -0.93, the optimal salinity of AMA in decane can be solved for.

$$0 = \ln(S) - 0.173 * 10 - 0.93 - 0$$

$$\ln(S) = 2.66$$

$$S_{AMA} = 14.3$$

So the scan will begin at 14g NaCl per 100mL of H_2O and will increase in increments of 0.5.

The cells on the left are the desired concentrations that are to be in the vial, and those cells titled volume in microliters are the necessary volumes of stock solution that needs to be added to the vial to achieve the desired concentrations in a total of 5mL of aqueous phase.

Table 15: Vial Preparation

AMA (M)	Surf. 3 (M)	NaCl (g/mL)	Surf. 3 Vol (uL)	AMA Vol (uL)	NaCl Vol (uL)	Vol H20 (uL)	total vol (uL)
0.014	0.001	14	611	355	2083	1950	5000
0.014	0.001	14.5	611	355	2158	1876	5000
0.014	0.001	15	611	355	2232	1801	5000
0.014	0.001	15.5	611	355	2307	1727	5000
0.014	0.001	16	611	355	2381	1652	5000

After all the aqueous phase volumes have been added to the vial and before the decane has been added, a line is drawn in permanent marker where the meniscus of the aqueous phase is as seen is Figure 73.

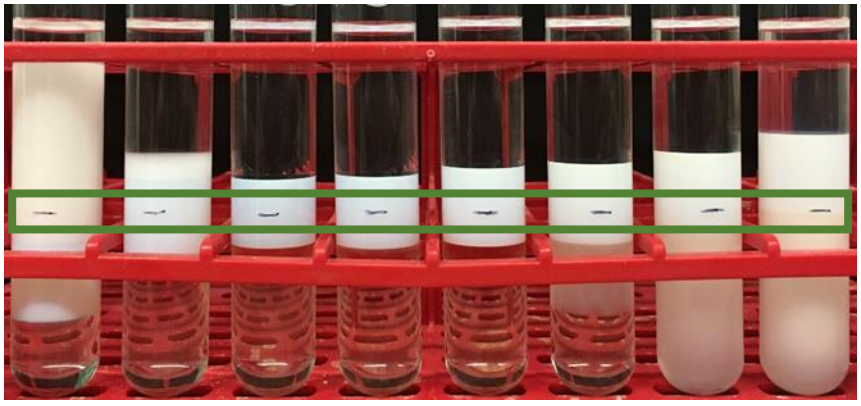

Figure 73: Aqueous phase meniscus lines

Once the line has been drawn, 5mL of decane is added to the vials and they are shaken vigorously until well mixed and then left to equilibrate. Once the emulsions have settled, it can be determined where the line is in the middle of the type III emulsion.

After the first scan, it was determined the optimal solubility was around 15.5g NaCl per 100mL, so another scan was performed for 15.2, 15.4, 15.7, and 15.9.

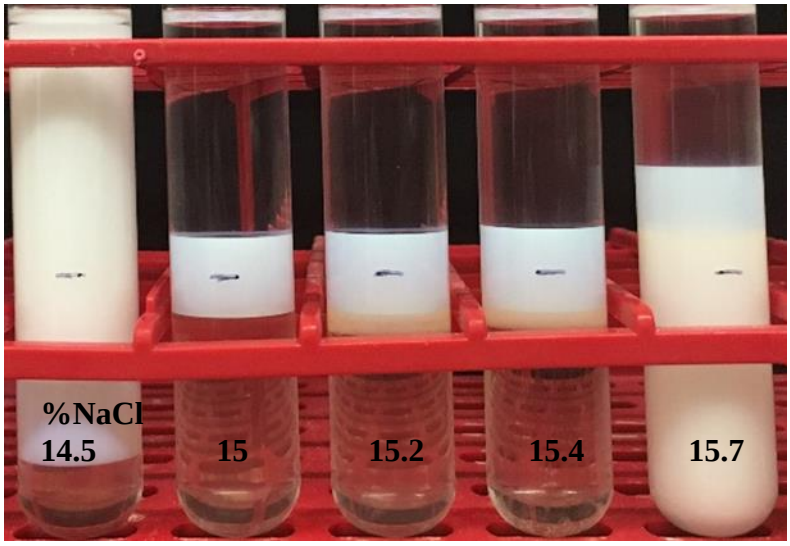

Figure 74: Completed Scan for 14mM AMA and 1.0mM Surfactant 3

The optimal salinity for a mole fraction of Surfactant 3 of 0.067 was determined to be 15.4g of NaCl per 100mL of H_2O. The same procedure was performed for three more mole fractions and their optimal salinities were found as well and recorded.

Table 16: Optimal Salinities for mole fractions of Surfactant 3

AMA (M)	Surfactant 3 (M)	x Surfactant 3	S*mixture
0.015	0	0	14.3
0.013	0.002	0.13	17.25
0.014	0.001	0.067	15.4
0.012	0.003	0.20	19.5
0.01	0.005	0.33	22.6

In order to determine the Cc of the target surfactant, it will be assumed no alcohol and 25°C.

$$HLD = \ln(S) - K * EACN + Cc - \alpha_T * \Delta T$$

$$HLD = \ln(S) - K * EACN + Cc$$

Assuming linear mixing occurs between the two surfactants;

$$HLD_{mix} = x_{AMA} HLD_{AMA} + x_{Surf3} HLD_{Surf3}$$

$$HLD_{mix} = x_{AMA}[\ln(S_{mix}) - K_{AMA} * EACN + Cc_{AMA}] + x_{Surf3}[\ln(S) - K_{Surf3} * EACN + Cc_{Surf3}]$$

Assume the K constants are equal and the optimum point occurs at $HLD_{mix} = 0$;

$$0 = (x_{AMA} + x_{Surf3}) \ln(S_{mix}) - K * EACN(x_{AMA} + x_{Surf3}) + x_{AMA} Cc_{AMA} + x_{Surf3} Cc_{Surf3}$$

$$x_{AMA} + x_{Surf3} = 1$$

$$0 = \ln(S_{mix}) - K * EACN + x_{AMA} Cc_{AMA} + x_{Surf3} Cc_{Surf3}$$

Subtracting the optimum HLD for AMA (i.e. $0 = \ln(S_{AMA}) - K * EACN + Cc_{AMA}$) gives;

$$\ln \frac{S_{mix}}{S_{AMA}} = x_{Surf3} * (Cc_{AMA} - Cc_{Surf3})$$ for ionic surfactants

Note: following the same procedure for nonionic surfactants gives;

$$b * (S_{mix} - S_{AMA}) = x_{Surf3} * (Cc_{AMA} - Cc_{XD70})$$

So to determine the Cc of Surfactant 3, $\ln \frac{S_{mix}}{S_{AMA}}$ will be graphed against the mole fraction of Surfactant 3 in the mixture and the linear slope between the data points and the origin will be the Cc of Surfactant 3 subtracted from the Cc of AMA.

Table 17: Mole fraction and corresponding natural logarithm of salinities

x Surfactant 3	ln(S*mix/S*AMA)
0	0
0.067	0.072
0.13	0.19
0.20	0.31
0.33	0.46

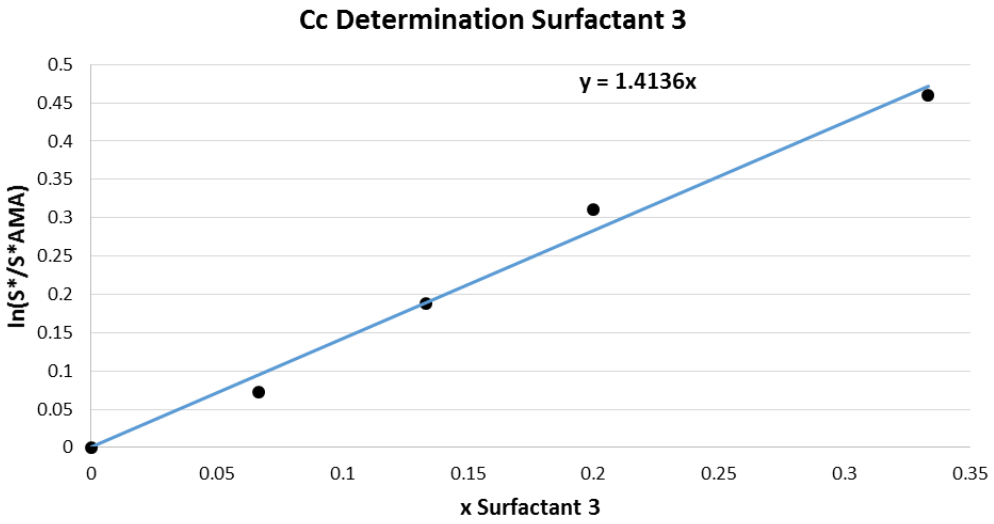

Figure 75: Optimal Salinity vs. Mole Fraction for Surfactant 3

The linear slope of this plot is 1.41 meaning that the Cc of Surfactant 3 is -2.34.

Appendix C: Sample Critical Micelle Concentration Determination

Materials Needed

- Surfactant to be tested
- Surface Tension Analyzer (Wilhelmy Plate, Maximum Bubble Pressure, or some other way to measure surface tension)
- Pipettes that measure in microliters
- DI water
- Various glassware

Procedure

Critical Micelle Concentration

1. Prepare a stock solution of the surfactant to be tested and record the molarity (weight of surfactant divided by molecular weight of surfactant multiplied by the volume of water and surfactant (in liters)). (i.e. 10 mM of surfactant) This stock solution will be used to prepare the dilutions for which the surface tension will be measured.
2. Since surface tension will be plotted against the log scale of concentration, prepare dilutions that are separated by a factor of 10 each time. (i.e. dilutions of 1 mM, 0.1 mM, 0.01 mM etc.)
    a. To ensure enough data has been collected to accurately determine the CMC, also prepare dilutions from other concentrations like 5 mM (i.e. 5 mM, 0.5 mM, 0.05 mM etc.)
3. Measure the surface tension of the dilutions prepared in Step 2.

a. The measurements shown below were completed using a Cahn DCA322 system which utilizes the Wilhelmy plate method (in this case a glass slide).
b. Other ways exist to determine surface tension such as tensiometers that utilize a pendant drop technique.

4. Construct a graphs of these surface tensions plotted against the log scale of concentration.
    a. Ideally there should be a certain point at which the surface tension no longer changes with concentration (or changes very slowly with concentration), which is due to the surface being saturated with surfactant molecules. If this phenomena is not represented in the data, the following steps may fix this problem.
    b. If the surface tension has not leveled off with increasing concentration, then the CMC has not been reached and more concentrated solutions must be measured.
    c. If the surface tension is not decreasing with increasing concentration, then the solutions being tested are still above the CMC and more dilute solutions must be measured.
    d. It is quite possible that a surfactant (e.g. lignin amine) does not have a CMC. However, the linear slope of the surface tension plotted against the log scale of concentration is needed for the Gibbs isotherm equation, not the actual CMC itself.

Area Per Surfactant Head Group

1. Using the Gibbs isotherm equation to determine the Gibbs surface excess for the surfactant.
    a. Ensure the units are correct.
    b. Note that a factor of 2 is present in the Gibbs isotherm equation for ionic surfactants without added salt. If the molar concentration of added salt is at least 10x the CMC then use the same equation for ionic surfactants and nonionic surfactants. The factor of 2 in the Gibbs isotherm equation comes from the change in chemical potential of the counterion of the surfactants ion.
2. Multiply the surface excess energy by Avogadro's number ($6.022*10^{23}$) and taking the inverse of that result yields the area per surfactant head group.
    a. Ensure the units are correct.

Example

As described in the procedure for CMC determination, surface tensions are measured for different surfactant concentrations as shown below in Table 18. In this example Surfactant 570S was used.

Table 18: Surfactant concentration and corresponding surface tensions

Concentration (mmol/L)	log(conc.)	Weight Percent	Surface Tension (mN/m)
1.81	-2.74	0.0566	33.57
1.0	-3.0	0.031	33.62
0.75	-3.1	0.023	33.94
0.50	-3.3	0.016	34.24
0.25	-3.6	0.0078	36.72
0.10	-4.0	0.0031	41.97
0.075	-4.1	0.0023	43.76
0.050	-4.3	0.0016	46.99
0.025	-4.6	0.0008	50.58
0.01	-5.0	0.0003	54.18

Now graph the surface tension against the log scale of concentration (or weight percent) as seen in Figure 76.

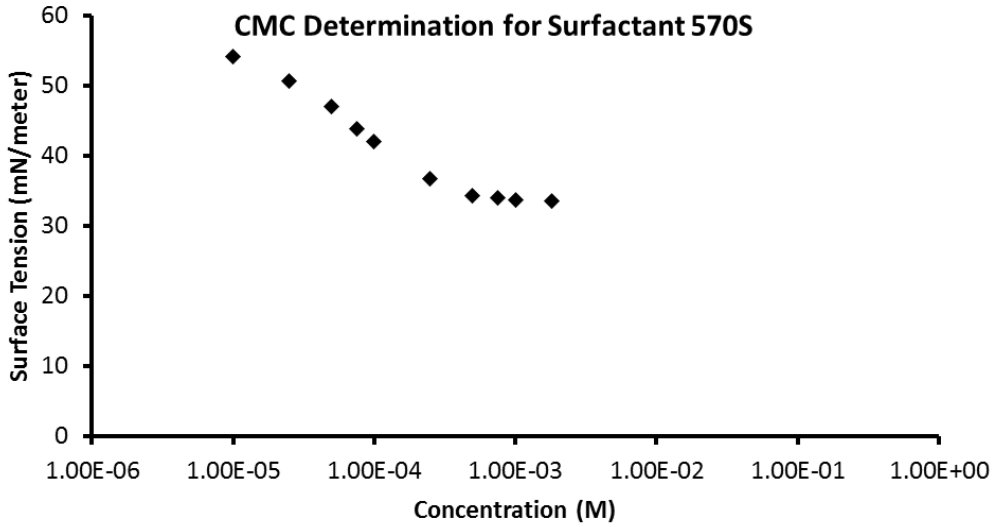

Figure 76: Surface Tension vs. Concentration for Surfactant 570S

The CMC occurs where the surface tension ceases to decrease linearly with the log scale of concentration and remains constant. This point is demonstrated in Figure 77 below. Assume the four data points to the right of the arrow are above the CMC and the six data points to the left of the arrow are below the CMC.

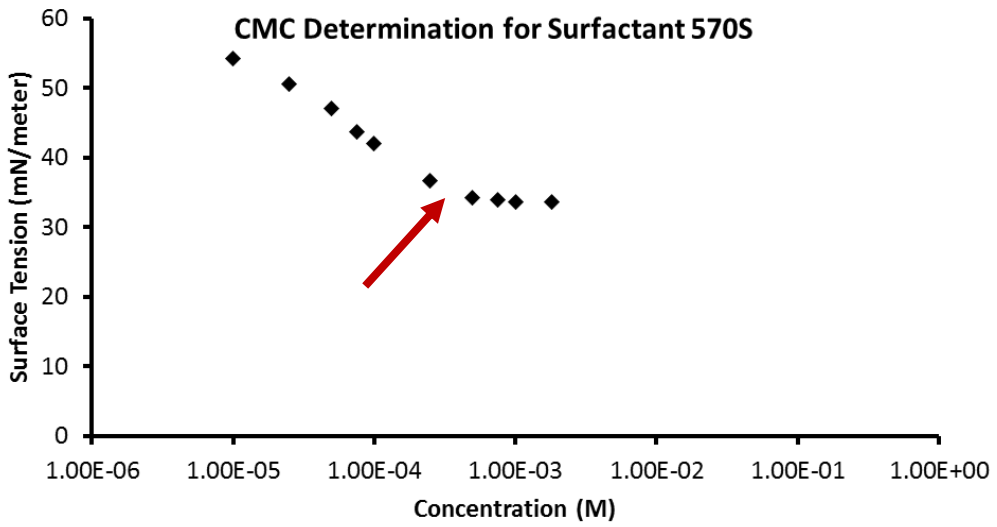

Figure 77: CMC approximation

Using a tool such as Excel, calculate the best "linear line fit" for the linear points below the CMC (the two lowest concentrations were excluded since they no longer trend linearly) and the best "linear line fit" with a slope of 0 for the points above the CMC. It is important to note that since the x-axis is in a logarithmic scale, the best "linear line fit" is actually a logarithmic fit. The line fit above the CMC has a slope of 0 because surface tension should ideally remain constant for concentrations above the CMC.

$$y = -14.42 * \log(x) - 15.42$$

$$y = 0 * \log(x) + 33.84$$

And calculate the intersection of these two best fit lines to find the CMC. (Graphically shown in Figure 78)

$$-14.42 * \log(x) - 15.42 = 33.84$$

$$\log(x) = -3.42$$

$$x = 3.83 * 10^{-4} M = .383 mM = CMC$$

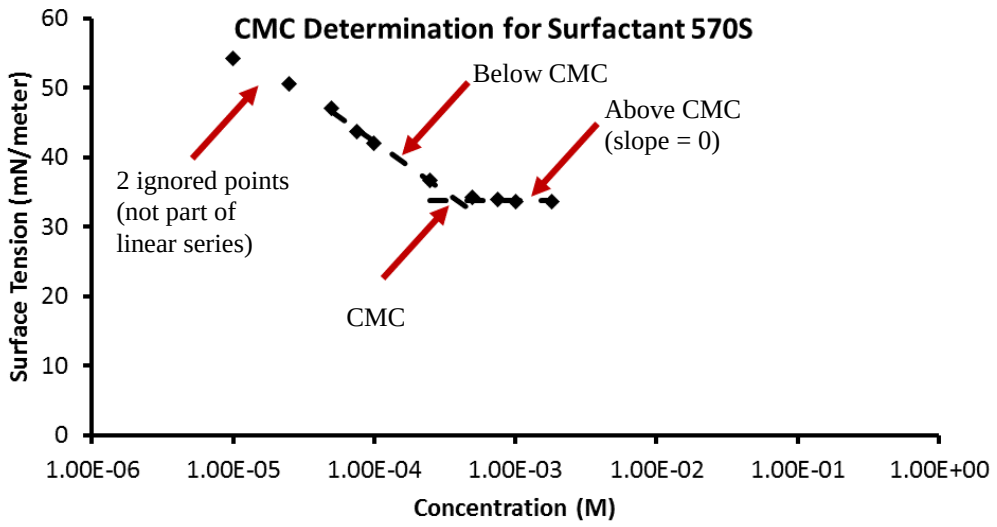

Figure 78: CMC Determination

Once the CMC has been determined, the area per surfactant head group may be calculated using the Gibbs isotherm equation and the linear slope calculated for the points below the CMC ($\frac{d\gamma}{d(logC)}$).

$$\Gamma_{2,1} = \frac{1}{RT}\frac{d\pi}{d(lnC)} = -\frac{1}{2.303 * RT}\frac{d\gamma}{d(logC)}$$ nonionics or ionics with swamping electrolyte

$$\Gamma_{2,1} = \frac{1}{RT}\frac{d\pi}{d(lnC)} = -\frac{1}{2.303 * 2 * RT}\frac{d\gamma}{d(logC)}$$ ionics without added electrolyte

The Gibbs isotherm equation allows the surface excess energy to be found, which is then in turn used in the area calculation along with Avogadro's number ($6.022*10^{23}$).

$$Area = \frac{1}{\Gamma_{2,1} N_A}$$

Applying unit conversions cause the final area per head group calculation to become:

$$Area = -\frac{T * 8.314 * 2.303}{\frac{d\gamma}{d(logC)} * 6.022}$$ nonionics

$$Area = -\frac{T * 8.314 * 2.303 * 2}{\frac{d\gamma}{d(logC)} * 6.022}$$ ionics

So for Surfactant 570S, which is an ionic surfactant, the area per surfactant head group is as follows:

$$Area = -\frac{298 * 8.314 * 2.303 * 2}{(-14.42) * 6.022} = 131\ \text{Å}^2/molecule$$